ISSN 0915-6364

NATIONAL INSTITUTE FOR FUSION SCIENCE

Energy Levels, Radiative Rates and Electron Impact Excitation Rates for Transitions in He-like C V

K.M. Aggarwal, T. Kato, F.P. Keenan and I. Murakami

(Received - June 11, 2010

NIFS-DATA-110 July 1, 2010

RESEARCH REPORT
NIFS-DATA Series

TOKI, JAPAN

Energy levels, radiative rates, and electron impact excitation rates for transitions in He-like C V

K. M. Aggarwal[1,⋆], T. Kato[2], F. P. Keenan[1], and I. Murakami[2]

[1]Astrophysics Research Centre, School of Mathematics and Physics, Queen's University Belfast, Belfast BT7 1NN, Northern Ireland, UK

⋆ e-mail: K.Aggarwal@qub.ac.uk

[2]National Institute for Fusion Science, Oroshi-cho, Toki, Gifu, 509-5292 Japan

Abstract

In this paper we report calculations for energy levels, radiative rates, and electron impact excitation rates for transitions in He-like C V. The GRASP (general-purpose relativistic atomic structure package) is adopted for calculating energy levels and radiative rates, and for determining the collision strengths and subsequently the excitation rates, the Dirac atomic R-matrix code (DARC) is used. Oscillator strengths, radiative rates, and line strengths are reported for all E1, E2, M1, and M2 transitions among the lowest 49 levels of C V. Collision strengths have been averaged over a Maxwellian velocity distribution and the effective collision strengths so obtained are reported over a wide temperature range below 10^6 K. Additionally, lifetimes are also reported for all calculated levels.

Keywords: He-like carbon, energy levels, radiative transition rates, oscillator strengths, line strengths, lifetimes, electron impact collision strengths, excitation rates

1 Introduction

Emission lines of He-like ions have been widely observed in a variety of astrophysical and laboratory plasmas. For example, lines of many He-like ions observed in solar plasmas in the x-ray region (1-50 Å) have been listed by Dere et al. [1]. Of particular interest are the resonance (w: 1s^2 ^{1}S$_0$ – 1s2p ^{1}P$^o_1$), intercombination (x and y: 1s^2 ^{1}S$_0$ – 1s2p ^{3}P$^o_{2,1}$), and forbidden (z: 1s^2 ^{1}S$_0$ – 1s2s ^{3}S$_1$) lines, which are highly useful for solar plasma diagnostics - see, for example, Gabriel and Jordan [2], Acton et al. [3], and Porquet et al. [4]. However to analyse observations, atomic data are required for a variety of parameters, such as energy levels, radiative rates (A- values), and excitation rates or equivalently the effective collision strengths (Υ), which are obtained from the electron impact collision strengths (Ω).

Emission lines from several ionisation stages of carbon, including He-like C V, have been observed in solar plasmas from rockets and satellites [1], and are useful for the determination of electron densities and temperatures in the solar corona and transition region [5]. Similarly, the resonance w line at 40.2 Å has been studied in a laser-produced carbon plasma by Chowdhury et al. [6]. Since this line lies in the water window spectral region, it has potential application in x-ray microscopic imaging of biological samples in wet conditions. Recently lines of C V have also been measured in the EUV range by Kato et al. [7] in fusion plasmas from Large Helical Device (LHD), as carbon is one of the main impurities in fusion reactors. Therefore, atomic data for C V are highly required for modelling and diagnostics of a variety of plasmas.

Experimentally, energy levels have been compiled by NIST (National Institute of Standards and Technology) and are available at their website `http://physics.nist.gov/PhysRefData`. Similarly, A- values are also available for some transitions on the NIST website. However, the collisional atomic data for C V are restricted to transitions only from the lowest three levels to higher excited levels [8]. These calculations of Sampson et al. [8] are based on the Coulomb-Born-Exchange method and do not include the contribution of resonances, which can be very important for an ion such as C V. Therefore, in this paper we report a complete set of results (namely energy levels, radiative rates, lifetimes, and effective collision strengths) for all transitions among the lowest 49 levels of C V. These levels belong to the 1s^2, 1s2ℓ, 1s3ℓ, 1s4ℓ, and 1s5ℓ configurations. Finally, we also report the A- values for four types of transitions, namely electric dipole (E1), electric quadrupole (E2), magnetic dipole (M1), and magnetic quadrupole (M2), because these are also required for plasma modelling.

For our calculations we employ the fully relativistic GRASP (general-purpose relativistic atomic structure package) code for the determination of wavefunctions, originally developed by Grant et al. [9] and revised by Dr. P. H. Norrington. It is a fully relativistic code, and is based on the jj coupling scheme. Further relativistic corrections arising from the Breit interaction and QED effects (vacuum polarization and Lamb shift) have also been included. Additionally, we have used the option of *extended average level* (EAL), in which a weighted (proportional to $2j$+1) trace of the Hamiltonian matrix is minimized. This produces a compromise set of orbitals describing closely lying states with moderate accuracy. Similarly, for our calculations of Ω, we have adopted the *Dirac atomic R-matrix code* (DARC) of P.H. Norrington and I.P. Grant (private communication). Finally, for comparison purposes we have performed parallel calculations from the *Flexible Atomic Code* (FAC) of Gu [10], available from the website `http://sprg.ssl.berkeley.edu/~mfgu/fac/`. This is also a fully relativistic code which provides a variety of atomic parameters, and (generally) yields results comparable to GRASP and DARC - see, for example, Aggarwal et al. [11] and references therein. Thus results from FAC will be helpful in assessing the accuracy of our energy levels, radiative rates, and collision strengths.

2 Energy levels

The 1s^2, 1s2ℓ, 1s3ℓ, 1s4ℓ, and 1s5ℓ configurations of C V give rise to the lowest 49 levels listed in Table 1, in which we compare our level energies from GRASP, obtained *without* and *with* the inclusion of Breit and QED effects, with the experimental energies compiled by NIST. Our level energies obtained without the Breit and QED effects (GRASP1) are consistently lower than the experimental ones by $\sim$ 0.2 Ryd, and agree within 1%. However, the orderings are slightly different from those of NIST, particularly for the ns ^{1}S$_0$ levels. The inclusion of Breit and QED effects has an insignificant effect ($\leq$ 0.01 Ryd) on the energy levels, which is expected also because C V is a light ion. Furthermore, the orderings have slightly altered in four instances, namely for levels 3/4, 9/10, 26/27, and 43/44. However, the energy differences for these swapping levels are very small. Our level energies obtained from the FAC code (FAC1), including the same CI (configuration interaction) as in GRASP1, are consistently higher by $\sim$ 0.1 Ryd and hence are comparatively in better agreement with the NIST orderings. The level orderings from FAC1 are in agreement with our calculations from GRASP for the lowest 36 levels, but differ for the higher ones not only with our calculations but also with the experimental compilations of NIST. This is mainly because degeneracy among the levels of the n = 5 configurations is very small. A further inclusion of 1s6ℓ configurations, as in the FAC2 calculations, makes no difference either in magnitude or orderings, mainly because the levels of the 1s6ℓ configurations lie *above* the lowest 49 levels listed in Table 1, and hence do not interact with those. To conclude, we may state that overall there is no discrepancy between theory and experiment for the energy levels of C V.

3 Radiative rates

The absorption oscillator strength (f_{ij}) and radiative rate A_{ji} (in s^{-1}) for a transition $i \rightarrow j$ are related by the following expression:

$$f_{ij} = \frac{mc}{8\pi^2e^2}\lambda^2_{ji}\frac{\omega_j}{\omega_i}A_{ji} = 1.49 \times 10^{-16}\lambda^2_{ji}(\omega_j/\omega_i)A_{ji} \tag{1}$$

where m and e are the electron mass and charge, respectively, c is the velocity of light, λ_{ji} is the transition energy/wavelength in Å, and ω_i and ω_j are the statistical weights of the lower (i) and upper (j) levels, respectively. Similarly, the oscillator strength f_{ij} (dimensionless) and the line strength S (in atomic unit, 1 a.u. = 6.460×10^{-36} cm^2 esu^2) are related by the following standard equations.

For the electric dipole (E1) transitions

$$A_{ji} = \frac{2.0261 \times 10^{18}}{\omega_j\lambda^3_{ji}}S^{\rm E1} \quad \text{and} \quad f_{ij} = \frac{303.75}{\lambda_{ji}\omega_i}S^{\rm E1}, \tag{2}$$

for the magnetic dipole (M1) transitions

$$A_{ji} = \frac{2.6974 \times 10^{13}}{\omega_j\lambda^3_{ji}}S^{\rm M1} \quad \text{and} \quad f_{ij} = \frac{4.044 \times 10^{-3}}{\lambda_{ji}\omega_i}S^{\rm M1}, \tag{3}$$

for the electric quadrupole (E2) transitions

$$A_{ji} = \frac{1.1199 \times 10^{18}}{\omega_j\lambda^5_{ji}}S^{\rm E2} \quad \text{and} \quad f_{ij} = \frac{167.89}{\lambda^3_{ji}\omega_i}S^{\rm E2}, \tag{4}$$

and for the magnetic quadrupole (M2) transitions

$$A_{ji} = \frac{1.4910 \times 10^{13}}{\omega_j\lambda^5_{ji}}S^{\rm M2} \quad \text{and} \quad f_{ij} = \frac{2.236 \times 10^{-3}}{\lambda^3_{ji}\omega_i}S^{\rm M2}. \tag{5}$$

In Table 2 we present transition energies/wavelengths (λ, in Å), radiative rates (A_{ji}, in s^{-1}), oscillator strengths (f_{ij}, dimensionless), and line strengths (S, in a.u.), in length form only, for all 336 electric dipole (E1) transitions among the 49 levels of C V. The *indices* used to represent the lower and upper levels of a transition have already been defined in Table 1. Similarly, there are 391 electric quadrupole (E2), 316 magnetic dipole (M1), and 410 magnetic quadrupole (M2) transitions among the 49 levels. However, for these transitions only the A- values are listed in Table 2, and the corresponding results for f- or S- values can be easily obtained by using Eqs. (1–5).

In Table 3 we compare our A-values from the GRASP and FAC codes for some of the transitions with those of Porquet and Dubau [12], who have adopted the *SuperStructure* (SS) code of Eissner et al. [13] and have reported A- values for only a few transitions among the lowest 17 levels of C V, although they performed calculations for all the 49 levels. For a majority of strong transitions (f $\geq$ 0.01), the A-values from GRASP and FAC agree to better than 10%, which is highly satisfactory. However, for some very weak transitions, such as 4–6 (f=8.7×10^{-8}), the two sets of A-values differ by an order of magnitude. For other weak transitions, such as 4–16 and 5–16, our A- values from

GRASP are higher than those from FAC by about a factor of two. Similarly, differences between the A-values of Porquet and Dubau and those presently calculated from GRASP are generally within 10% for all strong transitions, and are up to 50% for a few weak transitions, such as 4–16 and 5–16. This is because weak transitions are very sensitive to mixing coefficients, and hence differing amount of CI (and methods) produce different A-values, as discussed in detail by Hibbert [14]. However, we would like to emphasize that although the A-values for weak transitions may be required in modelling applications, their contribution is (generally) small in comparison to the stronger transitions with f $\geq$ 0.01. Furthermore, for a majority of the strong E1 transitions (f $\geq$ 0.01) the length and velocity forms in our GRASP calculations agree within 20%. However, the differences for 14 transitions are higher (by up to a factor of two), except for 48–49 for which the two forms differ by a factor of 5.6. For transitions for which the energy (ΔE) is very small (such as 48–49), a slight variation in ΔE affects the A-values considerably. Among weaker transitions only five, namely 2–26 (f = 6.0×10^{-4}), 2–40 (f = 1.4×10^{-11}), 4–6 (f = 8.7×10^{-8}), 43–45 (f = 5.6×10^{-8}), and 44–45 (f = 7.5×10^{-7}), differ by an order of magnitude, and the rest by smaller factors.

As a further assessment of accuracy for our calculated f- values from GRASP, we have compared these with the corresponding results from the FAC code, as shown already for some transitions in Table 3. For all strong transitions (f $\geq$ 0.01) the agreement between the two independent calculations is better than 20%, except for 13 (such as: 1–49, 27–47 and 29–44), for which the differences are up to a factor of 2.5. Therefore, on the basis of these comparisons and the discussion above, we may state that for a majority of strong E1 transitions, our radiative rates are accurate to better than 20%. However, for the weaker transitions this assessment of accuracy does not apply.

4 Lifetimes

The lifetime τ for a level j is defined as follows:

$$\tau_j = \frac{1}{\sum_i A_{ji}}. \tag{6}$$

Since this is a measurable parameter, it provides a check on the accuracy of the calculations. Therefore, in Table 1 we have also listed our calculated lifetimes, which *include* the contributions from four types of transitions, i.e. E1, E2, M1, and M2. To our knowledge, no calculations or measurements are available for lifetimes in C V. However, we hope the present results will be useful for future comparisons and may encourage experimentalists to measure lifetimes, particularly for levels (1s2s) $^3S_1$ and $^1S_0$ which have comparatively larger values.

5 Collision strengths

For the computation of collision strengths Ω, we have employed the *Dirac atomic R-matrix code* (DARC), which includes the relativistic effects in a systematic way, in both the target description and the scattering model. It is based on the jj coupling scheme, and uses the Dirac-Coulomb Hamiltonian in the R- matrix approach. The R-matrix radius adopted for C V is 19.36 and 60 continuum orbitals have been included for each channel angular momentum for the expansion of the wavefunction. This allows us to compute Ω up to an energy of 52 Ryd, sufficient to calculate values of Υ up to $T_e = 10^6$ K. The maximum number of channels for a partial wave is 217, and the corresponding size of the Hamiltonian matrix is 13076. In order to obtain convergence of Ω for all transitions and at all energies, we have included all partial waves with angular momentum $J \leq 40.5$, although a larger number would have been preferable for the convergence of some allowed transitions, especially at higher energies. However, to account for the inclusion of higher neglected partial waves, we have included a top-up, based on the Coulomb-Bethe approximation for allowed transitions and geometric series for others.

In Figs. 1-3 we show the variation of Ω with angular momentum J for three transitions of C V, namely 2–4 (1s2s $^3S_1$ – 1s2p $^3P^o_1$), 2–10 (1s2s $^3S_1$ – 1s3p $^3P^o_1$), and 9–11 (1s3p $^3P^o_0$ – 1s3p $^3P^o_2$), respectively, and at three energies of 30, 40, and 50 Ryd. Values of Ω have fully converged for all *resonance* transitions (including the allowed ones), plus most of the allowed transitions among the higher excited levels, as shown in Fig. 2 for the 2–10 transition. It is also clear from Fig. 2 that the need to include a larger range of partial waves increases with increasing energy. However, values of Ω have not converged for those allowed transitions whose ΔE is very small (mainly within the same n complex), as shown for the 2–4 transition in Fig. 1. Similarly, values of Ω have (almost) converged for all forbidden transitions, including those whose ΔE is very small, such as the 9–11 transition shown in Fig. 3. Therefore, primarily for the allowed transitions within the same n complex, our wide range of partial waves is not sufficient for the convergence of Ω, for which a top-up has been included as mentioned above, and has been found to be appreciable.

In Table 4 we list our values of Ω for resonance transitions of C V at energies *above* thresholds. The *indices* used to represent the levels of a transition have already been defined in Table 1. No similar data are available for comparison purpose as already stated in section 1. Therefore, in order to make an accuracy assessment of the values of Ω, particularly for the allowed transitions, we have performed another calculation using the FAC code of Gu [10]. This code is also fully relativistic, and is based on the well-known and widely-used *distorted-wave* (DW) method. Furthermore, the same CI is included in FAC as in the calculations from DARC. Therefore, also included in Table 4 for comparison purposes are the Ω values from FAC at a single *excited* energy E_j, which corresponds to $\sim$ 40 Ryd incident energy. Generally the two sets of Ω agree well (within $\sim$ 20%), but differences up to 50% are common for many weak transitions, such as 1–9/11/13/18/32. Similarly, for some transitions, particularly 1–27/29/41/43/45/46, discrepancies are up to a factor of two, although all such transitions are very *weak* ($\Omega \leq 10^{-5}$). For such weak transitions, values of Ω from the FAC code are not assessed to be accurate, as our corresponding results from the DARC code have fully converged within the adopted J values at *all* energies.

In Fig. 4 we show the variation of our values of Ω with energy for three *allowed* transitions among the excited levels of C V, namely 2–5 (1s2s $^3S_1$ – 1s2p $^3P^o_2$), 4–14 (1s2p $^3P^o_1$ – 1s3d $^3D_2$), and 10–24 (1s3p $^3P^o_1$ – 1s4d $^3D_2$). Also included in this figure are the corresponding results obtained from the FAC code. For all the above three (and many other) transitions there are no discrepancies between the f- values obtained from the two independent (GRASP and FAC) codes, and therefore the values of Ω also agree to better than 20%. However, the Ω obtained from FAC are slightly anomalous, for the 2–5 transition towards the lower end and for the 10–24 at the higher end of the energy range. Similar comparisons between the two calculations from DARC and FAC are made in Fig. 5 for three *forbidden* transitions, namely 2–8 (1s2s $^3S_1$ – 1s3s $^3S_1$), 2–15 (1s2s $^3S_1$ – 1s3d $^3D_3$), and 4–10 (1s2p $^3P^o_1$ – 1s3p $^3P^o_1$). For these transitions the agreement between the two calculations considerably improves with increasing energy, but differences are significant towards the lower end of the energy range. The main reason for such anomalies for some transitions from the calculations from FAC, is because of the interpolation and extrapolation techniques employed in the FAC code, which is designed to generate a large amount of atomic data in a comparatively very short period of time, and without too much loss of accuracy. Similarly, some differences in Ω are expected because the DW method generally overestimates the results for light ions due to the exclusion of channel coupling. Therefore, on the basis of these and other comparisons discussed above, collision strengths from the FAC code are not assessed to be very accurate for a majority of transitions of C V. On the other hand, we do not see any obvious deficiency in our calculations for Ω, and estimate our results to be accurate to better than 20% for a majority of the (strong) transitions.

6 Effective collision strengths

Excitation rates, along with energy levels and radiative rates, are required for plasma modelling, and are determined from the collision strengths (Ω). Since the threshold energy region is dominated by numerous closed-channel (Feshbach) resonances, values of Ω need to be calculated in a fine energy mesh in order to accurately account for their contribution. Furthermore, in a hot plasma electrons have a wide distribution of velocities, and therefore values of Ω are generally averaged over a *Maxwellian* distribution as follows:

$$\Upsilon(T_e) = \int_0^{\infty} \Omega(E) exp(-E_j/kT_e) d(E_j/kT_e), \quad (7)$$

where k is Boltzmann constant, T_e is electron temperature in K, and E_j is the electron energy with respect to the final (excited) state. Once the value of Υ is known the corresponding results for the excitation q(i,j) and de-excitation q(j,i) rates can be easily obtained from the following equations:

$$q(i,j) = \frac{8.63 \times 10^{-6}}{\omega_i T_e^{1/2}} \Upsilon exp(-E_{ij}/kT_e) \qquad \mathrm{cm^3 s^{-1}} \quad (8)$$

and

$$q(j,i) = \frac{8.63 \times 10^{-6}}{\omega_j T_e^{1/2}} \Upsilon \qquad \mathrm{cm^3 s^{-1}}, \quad (9)$$

where ω_i and ω_j are the statistical weights of the initial (i) and final (j) states, respectively, and E_{ij} is the transition energy. The contribution of resonances may enhance the values of Υ over those of the background values of collision strengths (Ω_B), especially for the forbidden transitions, by up to a factor of ten (or even more) depending on the transition and/or the temperature. Similarly, values of Ω need to be calculated over a wide energy range (above thresholds) in order to obtain convergence of the integral in Eq. (7), as demonstrated in Fig. 7 of Aggarwal and Keenan [15].

To delineate resonances, we have performed our calculations of Ω at over 3300 energies in the threshold region. Close to thresholds ($\sim$ 0.1 Ryd above a threshold) the energy mesh is 0.001 Ryd, and away from thresholds is 0.002 Ryd. Thus care has been taken to include as many resonances as possible, and with as fine a resolution as is computationally feasible. The density and importance of resonances can be appreciated from Figs. 6–9, where we show Ω in the thresholds region for the four most important transitions of C V, namely 1–2 (z: $1s^2\ {}^1S_0$ – $1s2s\ {}^3S_1$), 1–4 (y: $1s^2\ {}^1S_0$ – $1s2p\ {}^3P^o_1$), 1–5 (x: $1s^2\ {}^1S_0$ – $1s2p\ {}^3P^o_2$), and 1–7 (w: $1s^2\ {}^1S_0$ – $1s2p\ {}^1P^o_1$). For some transitions, such as 1–2, 1–4 and 1–5, resonances are dense particularly at energies just above the thresholds. These near threshold resonances affect the values of Υ particularly towards the lower end of the temperature range.

Our calculated values of Υ are listed in Table 5 over a wide temperature range up to 10^6 K, suitable for applications in solar and other plasmas. As stated earlier in section 1, there are no similar results available for comparison purpose except the *extrapolated* data of Porquet and Dubau [12] for only six resonance transitions. Their extrapolations are based on the Coulomb-Born-Exchange calculations of Zhang and Sampson [16] for He-like ions with $8 \leq Z \leq 74$, who also included the contribution of resonances in an approximate way. Therefore, in Table 6 we compare our results of Υ with theirs at four common temperatures of 8.64×10^4, 1.94×10^5, 4.32×10^5 and 9.72×10^5 K. The agreement between the two sets of results is within 20%, at all temperatures, for the 1–3/4/5/6 transitions. However, differences are larger (up to $\sim$40%) for the 1–7 ($1s^2\ {}^1S_0$ – $1s2p\ {}^1P^o_1$), and for the 1–2 ($1s^2\ {}^1S_0$ – $1s2s\ {}^3S_1$) transition our values of Υ are higher by up to a factor of three, particularly towards the lower end of the temperature range. As the temperature increases the differences between the two sets of Υ decrease. It is because there are dense and large resonances very close to the threshold (see Fig. 6), which have resulted in significantly higher values of Υ at lower temperatures. Since these comparisons are limited to only six resonance transitions, we have also calculated values of Υ from our non-resonant Ω data from the FAC code. These calculations are particularly helpful in providing an estimate of the importance of resonances in the determination of excitation rates. In Table 7 we compare the two sets of Υ obtained with (DARC) and without (FAC) resonances for the resonance transitions at three temperatures of 10^4, 10^5 and 10^6 K. At the lowest temperature of 10^4 K, our resonances-resolved values of Υ are up to an order of magnitude higher for some resonance transitions, such as 1–16/26/27/28/29. For the most prominent w, x, y, and z lines, resonances have enhanced the values of Υ by a factor of seven for the z (1–2: $1s^2\ {}^1S_0$ – $1s2s\ {}^3S_1$) transition. Similar enhancements (of up to an order of magnitude) are observed for many transitions among the higher excited levels, and examples include the 3–8/12/18/32, 4–8/12/18/32, and 5–8/12/18/32 transitions. Overall, Υ values for about 80% transitions of C V differ by over 20% between those from DARC and FAC at $T_e = 10^4$ K, but only 32% transitions differ at the highest temperature of 10^6 K. Clearly the importance of resonances decreases with increasing temperature, but their contribution remains appreciable even at the highest temperature of our calculations for about a third of the transitions.

7 Conclusions

In this paper we have presented results for energy levels and radiative rates for four types of transitions (E1, E2, M1, and M2) among the lowest 49 levels of C V belonging to the $n \leq 5$ configurations. Additionally, lifetimes of all the calculated levels have been reported, although no measurements or other theoretical results are available for comparisons. However, based on a variety of comparisons among various calculations from the GRASP and FAC codes, our energy levels are assessed to be accurate to better than 1%, and the results for radiative rates, oscillator strengths, line strengths, and lifetimes are assessed to be accurate to better than 20% for a majority of strong transitions (levels). Similarly, the accuracy of our results for collision strengths and effective collision strengths is estimated to be better than 20% for a majority of the transitions. This accuracy estimate is based on the comparison made between two independent calculations performed with the DARC and FAC codes and our experience with other He-like ions [17],[18]. Additionally, we have considered a large range of partial waves in order to achieve convergence of Ω at all energies, included a wide energy range to accurately calculate the values of Υ up to $T_e = 10^6$ K, and resolved resonances in a fine energy mesh in order to account for their contributions. Hence we see no obvious deficiency in our calculated results. However, the present results for effective collision strengths for transitions involving the levels of the $n = 5$ configurations can (perhaps) be improved by the inclusion of the levels of the $n = 6$ configurations, which will give rise to additional resonances. We believe the present set of complete results for radiative and excitation rates for transitions of C V will be highly useful for the modelling and diagnostics of a variety of plasmas.

Acknowledgment

This work has been jointly financed by the Engineering and Physical Sciences and Science and Technology Facilities Councils of the United Kingdom and the NIFS/NINS project of Formation of International Network for Scientific Collaborations. FPK is grateful to AWE Aldermaston for the award of a William Penney Fellowship, and KMA will like to acknowledge the hospitality of NIFS enjoyed during a visit in February 2010 when part of this work was performed. Finally, we thank Dr. P. H. Norrington for providing his revised GRASP and DARC codes prior to publication.

References

[1] K. P. Dere, E. Landi, P. R. Young and G. Del Zanna, *Astrophys. J. Suppl.* **134** (2001) 331.

[2] A. H. Gabriel and C. Jordan, *Mon. Not. R. Astron. Soc.* **145** (1969) 241.

[3] L. W. Acton, R. C. Catura, A. J. Meyerott, C. J. Wolfson and J. L. Culhane, *Sol. Phys.* **26** (1972) 183.

[4] D. Porquet, R. Mewe, J. Dubau, A. J. J. Raassen and J. S. Kaastra, *Astron. Astrophys.* **376** (2001) 1113.

[5] J. G. Doyle, *Astron. Astrophys.* **87** (1980) 18.

[6] A. Chowdhury, R. A. Joshi, G. P. Gupta, P. A. Naik and P. D. Gupta, *Pramana - J. Phys.* **61** (2003) 1121.

[7] T. Kato, H. Funaba, K. Sato, M. Goto, B. Peterson, I. Murakami, D. Kato and N. Yamamoto, *J. Phys. Conf. Series* **163** (2009) 012101.

[8] D. H. Sampson, S. J. Goett and R. E. H. Clark, *At. Data Nucl. Data Tables* **29** (1983) 467.

[9] I. P. Grant, B. J. McKenzie, P. H. Norrington, D. F. Mayers and N. C. Pyper, *Comput. Phys. Commun.* **21** (1980) 207.

[10] M. F. Gu, *Astrophys. J.* **582** (2003) 1241.

[11] K. M. Aggarwal, K. Hamada, A. Igarashi, V. Jonauskas, F. P. Keenan and S. Nakazaki, *Astron. Astrophys.* **484** (2008) 879.

[12] D. Porquet and J. Dubau, *Astron. Astrophys. Suppl.* **143** (2000) 495.

[13] W. Eissner, M. Jones and H. Nussbaumer, *Comput. Phys. Commun.* **8** (1974) 270.

[14] A. Hibbert, *AIP Conf. Proc.* **543** (2000) 242.

[15] K. M. Aggarwal and F. P. Keenan, *Eur. Phys. J.* D **46** (2008) 205.

[16] H. Zhang and D. H. Sampson, *Astrophys. J. Suppl.* **63** (1987) 487.

[17] K. M. Aggarwal and F. P. Keenan, *Astron. Astrophys.* **489** (2008) 1377.

[18] K. M. Aggarwal, F. P. Keenan and R. F. Heeter, *Phys. Scr.* **80** (2009) 045301.

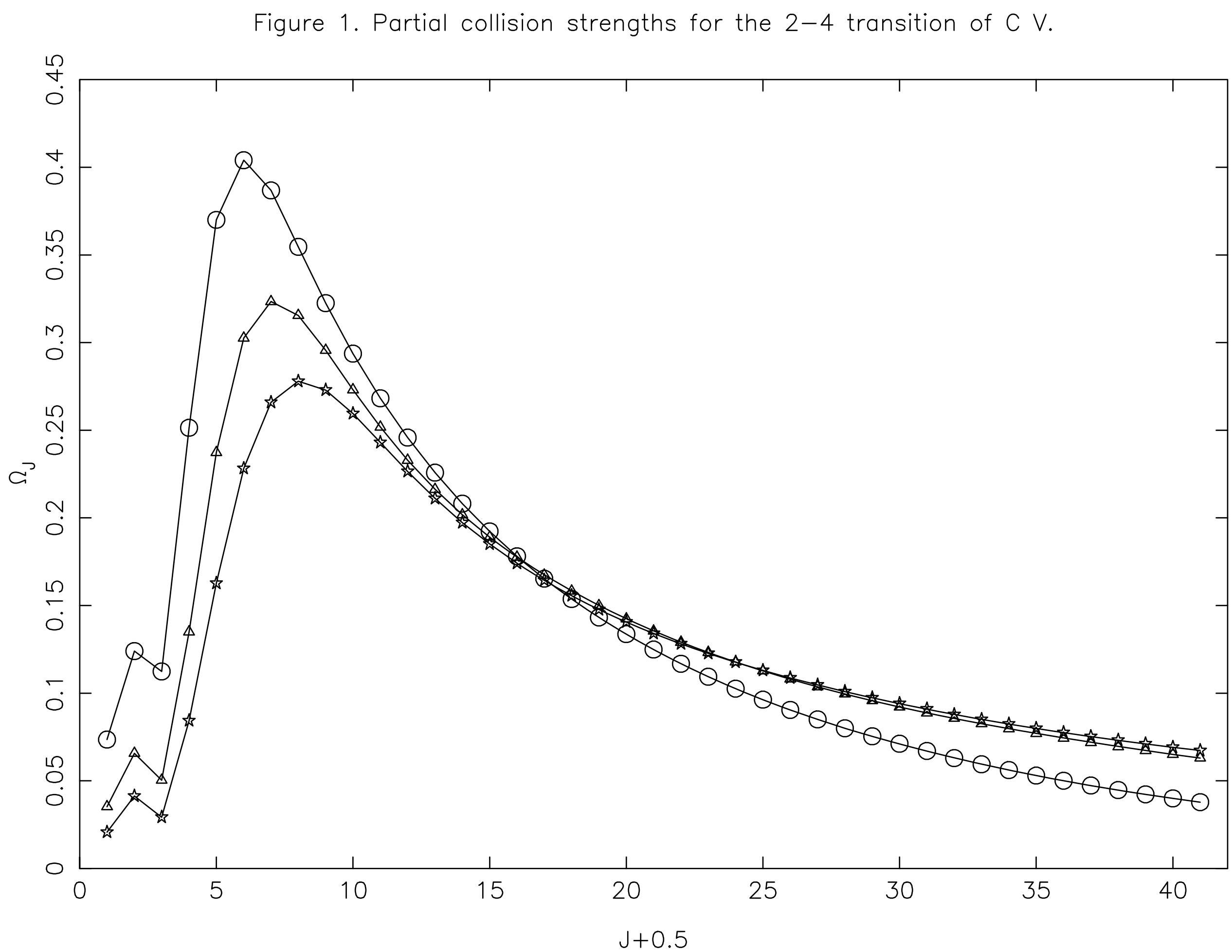

Figure 1: Partial collision strengths for the 1s2s $^3S_1$ - 1s2p $^3P_1^o$ (2-4) transition of C V, at three energies of: 30 Ryd (circles), 40 Ryd (triangles), and 50 Ryd (stars).

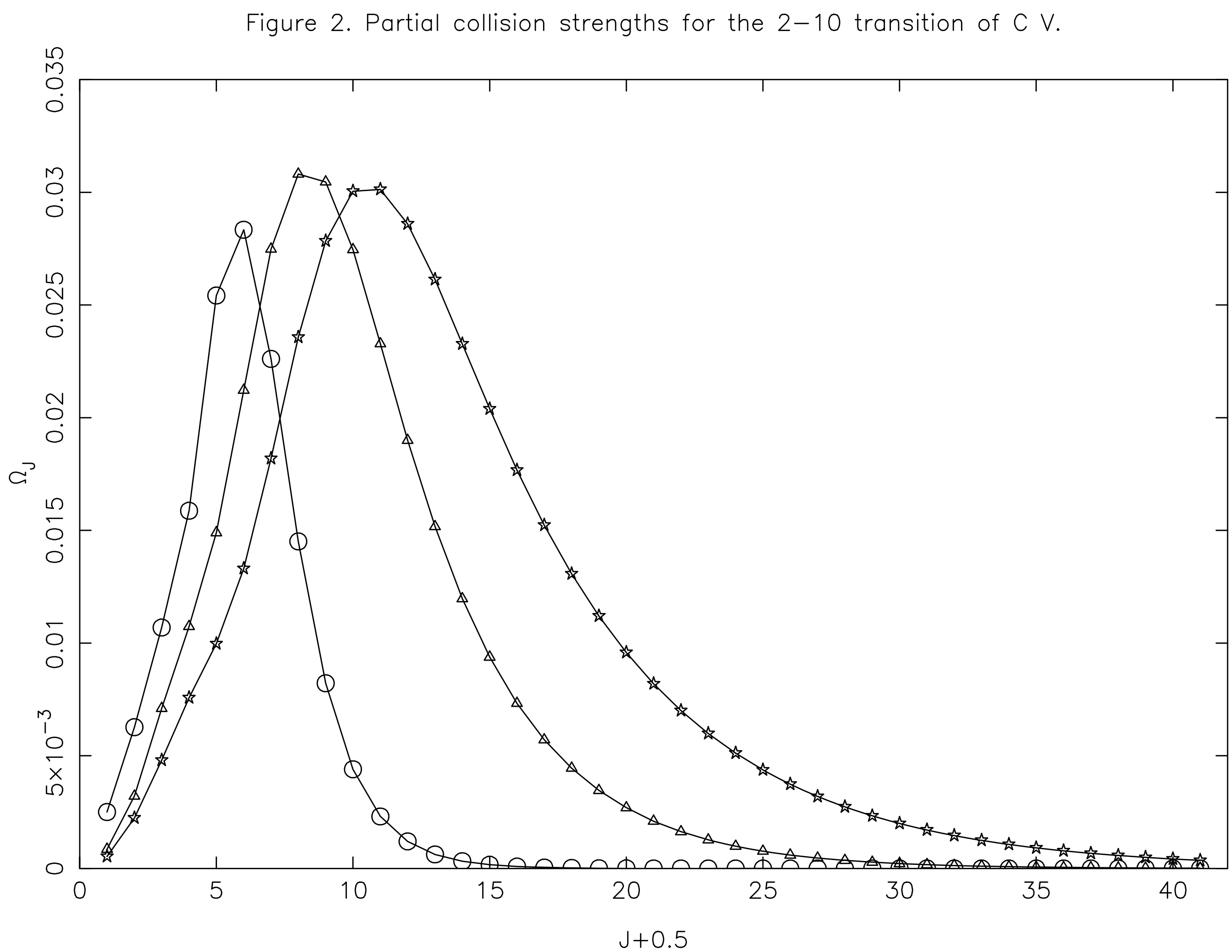

Figure 2: Partial collision strengths for the 1s2s $^3S_1$ - 1s3p $^3P_1^o$ (2-10) transition of C V, at three energies of: 30 Ryd (circles), 40 Ryd (triangles), and 50 Ryd (stars).

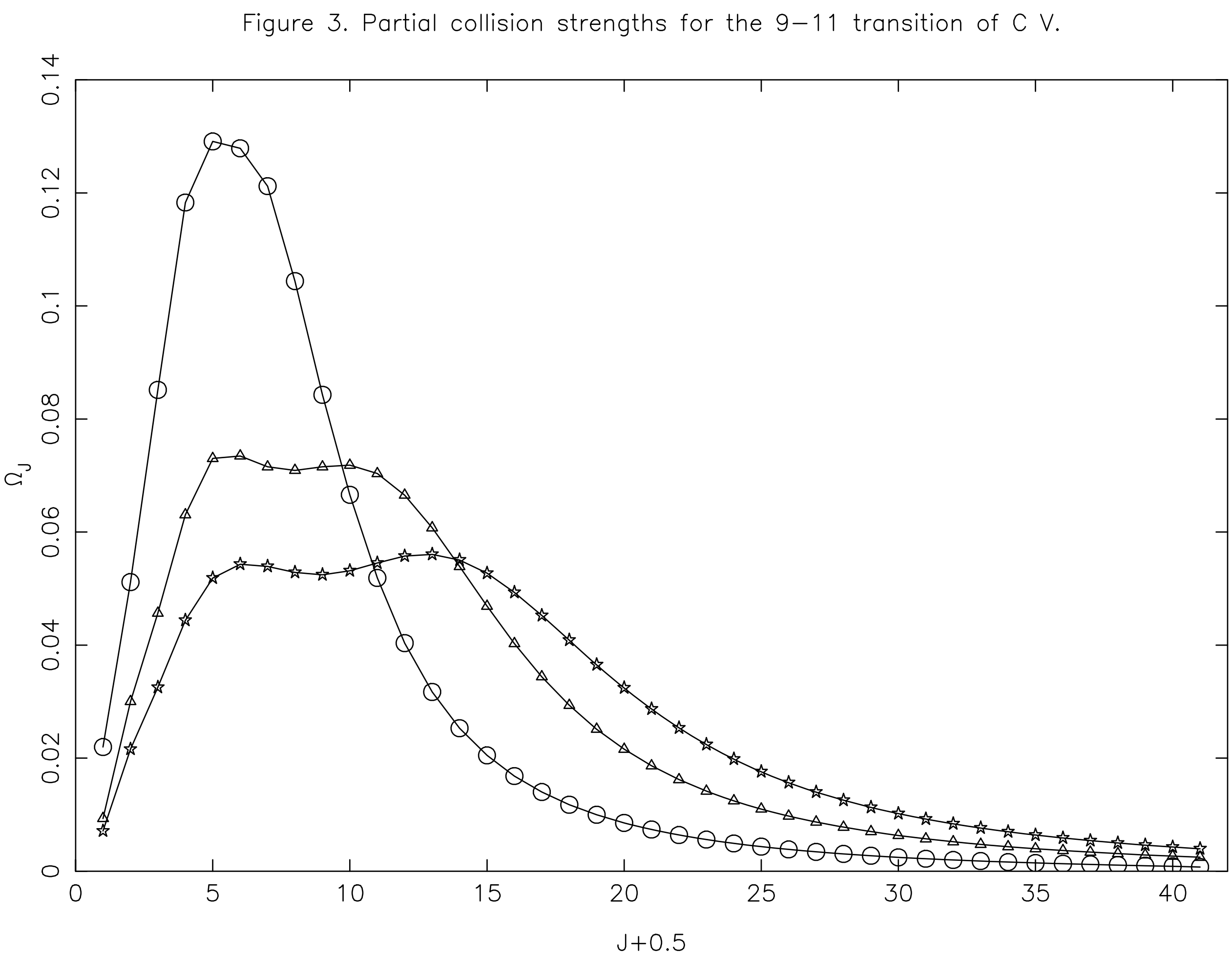

Figure 3: Partial collision strengths for the 1s3p $^3P^o_0$ - 1s3p $^3P^o_2$ (9-11) transition of C V, at three energies of: 30 Ryd (circles), 40 Ryd (triangles), and 50 Ryd (stars).

Figure 4. Comparison of collision strengths for the 2−5, 4−14, and 10−24 allowed transitions of C V.

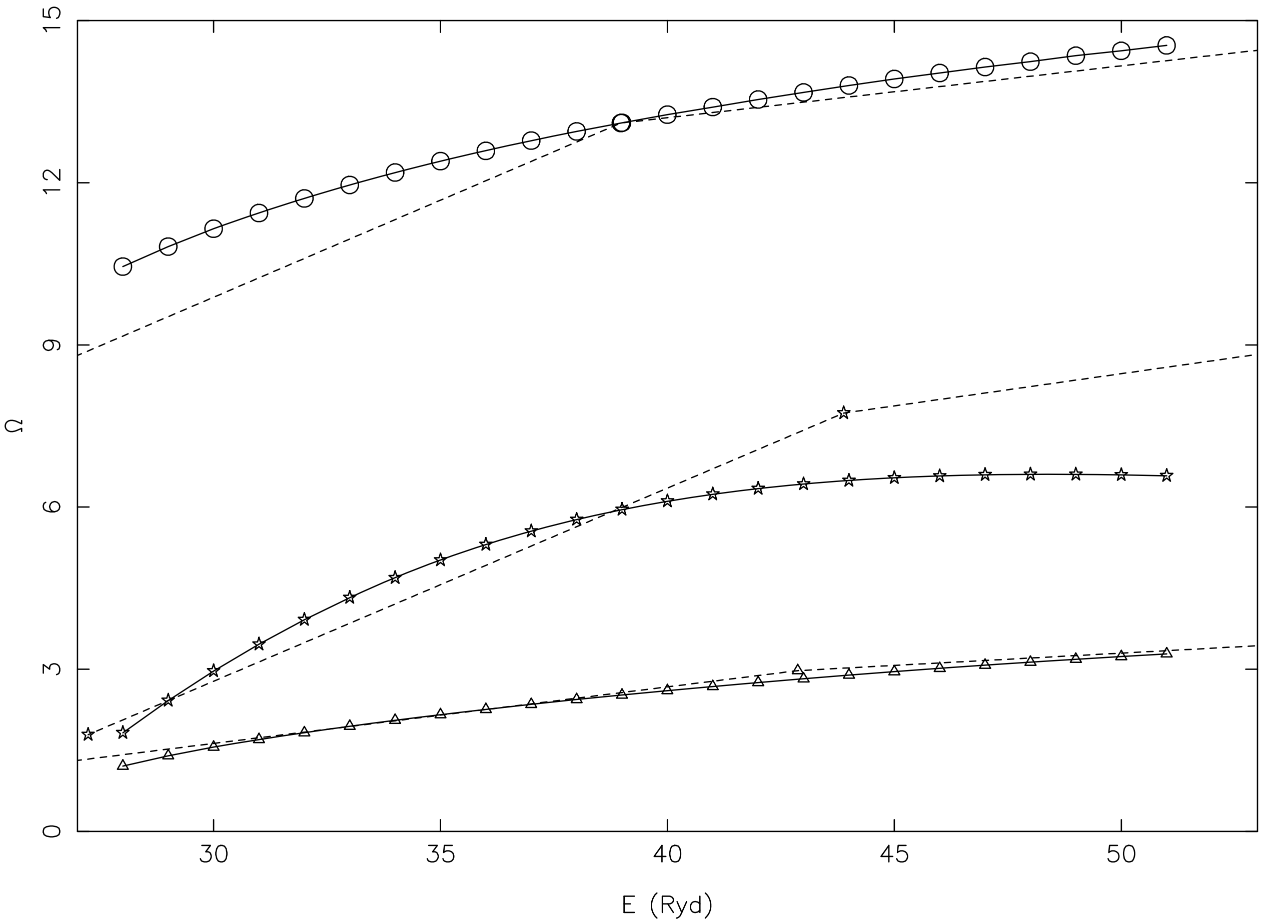

Figure 4: Comparison of collision strengths from our calculations from DARC (continuous curves) and FAC (broken curves) for the 2-5 (circles: 1s2s $^3S_1$ - 1s2p $^3P^o_2$), 4-14 (triangles: 1s2p $^3P^o_1$ - 1s3d $^3D_2$), and 10-24 (stars: 1s3p $^3P^o_1$ - 1s4d $^3D_2$) allowed transitions of C V.

Figure 5. Comparison of collision strengths for the 2–8, 2–15, and 4–10 forbidden transitions of C V.

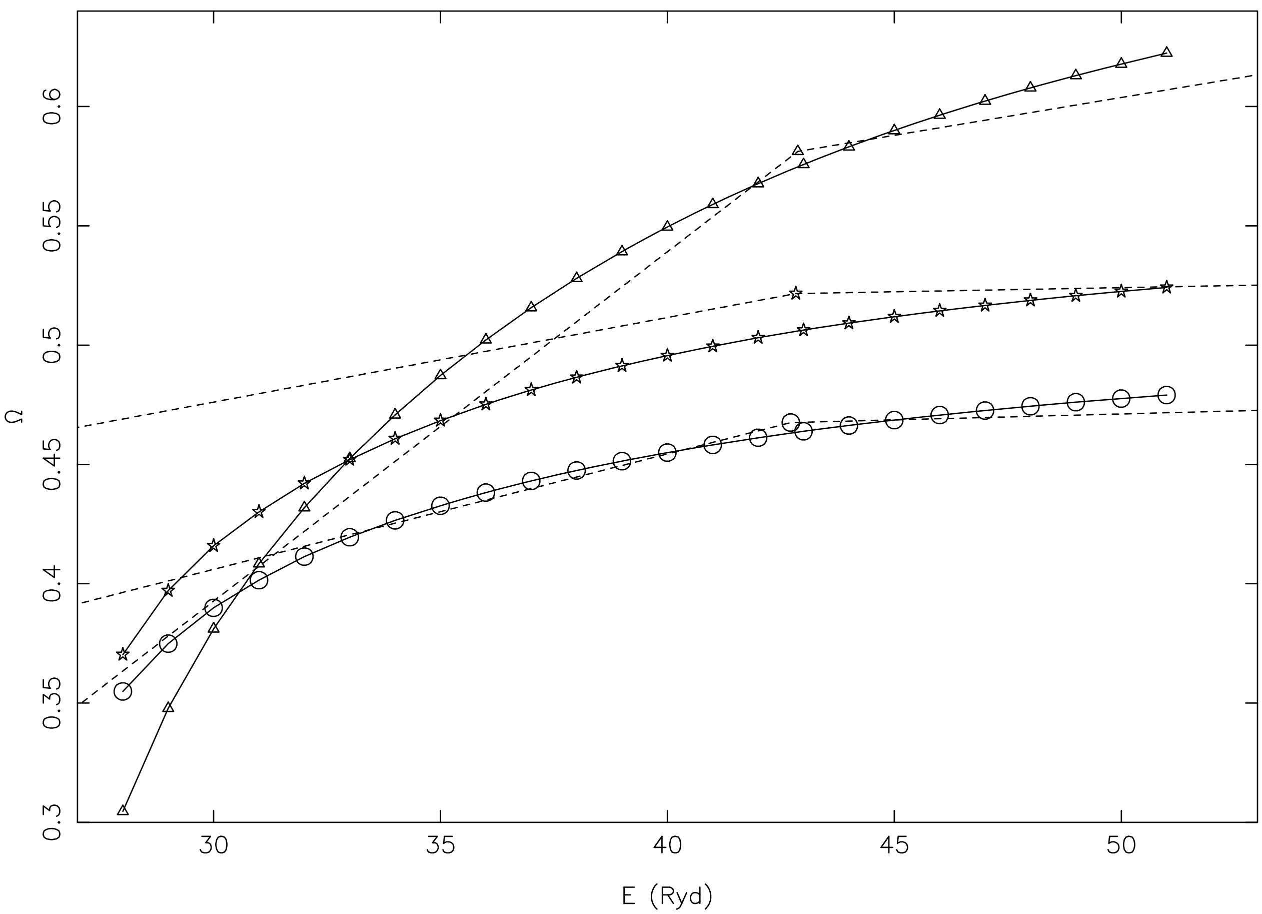

Figure 5: Comparison of collision strengths from our calculations from DARC (continuous curves) and FAC (broken curves) for the 2-8 (circles: 1s2s $^3S_1$ - 1s3s $^3S_1$), 2-15 (triangles: 1s2s $^3S_1$ - 1s3d $^3D_3$), and 4-10 (stars: 1s2p $^3P^o_1$ - 1s3p $^3P^o_1$) forbidden transitions of C V.

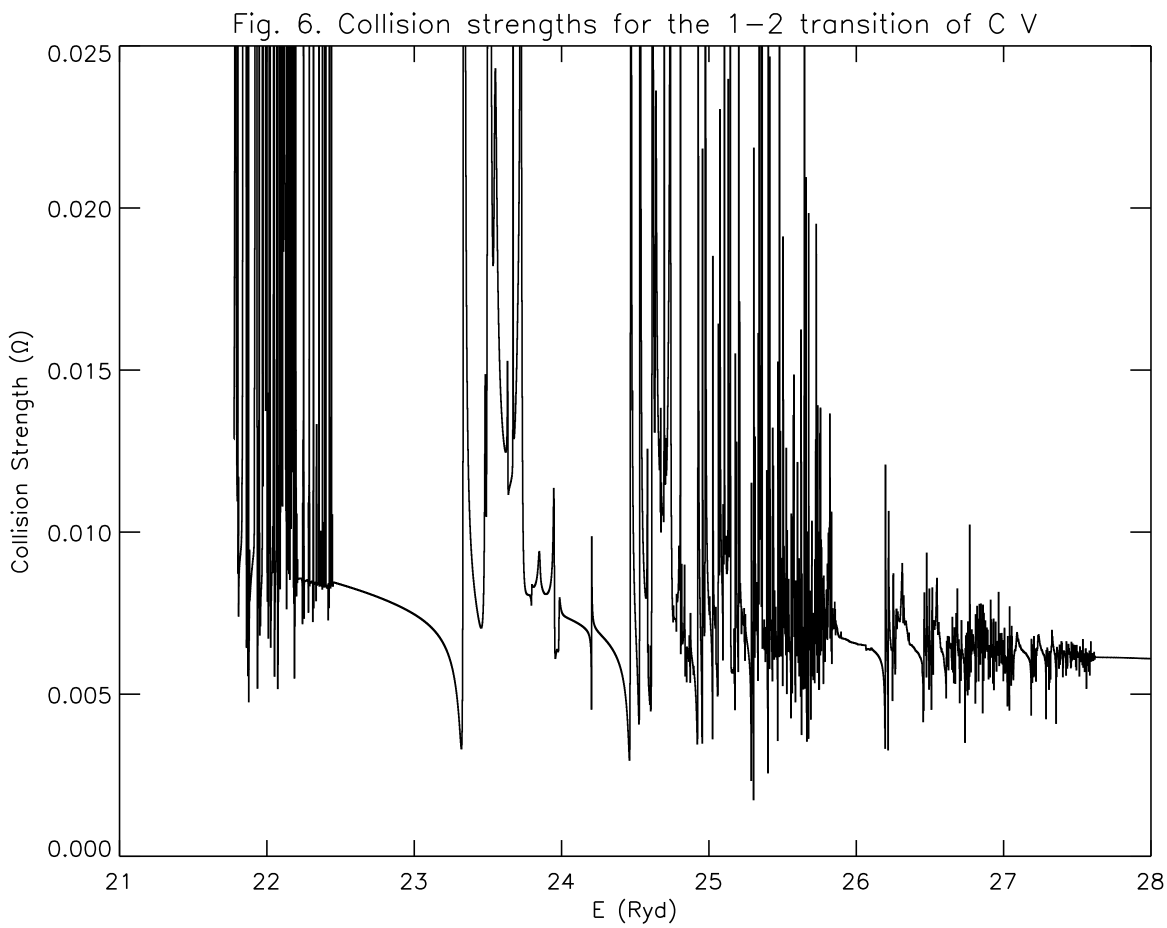

Figure 6: Collision strengths for the $1s^2\ ^1S_0$ - $1s2s\ ^3S_1$ (1-2) transition of C V.

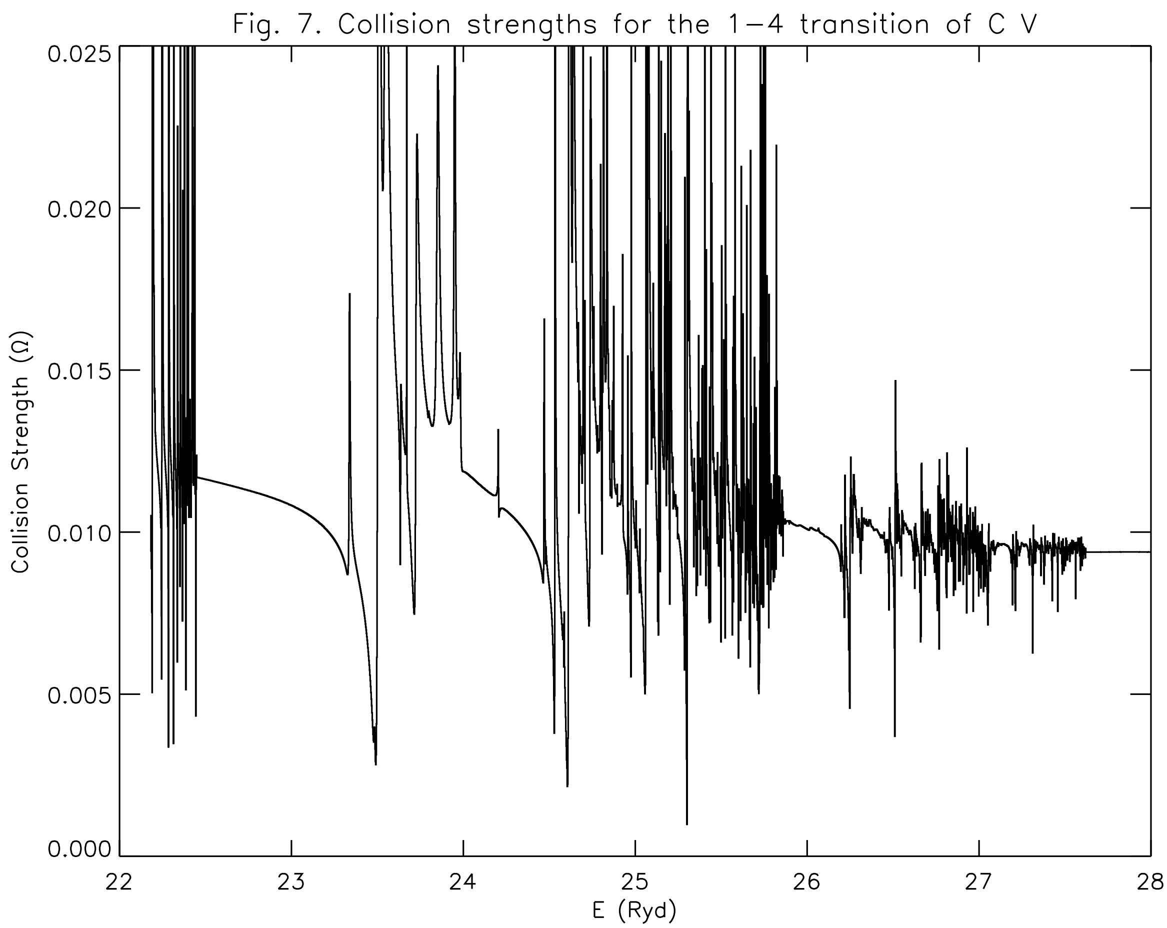

Figure 7: Collision strengths for the $1s^2\ ^1S_0$ - $1s2p\ ^3P^o_1$ (1-4) transition of C V.

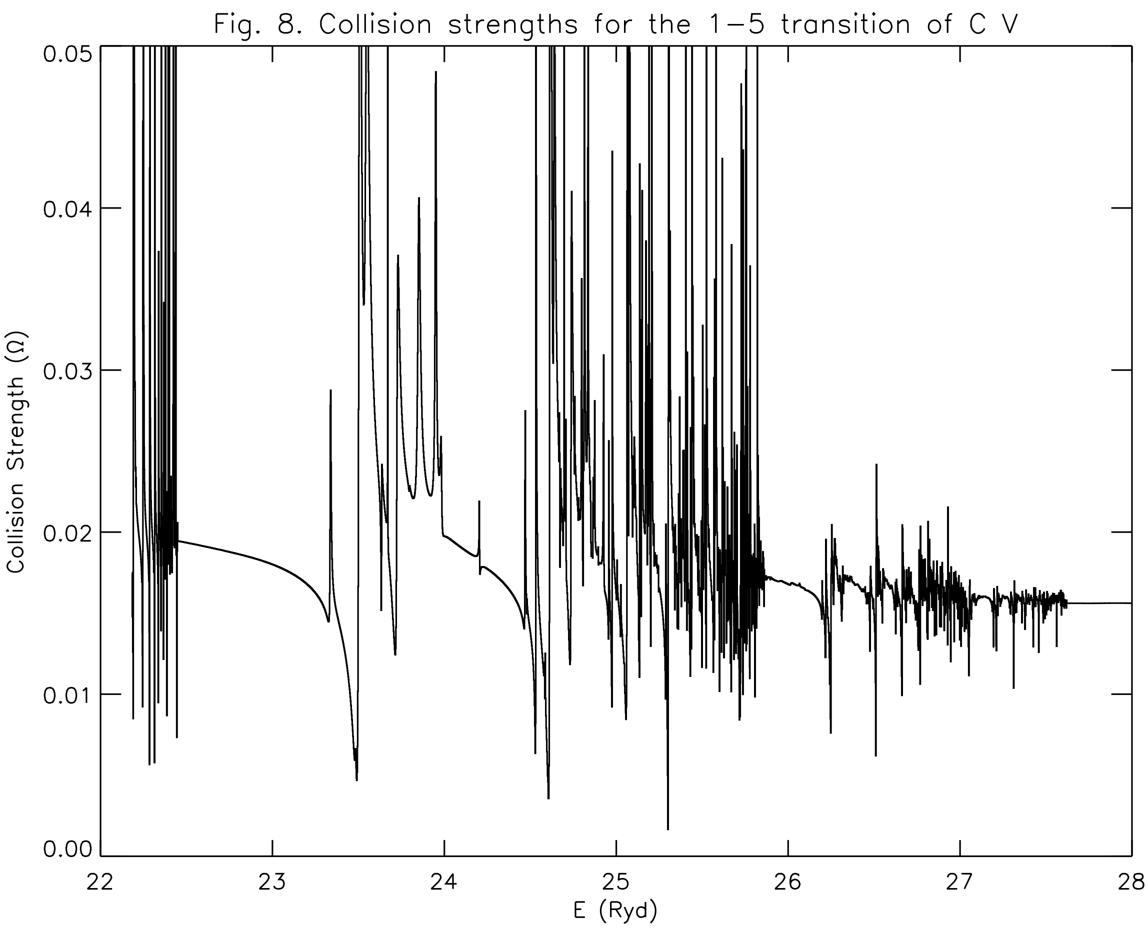

Figure 8: Collision strengths for the $1s^2\ ^1S_0$ - $1s2p\ ^3P^o_2$ (1-5) transition of C V.

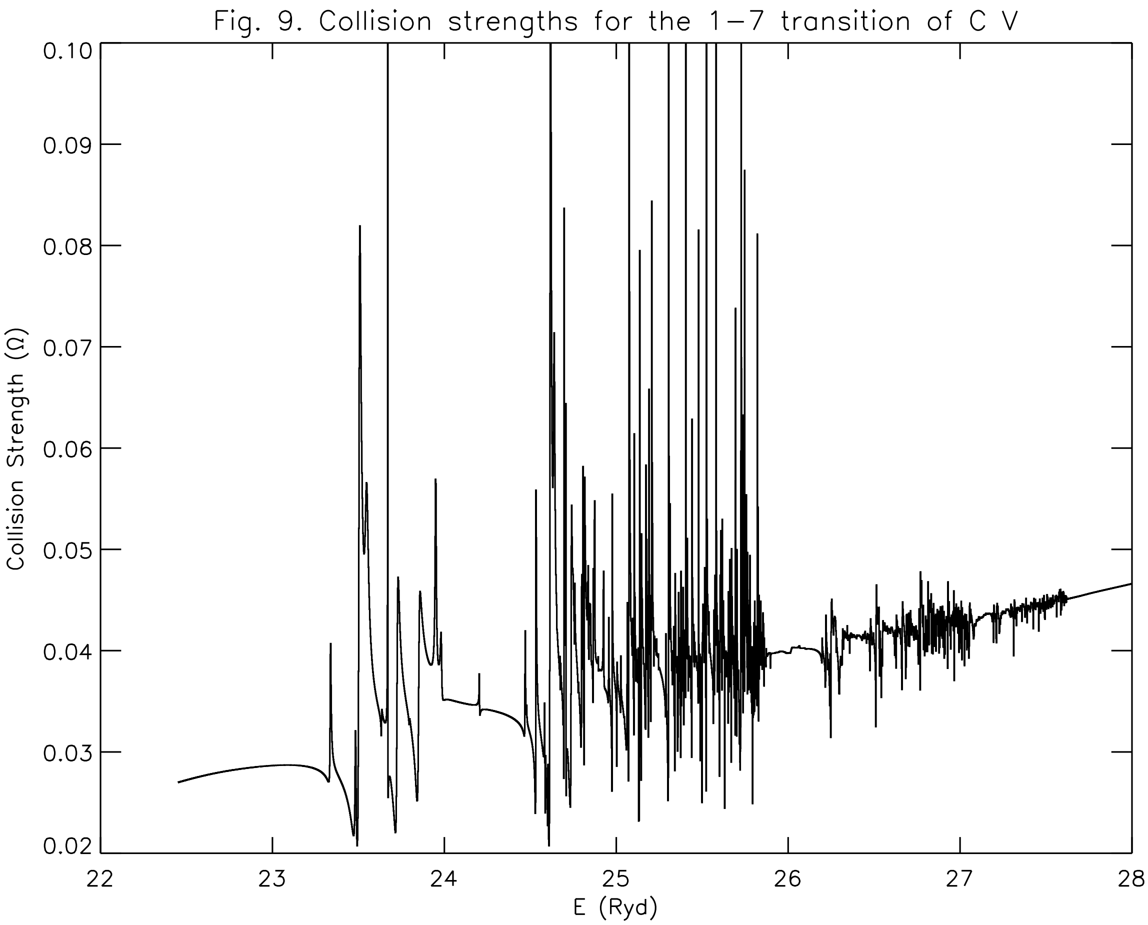

Figure 9: Collision strengths for the $1s^2\ ^1S_0$ - $1s2p\ ^1P^o_1$ (1-7) transition of C V.

Table 1: Energy levels (in Ryd) of C V and their lifetimes (τ, s). $a{\pm}b \equiv a{\times}10^{\pm b}$.

Index	Configuration/Level		NIST	GRASP1	GRASP2	FAC1	FAC2	τ (s)
1	$1s^2$	$^1S_0$	0.00000	0.00000	0.00000	0.00000	0.00000	.....
2	1s2s	$^3S_1$	21.97312	21.77571	21.76878	21.88477	21.88453	2.390-02
3	1s2p	$^3P^o_0$	22.37315	22.18028	22.17464	22.31951	22.31938	1.660-08
4	1s2p	$^3P^o_1$	22.37304	22.18109	22.17451	22.31936	22.31924	1.137-08
5	1s2p	$^3P^o_2$	22.37428	22.18273	22.17573	22.32047	22.32034	1.645-08
6	1s2s	$^1S_0$	22.37184	22.20944	22.20344	22.33293	22.33268	5.704-01
7	1s2p	$^1P^o_1$	22.63016	22.44973	22.44251	22.61483	22.61471	1.047-12
8	1s3s	$^3S_1$	25.87610	25.67483	25.66778	25.79924	25.79908	1.579-10
9	1s3p	$^3P^o_0$	25.98394	25.78365	25.77695	25.91049	25.91041	7.605-11
10	1s3p	$^3P^o_1$	25.98392	25.78389	25.77694	25.91050	25.91041	7.601-11
11	1s3p	$^3P^o_2$	25.98429	25.78437	25.77730	25.91086	25.91077	7.614-11
12	1s3s	$^1S_0$	25.98186	25.79391	25.78716	25.91487	25.91468	1.577-10
13	1s3d	$^3D_1$	26.03769	25.83547	25.82845	25.95381	25.95381	2.362-11
14	1s3d	$^3D_2$	26.03769	25.83555	25.82846	25.95381	25.95381	2.362-11
15	1s3d	$^3D_3$	26.03780	25.83568	25.82857	25.95391	25.95391	2.363-11
16	1s3d	$^1D_2$	26.03973	25.83807	25.83098	25.95716	25.95716	2.521-11
17	1s3p	$^1P^o_1$	26.05648	25.86161	25.85449	25.99178	25.99167	3.001-12
18	1s4s	$^3S_1$	27.18806	26.98592	26.97885	27.10247	27.10233	2.565-10
19	1s4p	$^3P^o_0$	27.23193	27.03024	27.02331	27.14077	27.14070	1.316-10
20	1s4p	$^3P^o_1$	27.23193	27.03034	27.02331	27.14079	27.14070	1.315-10
21	1s4p	$^3P^o_2$	27.23207	27.03054	27.02346	27.14095	27.14087	1.318-10
22	1s4s	$^1S_0$	27.23090	27.03580	27.02887	27.14910	27.14889	1.920-10
23	1s4d	$^3D_1$	27.25396	27.05162	27.04456	27.17316	27.17316	5.480-11
24	1s4d	$^3D_2$	27.25396	27.05165	27.04457	27.17316	27.17316	5.482-11
25	1s4d	$^3D_3$	27.25420	27.05171	27.04461	27.17319	27.17319	5.483-11
26	1s4f	$^3F^o_2$	27.25530	27.05260	27.04553	27.16645	27.16645	1.158-10
27	1s4f	$^3F^o_3$	27.25530	27.05261	27.04551	27.16644	27.16644	1.159-10
28	1s4f	$^3F^o_4$	27.25530	27.05265	27.04555	27.16647	27.16647	1.158-10
29	1s4f	$^1F^o_3$	27.25530	27.05266	27.04558	27.16650	27.16650	1.160-10
30	1s4d	$^1D_2$	27.25536	27.05304	27.04595	27.17497	27.17497	5.797-11
31	1s4p	$^1P^o_1$	27.26203	27.06321	27.05611	27.17424	27.17413	5.522-12
32	1s5s	$^3S_1$	27.78392	27.58151	27.57443	27.69462	27.69442	4.886-10
33	1s5p	$^3P^o_0$	27.80578	27.60378	27.59677	27.71331	27.71320	2.479-10
34	1s5p	$^3P^o_1$	27.80578	27.60384	27.59678	27.71332	27.71321	2.477-10
35	1s5p	$^3P^o_2$	27.80607	27.60394	27.59685	27.71340	27.71329	2.483-10
36	1s5s	$^1S_0$	27.80531	27.60786	27.60086	27.71812	27.71780	1.877-10
37	1s5d	$^3D_1$	28.81724	27.61458	27.60751	27.73519	27.73519	1.086-10
38	1s5d	$^3D_2$	27.81724	27.61460	27.60751	27.73519	27.73518	1.086-10
39	1s5d	$^3D_3$	27.81727	27.61463	27.60753	27.73520	27.73520	1.087-10
40	1s5f	$^3F^o_2$	27.81782	27.61513	27.60805	27.72869	27.72869	2.240-10
41	1s5f	$^3F^o_3$	27.81782	27.61514	27.60805	27.72868	27.72868	2.241-10
42	1s5f	$^3F^o_4$	27.81782	27.61515	27.60806	27.72870	27.72870	2.240-10
43	1s5g	$^3G_3$	27.81788	27.61516	27.60808	27.72866	27.72866	3.758-10
44	1s5g	$^3G_4$	27.81788	27.61516	27.60807	27.72865	27.72865	3.758-10
45	1s5f	$^1F^o_3$	27.81783	27.61516	27.60808	27.72872	27.72872	2.242-10
46	1s5g	$^3G_5$	27.81788	27.61518	27.60809	27.72866	27.72866	3.759-10
47	1s5g	$^1G_4$	27.81788	27.61518	27.60809	27.72867	27.72867	3.759-10
48	1s5d	$^1D_2$	27.81797	27.61538	27.60829	27.73620	27.73620	9.900-11
49	1s5p	$^1P^o_1$	27.82138	27.62104	27.61395	27.73030	27.73014	6.201-12

NIST: `http://physics.nist.gov/PhysRefData`

GRASP1: Energies from the GRASP code with 49 level calculations *without* Breit and QED effects

GRASP2: Energies from the GRASP code with 49 level calculations *with* Breit and QED effects

FAC1: Energies from the FAC code with 49 level calculations

FAC2: Energies from the FAC code with 71 level calculations

Table 2: Transition wavelengths (λ_{ij} in $\AA$), radiative rates (A_{ji} in s^{-1}), oscillator strengths (f_{ij}, dimensionless), and line strengths (S, in atomic units) for electric dipole (E1), and A_{ji} for E2, M1 and M2 transitions of C V. ($a{\pm}b \equiv a{\times}10^{\pm b}$).

i	j	λ_{ij}	A^{E1}_{ji}	f^{E1}_{ij}	S^{E1}	A^{E2}_{ji}	A^{M1}_{ji}	A^{M2}_{ji}
1	2	4.186+01	0.000+00	0.000+00	0.000+00	0.000+00	4.185+01	0.000+00
1	4	4.110+01	2.776+07	2.109−05	2.853−06	0.000+00	0.000+00	0.000+00
1	5	4.110+01	0.000+00	0.000+00	0.000+00	0.000+00	0.000+00	2.546+04
1	7	4.061+01	9.550+11	7.081−01	9.466−02	0.000+00	0.000+00	0.000+00
1	8	3.550+01	0.000+00	0.000+00	0.000+00	0.000+00	8.823+00	0.000+00
1	10	3.535+01	8.978+06	5.047−06	5.873−07	0.000+00	0.000+00	0.000+00
1	11	3.535+01	0.000+00	0.000+00	0.000+00	0.000+00	0.000+00	1.010+04
1	13	3.528+01	0.000+00	0.000+00	0.000+00	0.000+00	2.622−01	0.000+00
1	14	3.528+01	0.000+00	0.000+00	0.000+00	3.817+04	0.000+00	0.000+00
1	16	3.528+01	0.000+00	0.000+00	0.000+00	1.209+07	0.000+00	0.000+00
1	17	3.525+01	3.196+11	1.786−01	2.072−02	0.000+00	0.000+00	0.000+00
1	18	3.378+01	0.000+00	0.000+00	0.000+00	0.000+00	1.008+00	0.000+00
1	20	3.372+01	4.632+06	2.369−06	2.630−07	0.000+00	0.000+00	0.000+00
1	21	3.372+01	0.000+00	0.000+00	0.000+00	0.000+00	0.000+00	5.571+03
1	23	3.370+01	0.000+00	0.000+00	0.000+00	0.000+00	8.171−01	0.000+00
1	24	3.370+01	0.000+00	0.000+00	0.000+00	2.224+02	0.000+00	0.000+00
1	26	3.369+01	0.000+00	0.000+00	0.000+00	0.000+00	0.000+00	3.885−04
1	30	3.369+01	0.000+00	0.000+00	0.000+00	1.091+05	0.000+00	0.000+00
1	31	3.368+01	1.719+11	8.771−02	9.726−03	0.000+00	0.000+00	0.000+00
1	32	3.305+01	0.000+00	0.000+00	0.000+00	0.000+00	1.912+02	0.000+00
1	34	3.302+01	3.771+06	1.849−06	2.010−07	0.000+00	0.000+00	0.000+00
1	35	3.302+01	0.000+00	0.000+00	0.000+00	0.000+00	0.000+00	4.820+03
1	37	3.301+01	0.000+00	0.000+00	0.000+00	0.000+00	1.154+01	0.000+00
1	38	3.301+01	0.000+00	0.000+00	0.000+00	3.859+05	0.000+00	0.000+00
1	40	3.301+01	0.000+00	0.000+00	0.000+00	0.000+00	0.000+00	1.228−01
1	48	3.301+01	0.000+00	0.000+00	0.000+00	2.509+08	0.000+00	0.000+00
1	49	3.300+01	1.536+11	7.523−02	8.174−03	0.000+00	0.000+00	0.000+00
2	3	2.245+03	6.023+07	1.517−02	3.365−01	0.000+00	0.000+00	0.000+00
2	4	2.246+03	6.018+07	4.551−02	1.010+00	0.000+00	0.000+00	4.325−04
2	5	2.239+03	6.075+07	7.611−02	1.683+00	0.000+00	0.000+00	8.023−04
2	6	2.097+03	0.000+00	0.000+00	0.000+00	0.000+00	2.246−03	0.000+00
2	7	1.353+03	8.011+03	2.197−06	2.935−05	0.000+00	0.000+00	1.171−02
2	8	2.337+02	0.000+00	0.000+00	0.000+00	4.212−03	1.706−02	0.000+00
2	9	2.274+02	1.314+10	3.394−02	7.622−02	0.000+00	0.000+00	0.000+00
2	10	2.274+02	1.314+10	1.018−01	2.286−01	0.000+00	0.000+00	9.211+00
2	11	2.273+02	1.313+10	1.695−01	3.806−01	0.000+00	0.000+00	1.682+01
2	12	2.268+02	0.000+00	0.000+00	0.000+00	0.000+00	1.192−02	0.000+00
2	13	2.245+02	0.000+00	0.000+00	0.000+00	1.216+06	3.677−03	0.000+00
2	14	2.245+02	0.000+00	0.000+00	0.000+00	1.212+06	2.943−04	0.000+00
2	15	2.245+02	0.000+00	0.000+00	0.000+00	1.216+06	0.000+00	0.000+00
2	16	2.243+02	0.000+00	0.000+00	0.000+00	3.818+03	6.390−04	0.000+00
2	17	2.231+02	2.998+05	2.236−06	4.925−06	0.000+00	0.000+00	1.642+01
2	18	1.749+02	0.000+00	0.000+00	0.000+00	2.328−04	1.472−02	0.000+00
2	19	1.734+02	5.688+09	8.549−03	1.464−02	0.000+00	0.000+00	0.000+00
2	20	1.734+02	5.687+09	2.564−02	4.392−02	0.000+00	0.000+00	6.848+00
2	21	1.734+02	5.682+09	4.270−02	7.313−02	0.000+00	0.000+00	1.251+01
2	22	1.732+02	0.000+00	0.000+00	0.000+00	0.000+00	1.599−02	0.000+00
2	23	1.727+02	0.000+00	0.000+00	0.000+00	1.954+05	2.263−03	0.000+00
2	24	1.727+02	0.000+00	0.000+00	0.000+00	1.951+05	1.838−04	0.000+00
2	25	1.727+02	0.000+00	0.000+00	0.000+00	1.955+05	0.000+00	0.000+00

Table 2: Transition wavelengths (λ_{ij} in Å), radiative rates (A_{ji} in s^{-1}), oscillator strengths (f_{ij}, dimensionless), and line strengths (S, in atomic units) for electric dipole (E1), and A_{ji} for E2, M1, and M2 transitions of C V. ($a{\pm}b \equiv a{\times}10^{\pm b}$).

i	j	λ_{ij}	A^{E1}_{ji}	f^{E1}_{ij}	S^{E1}	A^{E2}_{ji}	A^{M1}_{ij}	A^{M2}_{ji}
2	26	1.727+02	8.065−03	6.010−14	1.025−13	0.000+00	0.000+00	2.257−08
2	27	1.727+02	0.000+00	0.000+00	0.000+00	0.000+00	0.000+00	3.246−08
2	29	1.727+02	0.000+00	0.000+00	0.000+00	0.000+00	0.000+00	7.056−09
2	30	1.727+02	0.000+00	0.000+00	0.000+00	3.667+02	4.092−04	0.000+00
2	31	1.724+02	1.378+05	6.137−07	1.045−06	0.000+00	0.000+00	1.355+01
2	32	1.570+02	0.000+00	0.000+00	0.000+00	5.862−02	1.601−02	0.000+00
2	33	1.564+02	2.556+09	3.122−03	4.822−03	0.000+00	0.000+00	0.000+00
2	34	1.564+02	2.555+09	9.366−03	1.446−02	0.000+00	0.000+00	3.782+00
2	35	1.564+02	2.552+09	1.559−02	2.407−02	0.000+00	0.000+00	6.912+00
2	36	1.563+02	0.000+00	0.000+00	0.000+00	0.000+00	2.380−02	0.000+00
2	37	1.561+02	0.000+00	0.000+00	0.000+00	1.314+04	1.561−03	0.000+00
2	38	1.561+02	0.000+00	0.000+00	0.000+00	1.318+04	2.167−04	0.000+00
2	39	1.561+02	0.000+00	0.000+00	0.000+00	1.318+04	0.000+00	0.000+00
2	40	1.561+02	2.228+00	1.356−11	2.089−11	0.000+00	0.000+00	7.485−09
2	41	1.561+02	0.000+00	0.000+00	0.000+00	0.000+00	0.000+00	6.625−12
2	43	1.561+02	0.000+00	0.000+00	0.000+00	2.056−03	0.000+00	0.000+00
2	45	1.561+02	0.000+00	0.000+00	0.000+00	0.000+00	0.000+00	1.814−10
2	48	1.561+02	0.000+00	0.000+00	0.000+00	2.102+01	3.553−04	0.000+00
2	49	1.559+02	6.040+04	2.201−07	3.389−07	0.000+00	0.000+00	8.501+00
3	5	8.400+05	0.000+00	0.000+00	0.000+00	2.716−13	0.000+00	0.000+00
3	7	3.402+03	0.000+00	0.000+00	0.000+00	0.000+00	1.403−02	0.000+00
3	8	2.609+02	7.044+08	2.156−02	1.852−02	0.000+00	0.000+00	0.000+00
3	10	2.530+02	0.000+00	0.000+00	0.000+00	0.000+00	4.866−05	0.000+00
3	11	2.529+02	0.000+00	0.000+00	0.000+00	7.885+04	0.000+00	0.000+00
3	13	2.494+02	2.352+10	6.580−01	5.403−01	0.000+00	0.000+00	0.000+00
3	14	2.494+02	0.000+00	0.000+00	0.000+00	0.000+00	0.000+00	1.239+00
3	16	2.492+02	0.000+00	0.000+00	0.000+00	0.000+00	0.000+00	1.047+01
3	17	2.476+02	0.000+00	0.000+00	0.000+00	0.000+00	3.467−02	0.000+00
3	18	1.897+02	2.402+08	3.887−03	2.427−03	0.000+00	0.000+00	0.000+00
3	20	1.879+02	0.000+00	0.000+00	0.000+00	0.000+00	8.412−05	0.000+00
3	21	1.879+02	0.000+00	0.000+00	0.000+00	2.891+04	0.000+00	0.000+00
3	23	1.871+02	7.748+09	1.220−01	7.517−02	0.000+00	0.000+00	0.000+00
3	24	1.871+02	0.000+00	0.000+00	0.000+00	0.000+00	0.000+00	7.800−01
3	26	1.871+02	0.000+00	0.000+00	0.000+00	4.576+05	0.000+00	0.000+00
3	30	1.871+02	0.000+00	0.000+00	0.000+00	0.000+00	0.000+00	6.102+00
3	31	1.867+02	0.000+00	0.000+00	0.000+00	0.000+00	1.814−02	0.000+00
3	32	1.688+02	8.302+07	1.063−03	5.908−04	0.000+00	0.000+00	0.000+00
3	34	1.681+02	0.000+00	0.000+00	0.000+00	0.000+00	5.647−06	0.000+00
3	35	1.681+02	0.000+00	0.000+00	0.000+00	2.368+03	0.000+00	0.000+00
3	37	1.677+02	3.444+09	4.358−02	2.407−02	0.000+00	0.000+00	0.000+00
3	38	1.677+02	0.000+00	0.000+00	0.000+00	0.000+00	0.000+00	4.412−01
3	40	1.677+02	0.000+00	0.000+00	0.000+00	3.528+05	0.000+00	0.000+00
3	48	1.677+02	0.000+00	0.000+00	0.000+00	0.000+00	0.000+00	3.389+00
3	49	1.675+02	0.000+00	0.000+00	0.000+00	0.000+00	9.976−03	0.000+00
4	5	7.493+05	0.000+00	0.000+00	0.000+00	1.082−12	3.202−05	0.000+00
4	6	3.150+04	1.751+00	8.681−08	2.701−05	0.000+00	0.000+00	0.000+00
4	7	3.400+03	0.000+00	0.000+00	0.000+00	8.246−05	1.231−02	0.000+00
4	8	2.609+02	2.109+09	2.152−02	5.544−02	0.000+00	0.000+00	1.123+00
4	9	2.530+02	0.000+00	0.000+00	0.000+00	0.000+00	2.239−03	0.000+00
4	10	2.530+02	0.000+00	0.000+00	0.000+00	9.856+04	1.584−02	0.000+00

Table 2: Transition wavelengths (λ_{ij} in $\mathring{A}$), radiative rates (A_{ji} in s^{-1}), oscillator strengths (f_{ij}, dimensionless), and line strengths (S, in atomic units) for electric dipole (E1), and A_{ji} for E2, M1, and M2 transitions of C V. ($a{\pm}b \equiv a{\times}10^{\pm b}$).

i	j	λ_{ij}	A^{E1}_{ji}	f^{E1}_{ij}	S^{E1}	A^{E2}_{ji}	A^{M1}_{ij}	A^{M2}_{ji}
4	11	2.529+02	0.000+00	0.000+00	0.000+00	1.774+05	2.637−02	0.000+00
4	12	2.523+02	1.271+05	4.043−07	1.007−06	0.000+00	0.000+00	0.000+00
4	13	2.494+02	1.764+10	1.645−01	4.052−01	0.000+00	0.000+00	1.682+00
4	14	2.494+02	3.168+10	4.923−01	1.212+00	0.000+00	0.000+00	2.383+01
4	15	2.494+02	0.000+00	0.000+00	0.000+00	0.000+00	0.000+00	1.745+00
4	16	2.492+02	7.917+07	1.229−03	3.024−03	0.000+00	0.000+00	2.510+01
4	17	2.476+02	0.000+00	0.000+00	0.000+00	2.458+01	2.394−02	0.000+00
4	18	1.897+02	7.182+08	3.874−03	7.257−03	0.000+00	0.000+00	7.212−01
4	19	1.879+02	0.000+00	0.000+00	0.000+00	0.000+00	1.041−03	0.000+00
4	20	1.879+02	0.000+00	0.000+00	0.000+00	3.606+04	1.250−02	0.000+00
4	21	1.879+02	0.000+00	0.000+00	0.000+00	6.493+04	1.474−02	0.000+00
4	22	1.877+02	7.101+04	1.250−07	2.318−07	0.000+00	0.000+00	0.000+00
4	23	1.871+02	5.811+09	3.050−02	5.637−02	0.000+00	0.000+00	9.840−01
4	24	1.871+02	1.044+10	9.138−02	1.689−01	0.000+00	0.000+00	1.431+01
4	25	1.871+02	0.000+00	0.000+00	0.000+00	0.000+00	0.000+00	1.021+00
4	26	1.871+02	0.000+00	0.000+00	0.000+00	4.576+05	1.839−04	0.000+00
4	27	1.871+02	0.000+00	0.000+00	0.000+00	4.347+05	0.000+00	0.000+00
4	29	1.871+02	0.000+00	0.000+00	0.000+00	2.190+05	0.000+00	0.000+00
4	30	1.871+02	1.429+07	1.249−04	2.308−04	0.000+00	0.000+00	1.439+01
4	31	1.867+02	0.000+00	0.000+00	0.000+00	1.311+01	1.127−02	0.000+00
4	32	1.688+02	2.472+08	1.055−03	1.759−03	0.000+00	0.000+00	3.106−01
4	33	1.681+02	0.000+00	0.000+00	0.000+00	0.000+00	1.113−04	0.000+00
4	34	1.681+02	0.000+00	0.000+00	0.000+00	2.842+03	9.985−03	0.000+00
4	35	1.681+02	0.000+00	0.000+00	0.000+00	5.115+03	8.068−03	0.000+00
4	36	1.679+02	6.800+04	9.583−08	1.589−07	0.000+00	0.000+00	0.000+00
4	37	1.677+02	2.582+09	1.089−02	1.804−02	0.000+00	0.000+00	5.441−01
4	38	1.677+02	4.642+09	3.263−02	5.405−02	0.000+00	0.000+00	7.970+00
4	39	1.677+02	0.000+00	0.000+00	0.000+00	0.000+00	0.000+00	5.664−01
4	40	1.677+02	0.000+00	0.000+00	0.000+00	3.534+05	1.306−04	0.000+00
4	41	1.677+02	0.000+00	0.000+00	0.000+00	3.630+05	0.000+00	0.000+00
4	43	1.677+02	0.000+00	0.000+00	0.000+00	0.000+00	0.000+00	2.729−09
4	45	1.677+02	0.000+00	0.000+00	0.000+00	1.418+05	0.000+00	0.000+00
4	48	1.677+02	4.928+06	3.463−05	5.736−05	0.000+00	0.000+00	7.942+00
4	49	1.675+02	0.000+00	0.000+00	0.000+00	1.795+01	4.081−03	0.000+00
5	6	3.288+04	0.000+00	0.000+00	0.000+00	0.000+00	0.000+00	3.909−09
5	7	3.416+03	0.000+00	0.000+00	0.000+00	2.762−05	1.135−02	0.000+00
5	8	2.610+02	3.520+09	2.156−02	9.262−02	0.000+00	0.000+00	3.424+00
5	9	2.531+02	0.000+00	0.000+00	0.000+00	3.941+05	0.000+00	0.000+00
5	10	2.531+02	0.000+00	0.000+00	0.000+00	2.956+05	3.829−02	0.000+00
5	11	2.530+02	0.000+00	0.000+00	0.000+00	1.379+05	3.946−02	0.000+00
5	12	2.523+02	0.000+00	0.000+00	0.000+00	0.000+00	0.000+00	4.515+00
5	13	2.495+02	1.176+09	6.581−03	2.703−02	0.000+00	0.000+00	4.477−09
5	14	2.495+02	1.055+10	9.842−02	4.042−01	0.000+00	0.000+00	1.010+01
5	15	2.495+02	4.233+10	5.529−01	2.270+00	0.000+00	0.000+00	8.340+01
5	16	2.493+02	3.317+07	3.090−04	1.268−03	0.000+00	0.000+00	1.913+01
5	17	2.477+02	0.000+00	0.000+00	0.000+00	8.027+00	9.709−02	0.000+00
5	18	1.897+02	1.198+09	3.879−03	1.211−02	0.000+00	0.000+00	2.204+00
5	19	1.880+02	0.000+00	0.000+00	0.000+00	1.441+05	0.000+00	0.000+00
5	20	1.880+02	0.000+00	0.000+00	0.000+00	1.080+05	2.118−02	0.000+00
5	21	1.880+02	0.000+00	0.000+00	0.000+00	5.041+04	3.167−02	0.000+00

Table 2: Transition wavelengths (λ_{ij} in Å), radiative rates (A_{ji} in s^{-1}), oscillator strengths (f_{ij}, dimensionless), and line strengths (S, in atomic units) for electric dipole (E1), and A_{ji} for E2, M1, and M2 transitions of C V. ($a \pm b \equiv a \times 10^{\pm b}$).

i	j	λ_{ij}	A^{E1}_{ji}	f^{E1}_{ij}	S^{E1}	A^{E2}_{ji}	A^{M1}_{ij}	A^{M2}_{ji}
5	22	1.878+02	0.000+00	0.000+00	0.000+00	0.000+00	0.000+00	3.153+00
5	23	1.872+02	3.871+08	1.220−03	3.758−03	0.000+00	0.000+00	1.804−09
5	24	1.872+02	3.477+09	1.826−02	5.627−02	0.000+00	0.000+00	6.116+00
5	25	1.872+02	1.394+10	1.025−01	3.157−01	0.000+00	0.000+00	4.879+01
5	26	1.871+02	0.000+00	0.000+00	0.000+00	6.538+04	1.660−04	0.000+00
5	27	1.871+02	0.000+00	0.000+00	0.000+00	2.154+05	3.408−04	0.000+00
5	28	1.871+02	0.000+00	0.000+00	0.000+00	9.805+05	0.000+00	0.000+00
5	29	1.871+02	0.000+00	0.000+00	0.000+00	1.114+05	1.320−05	0.000+00
5	30	1.871+02	6.479+06	3.401−05	1.047−04	0.000+00	0.000+00	1.104+01
5	31	1.867+02	0.000+00	0.000+00	0.000+00	3.181+00	6.614−02	0.000+00
5	32	1.688+02	4.114+08	1.054−03	2.930−03	0.000+00	0.000+00	9.566−01
5	33	1.681+02	0.000+00	0.000+00	0.000+00	1.119+04	0.000+00	0.000+00
5	34	1.681+02	0.000+00	0.000+00	0.000+00	8.344+03	1.280−02	0.000+00
5	35	1.681+02	0.000+00	0.000+00	0.000+00	3.895+03	2.845−02	0.000+00
5	36	1.680+02	0.000+00	0.000+00	0.000+00	0.000+00	0.000+00	1.526+00
5	37	1.678+02	1.720+08	4.355−04	1.203−03	0.000+00	0.000+00	2.241−09
5	38	1.678+02	1.545+09	6.519−03	1.800−02	0.000+00	0.000+00	3.416+00
5	39	1.678+02	6.190+09	3.657−02	1.010−01	0.000+00	0.000+00	2.697+01
5	40	1.678+02	0.000+00	0.000+00	0.000+00	5.050+04	1.266−04	0.000+00
5	41	1.678+02	0.000+00	0.000+00	0.000+00	1.805+05	2.219−04	0.000+00
5	42	1.678+02	0.000+00	0.000+00	0.000+00	7.577+05	0.000+00	0.000+00
5	43	1.678+02	7.160−02	4.229−13	1.168−12	0.000+00	0.000+00	4.603−10
5	44	1.678+02	0.000+00	0.000+00	0.000+00	0.000+00	0.000+00	1.046−08
5	45	1.678+02	0.000+00	0.000+00	0.000+00	7.211+04	1.653−05	0.000+00
5	47	1.678+02	0.000+00	0.000+00	0.000+00	0.000+00	0.000+00	3.495−13
5	48	1.678+02	2.374+06	1.001−05	2.765−05	0.000+00	0.000+00	6.107+00
5	49	1.676+02	0.000+00	0.000+00	0.000+00	2.283−01	5.144−02	0.000+00
6	7	3.812+03	1.308+07	8.549−02	1.073+00	0.000+00	0.000+00	0.000+00
6	8	2.630+02	0.000+00	0.000+00	0.000+00	0.000+00	1.805−02	0.000+00
6	10	2.550+02	4.473+05	1.308−05	1.098−05	0.000+00	0.000+00	0.000+00
6	11	2.550+02	0.000+00	0.000+00	0.000+00	0.000+00	0.000+00	1.053+01
6	13	2.514+02	0.000+00	0.000+00	0.000+00	0.000+00	7.748−04	0.000+00
6	14	2.514+02	0.000+00	0.000+00	0.000+00	2.865+03	0.000+00	0.000+00
6	16	2.512+02	0.000+00	0.000+00	0.000+00	9.138+05	0.000+00	0.000+00
6	17	2.496+02	1.364+10	3.822−01	3.140−01	0.000+00	0.000+00	0.000+00
6	18	1.908+02	0.000+00	0.000+00	0.000+00	0.000+00	1.127−02	0.000+00
6	20	1.891+02	2.154+05	3.464−06	2.156−06	0.000+00	0.000+00	0.000+00
6	21	1.891+02	0.000+00	0.000+00	0.000+00	0.000+00	0.000+00	8.931+00
6	23	1.882+02	0.000+00	0.000+00	0.000+00	0.000+00	3.801−04	0.000+00
6	24	1.882+02	0.000+00	0.000+00	0.000+00	2.836+02	0.000+00	0.000+00
6	26	1.882+02	0.000+00	0.000+00	0.000+00	0.000+00	0.000+00	2.091−09
6	30	1.882+02	0.000+00	0.000+00	0.000+00	1.551+05	0.000+00	0.000+00
6	31	1.878+02	7.159+09	1.135−01	7.019−02	0.000+00	0.000+00	0.000+00
6	32	1.697+02	0.000+00	0.000+00	0.000+00	0.000+00	4.098−04	0.000+00
6	34	1.690+02	1.510+05	1.938−06	1.078−06	0.000+00	0.000+00	0.000+00
6	35	1.690+02	0.000+00	0.000+00	0.000+00	0.000+00	0.000+00	7.823+00
6	37	1.686+02	0.000+00	0.000+00	0.000+00	0.000+00	6.025−07	0.000+00
6	38	1.686+02	0.000+00	0.000+00	0.000+00	5.597+02	0.000+00	0.000+00
6	40	1.686+02	0.000+00	0.000+00	0.000+00	0.000+00	0.000+00	1.215−07
6	48	1.686+02	0.000+00	0.000+00	0.000+00	3.718+05	0.000+00	0.000+00

Table 2: Transition wavelengths (λ_{ij} in Å), radiative rates (A_{ji} in s^{-1}), oscillator strengths (f_{ij}, dimensionless), and line strengths (S, in atomic units) for electric dipole (E1), and A_{ji} for E2, M1, and M2 transitions of C V. ($a{\pm}b \equiv a{\times}10^{\pm b}$).

i	j	λ_{ij}	A^{E1}_{ji}	f^{E1}_{ij}	S^{E1}	A^{E2}_{ji}	A^{M1}_{ij}	A^{M2}_{ji}
6	49	1.684+02	5.668+09	7.232−02	4.010−02	0.000+00	0.000+00	0.000+00
7	8	2.825+02	7.297+04	8.733−07	2.437−06	0.000+00	0.000+00	2.808+00
7	9	2.733+02	0.000+00	0.000+00	0.000+00	0.000+00	1.869−01	0.000+00
7	10	2.733+02	0.000+00	0.000+00	0.000+00	2.371+01	6.316−02	0.000+00
7	11	2.733+02	0.000+00	0.000+00	0.000+00	4.463+00	4.760−03	0.000+00
7	12	2.725+02	6.342+09	2.353−02	6.331−02	0.000+00	0.000+00	0.000+00
7	13	2.691+02	4.434+05	4.814−06	1.280−05	0.000+00	0.000+00	6.606−01
7	14	2.691+02	1.050+08	1.901−03	5.053−03	0.000+00	0.000+00	5.067+00
7	15	2.691+02	0.000+00	0.000+00	0.000+00	0.000+00	0.000+00	2.408+01
7	16	2.689+02	3.953+10	7.144−01	1.898+00	0.000+00	0.000+00	1.740+01
7	17	2.671+02	0.000+00	0.000+00	0.000+00	3.765+05	1.366−02	0.000+00
7	18	2.009+02	2.628+04	1.590−07	3.155−07	0.000+00	0.000+00	2.641+00
7	19	1.989+02	0.000+00	0.000+00	0.000+00	0.000+00	1.032−01	0.000+00
7	20	1.989+02	0.000+00	0.000+00	0.000+00	1.187+01	3.411−02	0.000+00
7	21	1.989+02	0.000+00	0.000+00	0.000+00	1.726+00	1.826−03	0.000+00
7	22	1.987+02	3.514+09	6.933−03	1.361−02	0.000+00	0.000+00	0.000+00
7	23	1.980+02	1.373+05	8.072−07	1.579−06	0.000+00	0.000+00	3.907−01
7	24	1.980+02	1.895+07	1.856−04	3.630−04	0.000+00	0.000+00	3.140+00
7	25	1.980+02	0.000+00	0.000+00	0.000+00	0.000+00	0.000+00	1.424+01
7	26	1.980+02	0.000+00	0.000+00	0.000+00	1.221+01	2.697−04	0.000+00
7	27	1.980+02	0.000+00	0.000+00	0.000+00	3.129+05	0.000+00	0.000+00
7	29	1.980+02	0.000+00	0.000+00	0.000+00	6.159+05	0.000+00	0.000+00
7	30	1.980+02	1.275+10	1.249−01	2.441−01	0.000+00	0.000+00	1.020+01
7	31	1.975+02	0.000+00	0.000+00	0.000+00	2.260+05	1.090−02	0.000+00
7	32	1.776+02	1.074+04	5.077−08	8.904−08	0.000+00	0.000+00	2.704+00
7	33	1.768+02	0.000+00	0.000+00	0.000+00	0.000+00	4.583−02	0.000+00
7	34	1.768+02	0.000+00	0.000+00	0.000+00	2.007+01	8.831−03	0.000+00
7	35	1.768+02	0.000+00	0.000+00	0.000+00	5.038−01	3.512−03	0.000+00
7	36	1.767+02	3.493+09	5.447−03	9.504−03	0.000+00	0.000+00	0.000+00
7	37	1.764+02	6.013+04	2.806−07	4.889−07	0.000+00	0.000+00	2.524−01
7	38	1.764+02	7.960+06	6.191−05	1.079−04	0.000+00	0.000+00	2.049+00
7	39	1.764+02	0.000+00	0.000+00	0.000+00	0.000+00	0.000+00	9.182+00
7	40	1.764+02	0.000+00	0.000+00	0.000+00	8.665+00	3.905−04	0.000+00
7	41	1.764+02	0.000+00	0.000+00	0.000+00	1.135+05	0.000+00	0.000+00
7	43	1.764+02	0.000+00	0.000+00	0.000+00	0.000+00	0.000+00	1.031−09
7	45	1.764+02	0.000+00	0.000+00	0.000+00	2.912+05	0.000+00	0.000+00
7	48	1.764+02	6.570+09	5.108−02	8.900−02	0.000+00	0.000+00	6.579+00
7	49	1.762+02	0.000+00	0.000+00	0.000+00	6.512+05	3.247−03	0.000+00
8	9	8.348+03	7.191+06	2.504−02	2.064+00	0.000+00	0.000+00	0.000+00
8	10	8.349+03	7.187+06	7.509−02	6.191+00	0.000+00	0.000+00	3.738−06
8	11	8.321+03	7.261+06	1.256−01	1.032+01	0.000+00	0.000+00	6.945−06
8	12	7.634+03	0.000+00	0.000+00	0.000+00	0.000+00	6.101−05	0.000+00
8	13	5.672+03	0.000+00	0.000+00	0.000+00	1.205+00	3.361−06	0.000+00
8	14	5.672+03	0.000+00	0.000+00	0.000+00	1.201+00	8.633−07	0.000+00
8	15	5.668+03	0.000+00	0.000+00	0.000+00	1.209+00	0.000+00	0.000+00
8	16	5.584+03	0.000+00	0.000+00	0.000+00	4.094−03	1.865−10	0.000+00
8	17	4.881+03	1.055+03	3.767−06	1.816−04	0.000+00	0.000+00	1.146−04
8	18	6.951+02	0.000+00	0.000+00	0.000+00	6.508−04	1.564−04	0.000+00
8	19	6.723+02	1.622+09	3.663−02	2.432−01	0.000+00	0.000+00	0.000+00
8	20	6.723+02	1.622+09	1.099−01	7.295−01	0.000+00	0.000+00	1.300−01

Table 2: Transition wavelengths (λ_{ij} in $\mathring{A}$), radiative rates (A_{ji} in s^{-1}), oscillator strengths (f_{ij}, dimensionless), and line strengths (S, in atomic units) for electric dipole (E1), and A_{ji} for E2, M1, and M2 transitions of C V. ($a \pm b \equiv a \times 10^{\pm b}$).

i	j	λ_{ij}	A^{E1}_{ji}	f^{E1}_{ij}	S^{E1}	A^{E2}_{ji}	A^{M1}_{ij}	A^{M2}_{ji}
8	21	6.722+02	1.620+09	1.829−01	1.214+00	0.000+00	0.000+00	2.374−01
8	22	6.695+02	0.000+00	0.000+00	0.000+00	0.000+00	1.422−06	0.000+00
8	23	6.619+02	0.000+00	0.000+00	0.000+00	7.558+04	4.816−05	0.000+00
8	24	6.619+02	0.000+00	0.000+00	0.000+00	7.543+04	3.175−07	0.000+00
8	25	6.619+02	0.000+00	0.000+00	0.000+00	7.557+04	0.000+00	0.000+00
8	26	6.615+02	3.405+01	3.722−09	2.431−08	0.000+00	0.000+00	2.120−09
8	27	6.615+02	0.000+00	0.000+00	0.000+00	0.000+00	0.000+00	1.413−12
8	29	6.614+02	0.000+00	0.000+00	0.000+00	0.000+00	0.000+00	2.889−09
8	30	6.612+02	0.000+00	0.000+00	0.000+00	1.400+02	2.368−06	0.000+00
8	31	6.564+02	3.517+04	2.271−06	1.472−05	0.000+00	0.000+00	2.259−01
8	32	4.780+02	0.000+00	0.000+00	0.000+00	8.563−06	2.064−04	0.000+00
8	33	4.724+02	8.471+08	9.447−03	4.408−02	0.000+00	0.000+00	0.000+00
8	34	4.724+02	8.469+08	2.833−02	1.322−01	0.000+00	0.000+00	1.374−01
8	35	4.724+02	8.458+08	4.716−02	2.200−01	0.000+00	0.000+00	2.510−01
8	36	4.714+02	0.000+00	0.000+00	0.000+00	0.000+00	6.384−05	0.000+00
8	37	4.698+02	0.000+00	0.000+00	0.000+00	2.524+04	4.734−05	0.000+00
8	38	4.698+02	0.000+00	0.000+00	0.000+00	2.521+04	4.569−09	0.000+00
8	39	4.698+02	0.000+00	0.000+00	0.000+00	2.525+04	0.000+00	0.000+00
8	40	4.697+02	9.976+00	5.498−10	2.550−09	0.000+00	0.000+00	1.023−09
8	41	4.697+02	0.000+00	0.000+00	0.000+00	0.000+00	0.000+00	2.603−14
8	43	4.697+02	0.000+00	0.000+00	0.000+00	9.056−04	0.000+00	0.000+00
8	45	4.697+02	0.000+00	0.000+00	0.000+00	0.000+00	0.000+00	2.044−09
8	48	4.696+02	0.000+00	0.000+00	0.000+00	3.875+01	3.543−06	0.000+00
8	49	4.683+02	1.866+04	6.135−07	2.837−06	0.000+00	0.000+00	2.715−01
9	11	2.628+06	0.000+00	0.000+00	0.000+00	3.440−14	0.000+00	0.000+00
9	13	1.769+04	3.332+05	4.691−02	2.732+00	0.000+00	0.000+00	0.000+00
9	14	1.769+04	0.000+00	0.000+00	0.000+00	0.000+00	0.000+00	3.489−09
9	16	1.687+04	0.000+00	0.000+00	0.000+00	0.000+00	0.000+00	3.747−08
9	17	1.175+04	0.000+00	0.000+00	0.000+00	0.000+00	3.606−04	0.000+00
9	18	7.582+02	1.937+08	5.009−02	1.250−01	0.000+00	0.000+00	0.000+00
9	20	7.312+02	0.000+00	0.000+00	0.000+00	0.000+00	1.439−06	0.000+00
9	21	7.311+02	0.000+00	0.000+00	0.000+00	8.282+03	0.000+00	0.000+00
9	23	7.189+02	2.389+09	5.554−01	1.314+00	0.000+00	0.000+00	0.000+00
9	24	7.189+02	0.000+00	0.000+00	0.000+00	0.000+00	0.000+00	1.630−02
9	26	7.184+02	0.000+00	0.000+00	0.000+00	4.846+04	0.000+00	0.000+00
9	30	7.181+02	0.000+00	0.000+00	0.000+00	0.000+00	0.000+00	1.265−01
9	31	7.124+02	0.000+00	0.000+00	0.000+00	0.000+00	2.070−03	0.000+00
9	32	5.070+02	8.076+07	9.336−03	1.558−02	0.000+00	0.000+00	0.000+00
9	34	5.008+02	0.000+00	0.000+00	0.000+00	0.000+00	3.030−06	0.000+00
9	35	5.008+02	0.000+00	0.000+00	0.000+00	3.676+03	0.000+00	0.000+00
9	37	4.978+02	1.171+09	1.305−01	2.139−01	0.000+00	0.000+00	0.000+00
9	38	4.978+02	0.000+00	0.000+00	0.000+00	0.000+00	0.000+00	1.703−02
9	40	4.977+02	0.000+00	0.000+00	0.000+00	5.967+02	0.000+00	0.000+00
9	48	4.976+02	0.000+00	0.000+00	0.000+00	0.000+00	0.000+00	1.297−01
9	49	4.961+02	0.000+00	0.000+00	0.000+00	0.000+00	1.553−03	0.000+00
10	11	2.526+06	0.000+00	0.000+00	0.000+00	9.429−14	8.358−07	0.000+00
10	12	8.915+04	4.961−01	1.970−07	1.735−04	0.000+00	0.000+00	0.000+00
10	13	1.769+04	2.502+05	1.173−02	2.050+00	0.000+00	0.000+00	4.743−09
10	14	1.769+04	4.493+05	3.511−02	6.134+00	0.000+00	0.000+00	6.721−08
10	15	1.765+04	0.000+00	0.000+00	0.000+00	0.000+00	0.000+00	4.973−09

Table 2: Transition wavelengths (λ_{ij} in Å), radiative rates (A_{ji} in s^{-1}), oscillator strengths (f_{ij}, dimensionless), and line strengths (S, in atomic units) for electric dipole (E1), and A_{ji} for E2, M1, and M2 transitions of C V. ($a{\pm}b \equiv a{\times}10^{\pm b}$).

i	j	λ_{ij}	A^{E1}_{ji}	f^{E1}_{ij}	S^{E1}	A^{E2}_{ji}	A^{M1}_{ij}	A^{M2}_{ji}
10	16	1.686+04	1.295+03	9.201−05	1.532−02	0.000+00	0.000+00	8.994−08
10	17	1.175+04	0.000+00	0.000+00	0.000+00	6.386−06	3.148−04	0.000+00
10	18	7.582+02	5.804+08	5.002−02	3.746−01	0.000+00	0.000+00	3.658−02
10	19	7.312+02	0.000+00	0.000+00	0.000+00	0.000+00	2.172−05	0.000+00
10	20	7.312+02	0.000+00	0.000+00	0.000+00	1.035+04	1.843−04	0.000+00
10	21	7.311+02	0.000+00	0.000+00	0.000+00	1.863+04	1.216−03	0.000+00
10	22	7.279+02	3.599+04	9.528−07	6.850−06	0.000+00	0.000+00	0.000+00
10	23	7.189+02	1.792+09	1.389−01	9.858−01	0.000+00	0.000+00	2.057−02
10	24	7.189+02	3.221+09	4.159−01	2.953+00	0.000+00	0.000+00	2.990−01
10	25	7.189+02	0.000+00	0.000+00	0.000+00	0.000+00	0.000+00	2.135−02
10	26	7.184+02	0.000+00	0.000+00	0.000+00	4.846+04	6.822−06	0.000+00
10	27	7.184+02	0.000+00	0.000+00	0.000+00	4.605+04	0.000+00	0.000+00
10	29	7.183+02	0.000+00	0.000+00	0.000+00	2.318+04	0.000+00	0.000+00
10	30	7.181+02	4.362+06	5.620−04	3.986−03	0.000+00	0.000+00	2.983−01
10	31	7.124+02	0.000+00	0.000+00	0.000+00	2.637+00	1.616−03	0.000+00
10	32	5.070+02	2.417+08	9.311−03	4.662−02	0.000+00	0.000+00	3.397−02
10	33	5.008+02	0.000+00	0.000+00	0.000+00	0.000+00	1.224−05	0.000+00
10	34	5.008+02	0.000+00	0.000+00	0.000+00	4.581+03	2.240−04	0.000+00
10	35	5.007+02	0.000+00	0.000+00	0.000+00	8.246+03	9.091−04	0.000+00
10	36	4.996+02	2.548+04	3.178−07	1.568−06	0.000+00	0.000+00	0.000+00
10	37	4.978+02	8.782+08	3.263−02	1.604−01	0.000+00	0.000+00	2.102−02
10	38	4.978+02	1.579+09	9.776−02	4.806−01	0.000+00	0.000+00	3.079−01
10	39	4.978+02	0.000+00	0.000+00	0.000+00	0.000+00	0.000+00	2.185−02
10	40	4.977+02	0.000+00	0.000+00	0.000+00	5.947+02	3.433−06	0.000+00
10	41	4.977+02	0.000+00	0.000+00	0.000+00	6.141+02	0.000+00	0.000+00
10	43	4.977+02	0.000+00	0.000+00	0.000+00	0.000+00	0.000+00	1.604−10
10	45	4.977+02	0.000+00	0.000+00	0.000+00	2.358+02	0.000+00	0.000+00
10	48	4.976+02	1.681+06	1.040−04	5.111−04	0.000+00	0.000+00	3.041−01
10	49	4.961+02	0.000+00	0.000+00	0.000+00	2.038+00	1.136−03	0.000+00
11	12	9.242+04	0.000+00	0.000+00	0.000+00	0.000+00	0.000+00	1.373−10
11	13	1.781+04	1.630+04	4.653−04	1.364−01	0.000+00	0.000+00	1.417−15
11	14	1.781+04	1.465+05	6.969−03	2.043+00	0.000+00	0.000+00	2.752−08
11	15	1.778+04	5.916+05	3.923−02	1.148+01	0.000+00	0.000+00	2.296−07
11	16	1.698+04	5.334+02	2.304−05	6.437−03	0.000+00	0.000+00	6.636−08
11	17	1.181+04	0.000+00	0.000+00	0.000+00	2.106−06	2.748−04	0.000+00
11	18	7.584+02	9.686+08	5.011−02	6.256−01	0.000+00	0.000+00	1.115−01
11	19	7.314+02	0.000+00	0.000+00	0.000+00	4.140+04	0.000+00	0.000+00
11	20	7.314+02	0.000+00	0.000+00	0.000+00	3.104+04	1.885−03	0.000+00
11	21	7.313+02	0.000+00	0.000+00	0.000+00	1.448+04	4.541−04	0.000+00
11	22	7.281+02	0.000+00	0.000+00	0.000+00	0.000+00	0.000+00	1.591−01
11	23	7.191+02	1.194+08	5.555−03	6.576−02	0.000+00	0.000+00	4.986−10
11	24	7.191+02	1.073+09	8.320−02	9.849−01	0.000+00	0.000+00	1.279−01
11	25	7.191+02	4.301+09	4.667−01	5.524+00	0.000+00	0.000+00	1.020+00
11	26	7.186+02	0.000+00	0.000+00	0.000+00	6.917+03	5.929−06	0.000+00
11	27	7.186+02	0.000+00	0.000+00	0.000+00	2.279+04	1.301−05	0.000+00
11	28	7.185+02	0.000+00	0.000+00	0.000+00	1.038+05	0.000+00	0.000+00
11	29	7.185+02	0.000+00	0.000+00	0.000+00	1.179+04	4.724−07	0.000+00
11	30	7.183+02	1.983+06	1.534−04	1.814−03	0.000+00	0.000+00	2.290−01
11	31	7.126+02	0.000+00	0.000+00	0.000+00	8.408−01	3.164−03	0.000+00
11	32	5.071+02	4.030+08	9.321−03	7.780−02	0.000+00	0.000+00	1.038−01

Table 2: Transition wavelengths (λ_{ij} in $\mathring{A}$), radiative rates (A_{ji} in s^{-1}), oscillator strengths (f_{ij}, dimensionless), and line strengths (S, in atomic units) for electric dipole (E1), and A_{ji} for E2, M1, and M2 transitions of C V. ($a{\pm}b \equiv a{\times}10^{\pm b}$).

i	j	λ_{ij}	A^{E1}_{ji}	f^{E1}_{ij}	S^{E1}	A^{E2}_{ji}	A^{M1}_{ij}	A^{M2}_{ji}
11	33	5.009+02	0.000+00	0.000+00	0.000+00	1.830+04	0.000+00	0.000+00
11	34	5.009+02	0.000+00	0.000+00	0.000+00	1.372+04	1.400−03	0.000+00
11	35	5.008+02	0.000+00	0.000+00	0.000+00	6.401+03	5.658−04	0.000+00
11	36	4.997+02	0.000+00	0.000+00	0.000+00	0.000+00	0.000+00	1.660−01
11	37	4.979+02	5.850+07	1.305−03	1.069−02	0.000+00	0.000+00	6.975−10
11	38	4.979+02	5.259+08	1.955−02	1.602−01	0.000+00	0.000+00	1.321−01
11	39	4.979+02	2.107+09	1.096−01	8.983−01	0.000+00	0.000+00	1.042+00
11	40	4.978+02	0.000+00	0.000+00	0.000+00	8.408+01	2.702−06	0.000+00
11	41	4.978+02	0.000+00	0.000+00	0.000+00	3.004+02	6.914−06	0.000+00
11	42	4.978+02	0.000+00	0.000+00	0.000+00	1.264+03	0.000+00	0.000+00
11	43	4.978+02	2.879−02	1.497−12	1.227−11	0.000+00	0.000+00	1.922−10
11	44	4.978+02	0.000+00	0.000+00	0.000+00	0.000+00	0.000+00	5.021−10
11	45	4.978+02	0.000+00	0.000+00	0.000+00	1.204+02	3.879−07	0.000+00
11	47	4.978+02	0.000+00	0.000+00	0.000+00	0.000+00	0.000+00	1.262−11
11	48	4.977+02	8.019+05	2.978−05	2.440−04	0.000+00	0.000+00	2.340−01
11	49	4.962+02	0.000+00	0.000+00	0.000+00	3.811−01	2.947−03	0.000+00
12	13	2.207+04	0.000+00	0.000+00	0.000+00	0.000+00	8.645−11	0.000+00
12	14	2.206+04	0.000+00	0.000+00	0.000+00	4.294−06	0.000+00	0.000+00
12	16	2.080+04	0.000+00	0.000+00	0.000+00	1.844−03	0.000+00	0.000+00
12	17	1.354+04	1.751+06	1.443−01	6.429+00	0.000+00	0.000+00	0.000+00
12	18	7.647+02	0.000+00	0.000+00	0.000+00	0.000+00	3.394−04	0.000+00
12	20	7.372+02	6.072+04	1.484−05	3.602−05	0.000+00	0.000+00	0.000+00
12	21	7.371+02	0.000+00	0.000+00	0.000+00	0.000+00	0.000+00	1.708−01
12	23	7.248+02	0.000+00	0.000+00	0.000+00	0.000+00	3.642−06	0.000+00
12	24	7.248+02	0.000+00	0.000+00	0.000+00	1.201+02	0.000+00	0.000+00
12	26	7.242+02	0.000+00	0.000+00	0.000+00	0.000+00	0.000+00	1.734−10
12	30	7.240+02	0.000+00	0.000+00	0.000+00	6.491+04	0.000+00	0.000+00
12	31	7.182+02	1.812+09	4.202−01	9.935−01	0.000+00	0.000+00	0.000+00
12	32	5.099+02	0.000+00	0.000+00	0.000+00	0.000+00	2.629−04	0.000+00
12	34	5.036+02	3.864+04	4.407−06	7.306−06	0.000+00	0.000+00	0.000+00
12	35	5.036+02	0.000+00	0.000+00	0.000+00	0.000+00	0.000+00	2.294−01
12	37	5.006+02	0.000+00	0.000+00	0.000+00	0.000+00	3.045−06	0.000+00
12	38	5.006+02	0.000+00	0.000+00	0.000+00	5.110+01	0.000+00	0.000+00
12	40	5.005+02	0.000+00	0.000+00	0.000+00	0.000+00	0.000+00	1.113−10
12	48	5.004+02	0.000+00	0.000+00	0.000+00	3.387+04	0.000+00	0.000+00
12	49	4.989+02	1.333+09	1.492−01	2.450−01	0.000+00	0.000+00	0.000+00
13	14	1.081+08	0.000+00	0.000+00	0.000+00	1.915−22	1.914−11	0.000+00
13	15	8.282+06	0.000+00	0.000+00	0.000+00	5.930−18	0.000+00	0.000+00
13	16	3.603+05	0.000+00	0.000+00	0.000+00	1.464−12	1.652−06	0.000+00
13	17	3.500+04	8.957−01	1.645−07	5.687−05	0.000+00	0.000+00	7.439−11
13	18	7.922+02	0.000+00	0.000+00	0.000+00	3.830+03	1.058−05	0.000+00
13	19	7.627+02	2.868+08	8.337−03	6.280−02	0.000+00	0.000+00	0.000+00
13	20	7.627+02	7.179+07	6.260−03	4.715−02	0.000+00	0.000+00	7.331−04
13	21	7.626+02	2.857+06	4.151−04	3.126−03	0.000+00	0.000+00	8.670−10
13	22	7.592+02	0.000+00	0.000+00	0.000+00	0.000+00	5.488−08	0.000+00
13	23	7.494+02	0.000+00	0.000+00	0.000+00	6.507+03	1.495−04	0.000+00
13	24	7.494+02	0.000+00	0.000+00	0.000+00	6.502+03	6.464−06	0.000+00
13	25	7.493+02	0.000+00	0.000+00	0.000+00	5.306+02	0.000+00	0.000+00
13	26	7.488+02	7.252+09	1.016+00	7.512+00	0.000+00	0.000+00	2.644−01
13	27	7.488+02	0.000+00	0.000+00	0.000+00	0.000+00	0.000+00	3.005−02

Table 2: Transition wavelengths (λ_{ij} in $\mathring{A}$), radiative rates (A_{ji} in s^{-1}), oscillator strengths (f_{ij}, dimensionless), and line strengths (S, in atomic units) for electric dipole (E1), and A_{ji} for E2, M1, and M2 transitions of C V. ($a{\pm}b \equiv a{\times}10^{\pm b}$).

i	j	λ_{ij}	A^{E1}_{ji}	f^{E1}_{ij}	S^{E1}	A^{E2}_{ji}	A^{M1}_{ij}	A^{M2}_{ji}
13	29	7.487+02	0.000+00	0.000+00	0.000+00	0.000+00	0.000+00	4.384−01
13	30	7.485+02	0.000+00	0.000+00	0.000+00	1.206+01	1.171−04	0.000+00
13	31	7.423+02	1.275+03	1.053−07	7.718−07	0.000+00	0.000+00	2.457−04
13	32	5.220+02	0.000+00	0.000+00	0.000+00	2.174+03	7.527−06	0.000+00
13	33	5.153+02	1.185+08	1.573−03	8.005−03	0.000+00	0.000+00	0.000+00
13	34	5.153+02	2.966+07	1.181−03	6.011−03	0.000+00	0.000+00	6.638−04
13	35	5.153+02	1.179+06	7.822−05	3.981−04	0.000+00	0.000+00	1.339−09
13	36	5.142+02	0.000+00	0.000+00	0.000+00	0.000+00	1.956−08	0.000+00
13	37	5.122+02	0.000+00	0.000+00	0.000+00	3.099+03	1.541−04	0.000+00
13	38	5.122+02	0.000+00	0.000+00	0.000+00	3.098+03	5.744−06	0.000+00
13	39	5.122+02	0.000+00	0.000+00	0.000+00	2.527+02	0.000+00	0.000+00
13	40	5.121+02	2.393+09	1.568−01	7.929−01	0.000+00	0.000+00	1.865−01
13	41	5.121+02	0.000+00	0.000+00	0.000+00	0.000+00	0.000+00	1.256−02
13	43	5.121+02	0.000+00	0.000+00	0.000+00	1.400+05	0.000+00	0.000+00
13	45	5.121+02	0.000+00	0.000+00	0.000+00	0.000+00	0.000+00	3.179−01
13	48	5.120+02	0.000+00	0.000+00	0.000+00	4.745+00	6.414−05	0.000+00
13	49	5.104+02	5.051+02	1.972−08	9.942−08	0.000+00	0.000+00	2.378−04
14	15	8.970+06	0.000+00	0.000+00	0.000+00	3.971−17	2.481−08	0.000+00
14	16	3.615+05	0.000+00	0.000+00	0.000+00	1.027−12	3.126−07	0.000+00
14	17	3.501+04	3.320+02	3.662−05	2.110−02	0.000+00	0.000+00	9.516−10
14	18	7.922+02	0.000+00	0.000+00	0.000+00	6.360+03	2.537−06	0.000+00
14	19	7.627+02	0.000+00	0.000+00	0.000+00	0.000+00	0.000+00	2.688−03
14	20	7.627+02	2.146+08	1.123−02	1.410−01	0.000+00	0.000+00	1.726−02
14	21	7.626+02	4.281+07	3.732−03	4.685−02	0.000+00	0.000+00	4.383−03
14	22	7.592+02	0.000+00	0.000+00	0.000+00	5.504+01	0.000+00	0.000+00
14	23	7.494+02	0.000+00	0.000+00	0.000+00	1.082+04	4.473−07	0.000+00
14	24	7.494+02	0.000+00	0.000+00	0.000+00	4.672+03	3.069−04	0.000+00
14	25	7.493+02	0.000+00	0.000+00	0.000+00	5.298+03	1.001−04	0.000+00
14	26	7.488+02	1.339+09	1.125−01	1.387+00	0.000+00	0.000+00	7.412−02
14	27	7.488+02	5.482+09	6.451−01	7.950+00	0.000+00	0.000+00	3.214−01
14	28	7.488+02	0.000+00	0.000+00	0.000+00	0.000+00	0.000+00	7.303−02
14	29	7.488+02	2.195+09	2.582−01	3.182+00	0.000+00	0.000+00	1.346+00
14	30	7.485+02	0.000+00	0.000+00	0.000+00	2.220+01	2.979−06	0.000+00
14	31	7.423+02	5.043+05	2.499−05	3.054−04	0.000+00	0.000+00	3.151−03
14	32	5.220+02	0.000+00	0.000+00	0.000+00	3.605+03	1.823−06	0.000+00
14	33	5.154+02	0.000+00	0.000+00	0.000+00	0.000+00	0.000+00	2.415−03
14	34	5.154+02	8.860+07	2.116−03	1.795−02	0.000+00	0.000+00	1.557−02
14	35	5.153+02	1.767+07	7.034−04	5.966−03	0.000+00	0.000+00	3.949−03
14	36	5.142+02	0.000+00	0.000+00	0.000+00	3.934+01	0.000+00	0.000+00
14	37	5.122+02	0.000+00	0.000+00	0.000+00	5.150+03	7.889−07	0.000+00
14	38	5.122+02	0.000+00	0.000+00	0.000+00	2.223+03	3.177−04	0.000+00
14	39	5.122+02	0.000+00	0.000+00	0.000+00	2.522+03	6.935−05	0.000+00
14	40	5.121+02	4.417+08	1.736−02	1.464−01	0.000+00	0.000+00	5.229−02
14	41	5.121+02	1.942+09	1.069−01	9.007−01	0.000+00	0.000+00	2.847−01
14	42	5.121+02	0.000+00	0.000+00	0.000+00	0.000+00	0.000+00	5.153−02
14	43	5.121+02	0.000+00	0.000+00	0.000+00	3.878+04	5.933−06	0.000+00
14	44	5.121+02	0.000+00	0.000+00	0.000+00	9.111+04	0.000+00	0.000+00
14	45	5.121+02	5.913+08	3.254−02	2.743−01	0.000+00	0.000+00	8.913−01
14	47	5.121+02	0.000+00	0.000+00	0.000+00	6.027+04	0.000+00	0.000+00
14	48	5.120+02	0.000+00	0.000+00	0.000+00	1.257+01	2.565−07	0.000+00

Table 2: Transition wavelengths (λ_{ij} in $\mathring{A}$), radiative rates (A_{ji} in s^{-1}), oscillator strengths (f_{ij}, dimensionless), and line strengths (S, in atomic units) for electric dipole (E1), and A_{ji} for E2, M1, and M2 transitions of C V. ($a{\pm}b \equiv a{\times}10^{\pm b}$).

i	j	λ_{ij}	A^{E1}_{ji}	f^{E1}_{ij}	S^{E1}	A^{E2}_{ji}	A^{M1}_{ij}	A^{M2}_{ji}
14	49	5.104+02	2.460+05	5.765−06	4.843−05	0.000+00	0.000+00	3.028−03
15	16	3.767+05	0.000+00	0.000+00	0.000+00	1.341−12	1.436−06	0.000+00
15	17	3.515+04	0.000+00	0.000+00	0.000+00	0.000+00	0.000+00	6.206−09
15	18	7.922+02	0.000+00	0.000+00	0.000+00	8.935+03	0.000+00	0.000+00
15	20	7.628+02	0.000+00	0.000+00	0.000+00	0.000+00	0.000+00	1.772−03
15	21	7.627+02	2.406+08	1.499−02	2.634−01	0.000+00	0.000+00	5.075−02
15	23	7.494+02	0.000+00	0.000+00	0.000+00	1.239+03	0.000+00	0.000+00
15	24	7.494+02	0.000+00	0.000+00	0.000+00	7.426+03	1.179−04	0.000+00
15	25	7.494+02	0.000+00	0.000+00	0.000+00	1.275+04	5.688−04	0.000+00
15	26	7.488+02	3.836+07	2.303−03	3.975−02	0.000+00	0.000+00	1.629−12
15	27	7.488+02	6.321+08	5.313−02	9.169−01	0.000+00	0.000+00	3.859−03
15	28	7.488+02	8.632+09	9.329−01	1.610+01	0.000+00	0.000+00	3.084+00
15	29	7.488+02	3.270+08	2.749−02	4.743−01	0.000+00	0.000+00	4.720−01
15	30	7.486+02	0.000+00	0.000+00	0.000+00	1.377+01	5.246−04	0.000+00
15	31	7.424+02	0.000+00	0.000+00	0.000+00	0.000+00	0.000+00	2.100−02
15	32	5.220+02	0.000+00	0.000+00	0.000+00	5.060+03	0.000+00	0.000+00
15	34	5.154+02	0.000+00	0.000+00	0.000+00	0.000+00	0.000+00	1.603−03
15	35	5.154+02	9.927+07	2.823−03	3.353−02	0.000+00	0.000+00	4.585−02
15	37	5.123+02	0.000+00	0.000+00	0.000+00	5.898+02	0.000+00	0.000+00
15	38	5.123+02	0.000+00	0.000+00	0.000+00	3.534+03	7.789−05	0.000+00
15	39	5.123+02	0.000+00	0.000+00	0.000+00	6.068+03	5.884−04	0.000+00
15	40	5.121+02	1.266+07	3.555−04	4.196−03	0.000+00	0.000+00	2.709−11
15	41	5.121+02	2.261+08	8.888−03	1.049−01	0.000+00	0.000+00	7.499−03
15	42	5.121+02	2.848+09	1.440−01	1.699+00	0.000+00	0.000+00	2.175+00
15	43	5.121+02	0.000+00	0.000+00	0.000+00	2.593+03	2.572−06	0.000+00
15	44	5.121+02	0.000+00	0.000+00	0.000+00	1.638+04	1.152−05	0.000+00
15	45	5.121+02	9.035+07	3.552−03	4.192−02	0.000+00	0.000+00	3.282−01
15	46	5.121+02	0.000+00	0.000+00	0.000+00	1.815+05	0.000+00	0.000+00
15	47	5.121+02	0.000+00	0.000+00	0.000+00	1.388+04	4.468−08	0.000+00
15	48	5.120+02	0.000+00	0.000+00	0.000+00	5.413+00	4.195−04	0.000+00
15	49	5.104+02	0.000+00	0.000+00	0.000+00	0.000+00	0.000+00	2.031−02
16	17	3.877+04	9.271+04	1.253−02	7.998+00	0.000+00	0.000+00	1.964−09
16	18	7.939+02	0.000+00	0.000+00	0.000+00	2.000+01	6.762−08	0.000+00
16	19	7.643+02	0.000+00	0.000+00	0.000+00	0.000+00	0.000+00	2.318−02
16	20	7.643+02	5.399+05	2.837−05	3.569−04	0.000+00	0.000+00	1.851−02
16	21	7.642+02	1.364+05	1.194−05	1.502−04	0.000+00	0.000+00	8.465−03
16	22	7.608+02	0.000+00	0.000+00	0.000+00	1.754+04	0.000+00	0.000+00
16	23	7.509+02	0.000+00	0.000+00	0.000+00	3.394+01	7.443−04	0.000+00
16	24	7.509+02	0.000+00	0.000+00	0.000+00	4.219+00	1.623−04	0.000+00
16	25	7.509+02	0.000+00	0.000+00	0.000+00	1.662+01	4.110−05	0.000+00
16	26	7.503+02	4.196+06	3.541−04	4.374−03	0.000+00	0.000+00	3.896−02
16	27	7.503+02	2.515+09	2.971−01	3.670+00	0.000+00	0.000+00	4.993−02
16	28	7.503+02	0.000+00	0.000+00	0.000+00	0.000+00	0.000+00	6.534−01
16	29	7.503+02	6.101+09	7.208−01	8.901+00	0.000+00	0.000+00	1.522+00
16	30	7.501+02	0.000+00	0.000+00	0.000+00	1.858+04	3.451−04	0.000+00
16	31	7.438+02	1.930+08	9.602−03	1.176−01	0.000+00	0.000+00	1.110−02
16	32	5.227+02	0.000+00	0.000+00	0.000+00	1.151+01	5.604−08	0.000+00
16	33	5.161+02	0.000+00	0.000+00	0.000+00	0.000+00	0.000+00	2.200−02
16	34	5.161+02	2.228+05	5.338−06	4.535−05	0.000+00	0.000+00	1.754−02
16	35	5.161+02	5.676+04	2.266−06	1.925−05	0.000+00	0.000+00	8.025−03

Table 2: Transition wavelengths (λ_{ij} in $\AA$), radiative rates (A_{ji} in s^{-1}), oscillator strengths (f_{ij}, dimensionless), and line strengths (S, in atomic units) for electric dipole (E1), and A_{ji} for E2, M1, and M2 transitions of C V. ($a \pm b \equiv a \times 10^{\pm b}$).

i	j	λ_{ij}	A^{E1}_{ji}	f^{E1}_{ij}	S^{E1}	A^{E2}_{ji}	A^{M1}_{ij}	A^{M2}_{ji}
16	36	5.149+02	0.000+00	0.000+00	0.000+00	1.272+04	0.000+00	0.000+00
16	37	5.130+02	0.000+00	0.000+00	0.000+00	1.624+01	5.666−04	0.000+00
16	38	5.130+02	0.000+00	0.000+00	0.000+00	1.231+00	1.359−04	0.000+00
16	39	5.130+02	0.000+00	0.000+00	0.000+00	7.953+00	1.707−05	0.000+00
16	40	5.128+02	1.381+06	5.445−05	4.596−04	0.000+00	0.000+00	2.749−02
16	41	5.128+02	6.787+08	3.746−02	3.162−01	0.000+00	0.000+00	1.571−02
16	42	5.128+02	0.000+00	0.000+00	0.000+00	0.000+00	0.000+00	4.609−01
16	43	5.128+02	0.000+00	0.000+00	0.000+00	1.218+02	8.563−06	0.000+00
16	44	5.128+02	0.000+00	0.000+00	0.000+00	7.394+04	0.000+00	0.000+00
16	45	5.128+02	2.161+09	1.192−01	1.007+00	0.000+00	0.000+00	1.093+00
16	47	5.128+02	0.000+00	0.000+00	0.000+00	1.072+05	0.000+00	0.000+00
16	48	5.128+02	0.000+00	0.000+00	0.000+00	9.266+03	3.542−04	0.000+00
16	49	5.111+02	9.356+07	2.198−03	1.850−02	0.000+00	0.000+00	1.137−02
17	18	8.105+02	2.025+04	1.994−06	1.596−05	0.000+00	0.000+00	8.717−02
17	19	7.797+02	0.000+00	0.000+00	0.000+00	0.000+00	7.672−03	0.000+00
17	20	7.797+02	0.000+00	0.000+00	0.000+00	2.572+00	2.431−03	0.000+00
17	21	7.796+02	0.000+00	0.000+00	0.000+00	4.996−01	4.995−04	0.000+00
17	22	7.760+02	1.693+09	5.095−02	3.905−01	0.000+00	0.000+00	0.000+00
17	23	7.658+02	5.204+04	4.574−06	3.459−05	0.000+00	0.000+00	9.238−03
17	24	7.658+02	6.641+06	9.729−04	7.358−03	0.000+00	0.000+00	7.435−02
17	25	7.657+02	0.000+00	0.000+00	0.000+00	0.000+00	0.000+00	3.369−01
17	26	7.651+02	0.000+00	0.000+00	0.000+00	1.115+00	7.953−06	0.000+00
17	27	7.652+02	0.000+00	0.000+00	0.000+00	2.864+04	0.000+00	0.000+00
17	29	7.651+02	0.000+00	0.000+00	0.000+00	5.639+04	0.000+00	0.000+00
17	30	7.649+02	4.470+09	6.534−01	4.936+00	0.000+00	0.000+00	2.396−01
17	31	7.584+02	0.000+00	0.000+00	0.000+00	4.072+04	1.980−04	0.000+00
17	32	5.298+02	8.712+03	3.666−07	1.919−06	0.000+00	0.000+00	1.176−01
17	33	5.230+02	0.000+00	0.000+00	0.000+00	0.000+00	5.492−03	0.000+00
17	34	5.230+02	0.000+00	0.000+00	0.000+00	1.874+00	1.701−03	0.000+00
17	35	5.230+02	0.000+00	0.000+00	0.000+00	2.391−01	2.971−04	0.000+00
17	36	5.218+02	1.212+09	1.650−02	8.501−02	0.000+00	0.000+00	0.000+00
17	37	5.198+02	2.416+04	9.787−07	5.025−06	0.000+00	0.000+00	1.006−02
17	38	5.198+02	2.708+06	1.828−04	9.386−04	0.000+00	0.000+00	8.201−02
17	39	5.198+02	0.000+00	0.000+00	0.000+00	0.000+00	0.000+00	3.667−01
17	40	5.197+02	0.000+00	0.000+00	0.000+00	9.260−04	3.068−06	0.000+00
17	41	5.197+02	0.000+00	0.000+00	0.000+00	1.966+02	0.000+00	0.000+00
17	43	5.197+02	0.000+00	0.000+00	0.000+00	0.000+00	0.000+00	9.109−11
17	45	5.197+02	0.000+00	0.000+00	0.000+00	4.976+02	0.000+00	0.000+00
17	48	5.196+02	2.260+09	1.524−01	7.823−01	0.000+00	0.000+00	2.610−01
17	49	5.180+02	0.000+00	0.000+00	0.000+00	4.096+04	2.354−04	0.000+00
18	19	2.050+04	1.639+06	3.442−02	6.967+00	0.000+00	0.000+00	0.000+00
18	20	2.050+04	1.638+06	1.032−01	2.090+01	0.000+00	0.000+00	1.414−07
18	21	2.043+04	1.656+06	1.727−01	3.484+01	0.000+00	0.000+00	2.628−07
18	22	1.822+04	0.000+00	0.000+00	0.000+00	0.000+00	4.878−06	0.000+00
18	23	1.387+04	0.000+00	0.000+00	0.000+00	1.969−01	3.317−07	0.000+00
18	24	1.387+04	0.000+00	0.000+00	0.000+00	1.966−01	7.795−08	0.000+00
18	25	1.386+04	0.000+00	0.000+00	0.000+00	1.976−01	0.000+00	0.000+00
18	26	1.367+04	1.321−02	6.164−10	8.319−08	0.000+00	0.000+00	8.977−16
18	27	1.367+04	0.000+00	0.000+00	0.000+00	0.000+00	0.000+00	1.877−16
18	29	1.366+04	0.000+00	0.000+00	0.000+00	0.000+00	0.000+00	4.254−15

Table 2: Transition wavelengths (λ_{ij} in $\mathring{A}$), radiative rates (A_{ji} in s^{-1}), oscillator strengths (f_{ij}, dimensionless), and line strengths (S, in atomic units) for electric dipole (E1), and A_{ji} for E2, M1, and M2 transitions of C V. ($a \pm b \equiv a \times 10^{\pm b}$).

i	j	λ_{ij}	A^{E1}_{ji}	f^{E1}_{ij}	S^{E1}	A^{E2}_{ji}	A^{M1}_{ij}	A^{M2}_{ji}
18	30	1.358+04	0.000+00	0.000+00	0.000+00	4.058−04	8.885−13	0.000+00
18	31	1.180+04	2.477+02	5.167−06	6.019−04	0.000+00	0.000+00	4.626−06
18	32	1.530+03	0.000+00	0.000+00	0.000+00	1.094−04	5.098−06	0.000+00
18	33	1.475+03	3.633+08	3.948−02	5.751−01	0.000+00	0.000+00	0.000+00
18	34	1.475+03	3.632+08	1.184−01	1.725+00	0.000+00	0.000+00	6.051−03
18	35	1.475+03	3.627+08	1.971−01	2.870+00	0.000+00	0.000+00	1.105−02
18	36	1.465+03	0.000+00	0.000+00	0.000+00	0.000+00	5.152−06	0.000+00
18	37	1.450+03	0.000+00	0.000+00	0.000+00	9.884+03	2.976−06	0.000+00
18	38	1.450+03	0.000+00	0.000+00	0.000+00	9.868+03	2.430−07	0.000+00
18	39	1.450+03	0.000+00	0.000+00	0.000+00	9.883+03	0.000+00	0.000+00
18	40	1.448+03	7.128+00	3.736−09	5.344−08	0.000+00	0.000+00	7.255−11
18	41	1.448+03	0.000+00	0.000+00	0.000+00	0.000+00	0.000+00	7.789−13
18	43	1.448+03	0.000+00	0.000+00	0.000+00	1.176−04	0.000+00	0.000+00
18	45	1.448+03	0.000+00	0.000+00	0.000+00	0.000+00	0.000+00	1.429−10
18	48	1.448+03	0.000+00	0.000+00	0.000+00	1.505+01	3.469−08	0.000+00
18	49	1.435+03	7.324+03	2.261−06	3.204−05	0.000+00	0.000+00	1.063−02
19	21	6.021+06	0.000+00	0.000+00	0.000+00	6.193−15	0.000+00	0.000+00
19	23	4.288+04	9.953+04	8.229−02	1.161+01	0.000+00	0.000+00	0.000+00
19	24	4.287+04	0.000+00	0.000+00	0.000+00	0.000+00	0.000+00	1.912−10
19	26	4.101+04	0.000+00	0.000+00	0.000+00	2.526−04	0.000+00	0.000+00
19	30	4.025+04	0.000+00	0.000+00	0.000+00	0.000+00	0.000+00	2.037−09
19	31	2.778+04	0.000+00	0.000+00	0.000+00	0.000+00	2.740−05	0.000+00
19	32	1.654+03	6.443+07	7.923−02	4.313−01	0.000+00	0.000+00	0.000+00
19	34	1.589+03	0.000+00	0.000+00	0.000+00	0.000+00	1.862−07	0.000+00
19	35	1.589+03	0.000+00	0.000+00	0.000+00	1.427+03	0.000+00	0.000+00
19	37	1.560+03	4.849+08	5.306−01	2.725+00	0.000+00	0.000+00	0.000+00
19	38	1.560+03	0.000+00	0.000+00	0.000+00	0.000+00	0.000+00	7.183−04
19	40	1.558+03	0.000+00	0.000+00	0.000+00	7.528+03	0.000+00	0.000+00
19	48	1.558+03	0.000+00	0.000+00	0.000+00	0.000+00	0.000+00	5.436−03
19	49	1.543+03	0.000+00	0.000+00	0.000+00	0.000+00	2.411−04	0.000+00
20	21	5.968+06	0.000+00	0.000+00	0.000+00	1.456−14	6.336−08	0.000+00
20	22	1.639+05	2.670−01	3.584−07	5.800−04	0.000+00	0.000+00	0.000+00
20	23	4.288+04	7.469+04	2.058−02	8.715+00	0.000+00	0.000+00	2.411−10
20	24	4.287+04	1.343+05	6.166−02	2.610+01	0.000+00	0.000+00	3.508−09
20	25	4.278+04	0.000+00	0.000+00	0.000+00	0.000+00	0.000+00	2.528−10
20	26	4.101+04	0.000+00	0.000+00	0.000+00	2.527−04	3.899−11	0.000+00
20	27	4.104+04	0.000+00	0.000+00	0.000+00	2.393−04	0.000+00	0.000+00
20	29	4.092+04	0.000+00	0.000+00	0.000+00	1.222−04	0.000+00	0.000+00
20	30	4.025+04	2.219+02	8.983−05	3.571−02	0.000+00	0.000+00	4.805−09
20	31	2.778+04	0.000+00	0.000+00	0.000+00	9.608−07	2.391−05	0.000+00
20	32	1.654+03	1.931+08	7.913−02	1.292+00	0.000+00	0.000+00	2.558−03
20	33	1.589+03	0.000+00	0.000+00	0.000+00	0.000+00	2.911−07	0.000+00
20	34	1.589+03	0.000+00	0.000+00	0.000+00	1.783+03	6.573−06	0.000+00
20	35	1.589+03	0.000+00	0.000+00	0.000+00	3.208+03	1.227−04	0.000+00
20	36	1.578+03	1.319+04	1.641−06	2.558−05	0.000+00	0.000+00	0.000+00
20	37	1.560+03	3.637+08	1.327−01	2.044+00	0.000+00	0.000+00	8.867−04
20	38	1.560+03	6.538+08	3.975−01	6.123+00	0.000+00	0.000+00	1.299−02
20	39	1.560+03	0.000+00	0.000+00	0.000+00	0.000+00	0.000+00	9.203−04
20	40	1.558+03	0.000+00	0.000+00	0.000+00	7.527+03	1.831−07	0.000+00
20	41	1.558+03	0.000+00	0.000+00	0.000+00	7.747+03	0.000+00	0.000+00

Table 2: Transition wavelengths (λ_{ij} in Å), radiative rates (A_{ji} in s^{-1}), oscillator strengths (f_{ij}, dimensionless), and line strengths (S, in atomic units) for electric dipole (E1), and A_{ji} for E2, M1, and M2 transitions of C V. ($a{\pm}b \equiv a{\times}10^{\pm b}$).

i	j	λ_{ij}	A^{E1}_{ji}	f^{E1}_{ij}	S^{E1}	A^{E2}_{ji}	A^{M1}_{ij}	A^{M2}_{ji}
20	43	1.558+03	0.000+00	0.000+00	0.000+00	0.000+00	0.000+00	6.031−13
20	45	1.558+03	0.000+00	0.000+00	0.000+00	3.006+03	0.000+00	0.000+00
20	48	1.558+03	6.992+05	4.240−04	6.523−03	0.000+00	0.000+00	1.275−02
20	49	1.543+03	0.000+00	0.000+00	0.000+00	4.772−01	1.967−04	0.000+00
21	22	1.685+05	0.000+00	0.000+00	0.000+00	0.000+00	0.000+00	2.288−11
21	23	4.318+04	4.866+03	8.162−04	5.801−01	0.000+00	0.000+00	6.816−17
21	24	4.318+04	4.379+04	1.224−02	8.696+00	0.000+00	0.000+00	1.448−09
21	25	4.309+04	1.766+05	6.880−02	4.879+01	0.000+00	0.000+00	1.166−08
21	26	4.129+04	0.000+00	0.000+00	0.000+00	3.487−05	4.118−10	0.000+00
21	27	4.132+04	0.000+00	0.000+00	0.000+00	1.145−04	1.010−10	0.000+00
21	28	4.125+04	0.000+00	0.000+00	0.000+00	5.261−04	0.000+00	0.000+00
21	29	4.120+04	0.000+00	0.000+00	0.000+00	6.011−05	3.231−11	0.000+00
21	30	4.052+04	9.845+01	2.423−05	1.616−02	0.000+00	0.000+00	3.567−09
21	31	2.791+04	0.000+00	0.000+00	0.000+00	3.173−07	2.037−05	0.000+00
21	32	1.654+03	3.221+08	7.926−02	2.158+00	0.000+00	0.000+00	7.799−03
21	33	1.590+03	0.000+00	0.000+00	0.000+00	7.130+03	0.000+00	0.000+00
21	34	1.590+03	0.000+00	0.000+00	0.000+00	5.347+03	1.959−04	0.000+00
21	35	1.589+03	0.000+00	0.000+00	0.000+00	2.495+03	1.612−05	0.000+00
21	36	1.578+03	0.000+00	0.000+00	0.000+00	0.000+00	0.000+00	1.201−02
21	37	1.560+03	2.424+07	5.308−03	1.363−01	0.000+00	0.000+00	4.619−11
21	38	1.560+03	2.179+08	7.953−02	2.043+00	0.000+00	0.000+00	5.573−03
21	39	1.560+03	8.728+08	4.459−01	1.145+01	0.000+00	0.000+00	4.397−02
21	40	1.559+03	0.000+00	0.000+00	0.000+00	1.074+03	2.003−07	0.000+00
21	41	1.559+03	0.000+00	0.000+00	0.000+00	3.839+03	2.704−07	0.000+00
21	42	1.559+03	0.000+00	0.000+00	0.000+00	1.612+04	0.000+00	0.000+00
21	43	1.559+03	4.056−01	2.068−10	5.307−09	0.000+00	0.000+00	1.248−11
21	44	1.559+03	0.000+00	0.000+00	0.000+00	0.000+00	0.000+00	3.065−13
21	45	1.559+03	0.000+00	0.000+00	0.000+00	1.534+03	2.482−08	0.000+00
21	47	1.559+03	0.000+00	0.000+00	0.000+00	0.000+00	0.000+00	8.345−12
21	48	1.558+03	3.303+05	1.202−04	3.083−03	0.000+00	0.000+00	9.811−03
21	49	1.543+03	0.000+00	0.000+00	0.000+00	1.399−01	2.801−04	0.000+00
22	23	5.806+04	0.000+00	0.000+00	0.000+00	0.000+00	2.866−12	0.000+00
22	24	5.805+04	0.000+00	0.000+00	0.000+00	2.857−07	0.000+00	0.000+00
22	26	5.469+04	0.000+00	0.000+00	0.000+00	0.000+00	0.000+00	4.398−19
22	30	5.335+04	0.000+00	0.000+00	0.000+00	2.357−04	0.000+00	0.000+00
22	31	3.345+04	3.842+05	1.933−01	2.129+01	0.000+00	0.000+00	0.000+00
22	32	1.670+03	0.000+00	0.000+00	0.000+00	0.000+00	2.187−05	0.000+00
22	34	1.605+03	1.496+04	1.732−05	9.149−05	0.000+00	0.000+00	0.000+00
22	35	1.604+03	0.000+00	0.000+00	0.000+00	0.000+00	0.000+00	9.037−03
22	37	1.575+03	0.000+00	0.000+00	0.000+00	0.000+00	5.587−08	0.000+00
22	38	1.575+03	0.000+00	0.000+00	0.000+00	1.462+01	0.000+00	0.000+00
22	40	1.573+03	0.000+00	0.000+00	0.000+00	0.000+00	0.000+00	7.696−12
22	48	1.573+03	0.000+00	0.000+00	0.000+00	9.612+03	0.000+00	0.000+00
22	49	1.558+03	4.664+08	5.089−01	2.609+00	0.000+00	0.000+00	0.000+00
23	24	2.084+08	0.000+00	0.000+00	0.000+00	1.152−22	2.673−12	0.000+00
23	25	1.969+07	0.000+00	0.000+00	0.000+00	1.249−18	0.000+00	0.000+00
23	26	9.422+05	8.800+00	1.952−03	1.816+01	0.000+00	0.000+00	2.026−16
23	27	9.569+05	0.000+00	0.000+00	0.000+00	0.000+00	0.000+00	2.132−17
23	29	8.972+05	0.000+00	0.000+00	0.000+00	0.000+00	0.000+00	4.290−16
23	30	6.571+05	0.000+00	0.000+00	0.000+00	6.872−13	1.619−07	0.000+00

Table 2: Transition wavelengths (λ_{ij} in Å), radiative rates (A_{ji} in s^{-1}), oscillator strengths (f_{ij}, dimensionless), and line strengths (S, in atomic units) for electric dipole (E1), and A_{ji} for E2, M1, and M2 transitions of C V. ($a{\pm}b \equiv a{\times}10^{\pm b}$).

i	j	λ_{ij}	A^{E1}_{ji}	f^{E1}_{ij}	S^{E1}	A^{E2}_{ji}	A^{M1}_{ij}	A^{M2}_{ji}
23	31	7.891+04	3.326−01	3.104−07	2.419−04	0.000+00	0.000+00	5.460−12
23	32	1.720+03	0.000+00	0.000+00	0.000+00	1.145+03	1.420−06	0.000+00
23	33	1.650+03	1.491+08	2.029−02	3.308−01	0.000+00	0.000+00	0.000+00
23	34	1.650+03	3.731+07	1.523−02	2.483−01	0.000+00	0.000+00	8.136−05
23	35	1.650+03	1.486+06	1.011−03	1.647−02	0.000+00	0.000+00	6.928−11
23	36	1.638+03	0.000+00	0.000+00	0.000+00	0.000+00	5.732−09	0.000+00
23	37	1.619+03	0.000+00	0.000+00	0.000+00	1.452+03	7.136−06	0.000+00
23	38	1.619+03	0.000+00	0.000+00	0.000+00	1.451+03	5.239−07	0.000+00
23	39	1.619+03	0.000+00	0.000+00	0.000+00	1.184+02	0.000+00	0.000+00
23	40	1.617+03	1.357+09	8.868−01	1.416+01	0.000+00	0.000+00	1.061−02
23	41	1.617+03	0.000+00	0.000+00	0.000+00	0.000+00	0.000+00	7.143−04
23	43	1.617+03	0.000+00	0.000+00	0.000+00	1.212+04	0.000+00	0.000+00
23	45	1.617+03	0.000+00	0.000+00	0.000+00	0.000+00	0.000+00	1.808−02
23	48	1.617+03	0.000+00	0.000+00	0.000+00	2.213+00	1.940−05	0.000+00
23	49	1.600+03	6.654+02	2.555−07	4.039−06	0.000+00	0.000+00	2.965−05
24	25	2.175+07	0.000+00	0.000+00	0.000+00	7.599−18	1.743−09	0.000+00
24	26	9.464+05	1.605+00	2.155−04	3.357+00	0.000+00	0.000+00	5.449−17
24	27	9.613+05	6.152+00	1.193−03	1.888+01	0.000+00	0.000+00	2.205−16
24	28	9.226+05	0.000+00	0.000+00	0.000+00	0.000+00	0.000+00	5.740−17
24	29	9.011+05	3.177+00	5.414−04	8.031+00	0.000+00	0.000+00	1.324−15
24	30	6.592+05	0.000+00	0.000+00	0.000+00	4.818−13	3.104−08	0.000+00
24	31	7.894+04	6.922+01	3.879−05	5.040−02	0.000+00	0.000+00	7.320−11
24	32	1.720+03	0.000+00	0.000+00	0.000+00	1.904+03	3.579−07	0.000+00
24	33	1.650+03	0.000+00	0.000+00	0.000+00	0.000+00	0.000+00	3.215−04
24	34	1.650+03	1.117+08	2.736−02	7.432−01	0.000+00	0.000+00	1.967−03
24	35	1.650+03	2.228+07	9.095−03	2.470−01	0.000+00	0.000+00	5.042−04
24	36	1.638+03	0.000+00	0.000+00	0.000+00	1.043+01	0.000+00	0.000+00
24	37	1.619+03	0.000+00	0.000+00	0.000+00	2.417+03	1.584−08	0.000+00
24	38	1.619+03	0.000+00	0.000+00	0.000+00	1.041+03	1.488−05	0.000+00
24	39	1.619+03	0.000+00	0.000+00	0.000+00	1.184+03	1.137−05	0.000+00
24	40	1.617+03	2.508+08	9.835−02	2.618+00	0.000+00	0.000+00	2.917−03
24	41	1.617+03	1.084+09	5.951−01	1.584+01	0.000+00	0.000+00	1.609−02
24	42	1.617+03	0.000+00	0.000+00	0.000+00	0.000+00	0.000+00	2.705−03
24	43	1.617+03	0.000+00	0.000+00	0.000+00	3.361+03	2.191−07	0.000+00
24	44	1.617+03	0.000+00	0.000+00	0.000+00	7.702+03	0.000+00	0.000+00
24	45	1.617+03	3.521+08	1.933−01	5.144+00	0.000+00	0.000+00	5.214−02
24	47	1.617+03	0.000+00	0.000+00	0.000+00	5.399+03	0.000+00	0.000+00
24	48	1.617+03	0.000+00	0.000+00	0.000+00	2.320+00	1.537−06	0.000+00
24	49	1.600+03	1.598+05	3.682−05	9.699−04	0.000+00	0.000+00	3.979−04
25	26	9.895+05	4.016−02	4.210−06	9.600−02	0.000+00	0.000+00	6.925−25
25	27	1.006+06	6.305−01	9.562−05	2.216+00	0.000+00	0.000+00	2.134−18
25	28	9.635+05	9.795+00	1.753−03	3.891+01	0.000+00	0.000+00	2.114−15
25	29	9.401+05	3.996−01	5.293−05	1.147+00	0.000+00	0.000+00	3.659−16
25	30	6.798+05	0.000+00	0.000+00	0.000+00	6.630−13	1.431−07	0.000+00
25	31	7.922+04	0.000+00	0.000+00	0.000+00	0.000+00	0.000+00	4.559−10
25	32	1.720+03	0.000+00	0.000+00	0.000+00	2.671+03	0.000+00	0.000+00
25	34	1.650+03	0.000+00	0.000+00	0.000+00	0.000+00	0.000+00	1.967−04
25	35	1.650+03	1.251+08	3.647−02	1.387+00	0.000+00	0.000+00	5.634−03
25	37	1.619+03	0.000+00	0.000+00	0.000+00	2.765+02	0.000+00	0.000+00
25	38	1.619+03	0.000+00	0.000+00	0.000+00	1.658+03	1.421−05	0.000+00

Table 2: Transition wavelengths (λ_{ij} in $\AA$), radiative rates (A_{ji} in s^{-1}), oscillator strengths (f_{ij}, dimensionless), and line strengths (S, in atomic units) for electric dipole (E1), and A_{ji} for E2, M1, and M2 transitions of C V. ($a{\pm}b \equiv a{\times}10^{\pm b}$).

i	j	λ_{ij}	A^{E1}_{ji}	f^{E1}_{ij}	S^{E1}	A^{E2}_{ji}	A^{M1}_{ij}	A^{M2}_{ji}
25	39	1.619+03	0.000+00	0.000+00	0.000+00	2.846+03	2.714−05	0.000+00
25	40	1.617+03	7.179+06	2.011−03	7.494−02	0.000+00	0.000+00	1.717−12
25	41	1.617+03	1.282+08	5.029−02	1.875+00	0.000+00	0.000+00	4.266−04
25	42	1.617+03	1.615+09	8.144−01	3.035+01	0.000+00	0.000+00	1.237−01
25	43	1.617+03	0.000+00	0.000+00	0.000+00	2.244+02	7.167−08	0.000+00
25	44	1.617+03	0.000+00	0.000+00	0.000+00	1.417+03	4.709−07	0.000+00
25	45	1.617+03	5.124+07	2.009−02	7.487−01	0.000+00	0.000+00	1.866−02
25	46	1.617+03	0.000+00	0.000+00	0.000+00	1.571+04	0.000+00	0.000+00
25	47	1.617+03	0.000+00	0.000+00	0.000+00	1.202+03	6.613−10	0.000+00
25	48	1.617+03	0.000+00	0.000+00	0.000+00	2.527+00	4.847−05	0.000+00
25	49	1.601+03	0.000+00	0.000+00	0.000+00	0.000+00	0.000+00	2.530−03
26	28	3.668+07	0.000+00	0.000+00	0.000+00	7.397−21	0.000+00	0.000+00
26	29	1.882+07	0.000+00	0.000+00	0.000+00	1.917−18	1.315−09	0.000+00
26	30	2.172+06	2.460−04	1.739−07	6.216−03	0.000+00	0.000+00	4.774−19
26	31	8.612+04	0.000+00	0.000+00	0.000+00	2.845−10	2.939−13	0.000+00
26	32	1.723+03	1.779−01	4.751−11	1.347−09	0.000+00	0.000+00	1.581−13
26	33	1.653+03	0.000+00	0.000+00	0.000+00	7.983+02	0.000+00	0.000+00
26	34	1.653+03	0.000+00	0.000+00	0.000+00	2.661+02	1.903−09	0.000+00
26	35	1.653+03	0.000+00	0.000+00	0.000+00	2.280+01	5.363−09	0.000+00
26	36	1.641+03	0.000+00	0.000+00	0.000+00	0.000+00	0.000+00	3.983−12
26	37	1.622+03	3.208+07	7.588−03	2.025−01	0.000+00	0.000+00	2.494−04
26	38	1.622+03	3.560+06	1.403−03	3.745−02	0.000+00	0.000+00	4.093−05
26	39	1.622+03	7.258+04	4.005−05	1.069−03	0.000+00	0.000+00	4.343−12
26	40	1.620+03	0.000+00	0.000+00	0.000+00	1.639+03	1.168−05	0.000+00
26	41	1.620+03	0.000+00	0.000+00	0.000+00	3.661+02	2.603−08	0.000+00
26	42	1.620+03	0.000+00	0.000+00	0.000+00	1.895+01	0.000+00	0.000+00
26	43	1.620+03	2.443+09	1.346+00	3.588+01	0.000+00	0.000+00	5.595−02
26	44	1.620+03	0.000+00	0.000+00	0.000+00	0.000+00	0.000+00	5.197−03
26	45	1.620+03	0.000+00	0.000+00	0.000+00	1.462+02	2.591−06	0.000+00
26	47	1.620+03	0.000+00	0.000+00	0.000+00	0.000+00	0.000+00	3.122−02
26	48	1.619+03	5.303+03	2.085−06	5.557−05	0.000+00	0.000+00	2.278−05
26	49	1.603+03	0.000+00	0.000+00	0.000+00	6.296−03	1.339−10	0.000+00
27	28	2.293+07	0.000+00	0.000+00	0.000+00	1.119−18	1.106−09	0.000+00
27	29	1.439+07	0.000+00	0.000+00	0.000+00	1.410−18	1.698−10	0.000+00
27	30	2.097+06	4.023−01	1.895−04	9.155+00	0.000+00	0.000+00	1.050−18
27	31	8.600+04	0.000+00	0.000+00	0.000+00	1.024−05	0.000+00	0.000+00
27	32	1.723+03	0.000+00	0.000+00	0.000+00	0.000+00	0.000+00	6.627−13
27	34	1.653+03	0.000+00	0.000+00	0.000+00	3.539+02	0.000+00	0.000+00
27	35	1.653+03	0.000+00	0.000+00	0.000+00	1.051+02	7.201−11	0.000+00
27	37	1.622+03	0.000+00	0.000+00	0.000+00	0.000+00	0.000+00	3.972−05
27	38	1.622+03	1.989+07	5.600−03	2.093−01	0.000+00	0.000+00	2.510−04
27	39	1.622+03	1.676+06	6.605−04	2.468−02	0.000+00	0.000+00	2.176−06
27	40	1.620+03	0.000+00	0.000+00	0.000+00	4.727+02	3.978−06	0.000+00
27	41	1.620+03	0.000+00	0.000+00	0.000+00	1.634+03	1.198−05	0.000+00
27	42	1.620+03	0.000+00	0.000+00	0.000+00	2.735+02	3.100−06	0.000+00
27	43	1.620+03	1.409+08	5.543−02	2.069+00	0.000+00	0.000+00	9.251−03
27	44	1.620+03	2.523+09	1.276+00	4.763+01	0.000+00	0.000+00	5.925−02
27	45	1.620+03	0.000+00	0.000+00	0.000+00	6.772+01	3.845−07	0.000+00
27	46	1.620+03	0.000+00	0.000+00	0.000+00	0.000+00	0.000+00	2.998−02
27	47	1.620+03	2.815+07	1.424−02	5.314−01	0.000+00	0.000+00	1.042−02

Table 2: Transition wavelengths (λ_{ij} in Å), radiative rates (A_{ji} in s^{-1}), oscillator strengths (f_{ij}, dimensionless), and line strengths (S, in atomic units) for electric dipole (E1), and A_{ji} for E2, M1, and M2 transitions of C V. ($a{\pm}b \equiv a{\times}10^{\pm b}$).

i	j	λ_{ij}	A^{E1}_{ji}	f^{E1}_{ij}	S^{E1}	A^{E2}_{ji}	A^{M1}_{ij}	A^{M2}_{ji}
27	48	1.619+03	9.624+06	2.702−03	1.008−01	0.000+00	0.000+00	4.252−05
27	49	1.603+03	0.000+00	0.000+00	0.000+00	2.437+02	0.000+00	0.000+00
28	29	3.864+07	0.000+00	0.000+00	0.000+00	5.470−20	1.532−10	0.000+00
28	30	2.308+06	0.000+00	0.000+00	0.000+00	0.000+00	0.000+00	1.034−17
28	35	1.653+03	0.000+00	0.000+00	0.000+00	6.154+02	0.000+00	0.000+00
28	38	1.622+03	0.000+00	0.000+00	0.000+00	0.000+00	0.000+00	6.700−05
28	39	1.622+03	2.944+07	9.027−03	4.337−01	0.000+00	0.000+00	2.243−03
28	40	1.620+03	0.000+00	0.000+00	0.000+00	3.414+01	0.000+00	0.000+00
28	41	1.620+03	0.000+00	0.000+00	0.000+00	3.812+02	9.492−06	0.000+00
28	42	1.620+03	0.000+00	0.000+00	0.000+00	1.956+03	2.870−05	0.000+00
28	43	1.620+03	3.393+06	1.038−03	4.984−02	0.000+00	0.000+00	7.437−14
28	44	1.620+03	8.998+07	3.540−02	1.699+00	0.000+00	0.000+00	5.491−06
28	45	1.620+03	0.000+00	0.000+00	0.000+00	1.523+02	5.694−06	0.000+00
28	46	1.620+03	2.660+09	1.279+00	6.140+01	0.000+00	0.000+00	3.021−01
28	47	1.620+03	7.629+07	3.001−02	1.441+00	0.000+00	0.000+00	2.637−02
28	48	1.619+03	0.000+00	0.000+00	0.000+00	0.000+00	0.000+00	6.645−04
29	30	2.455+06	5.768−01	3.722−04	2.106+01	0.000+00	0.000+00	1.333−17
29	31	8.652+04	0.000+00	0.000+00	0.000+00	1.956−05	0.000+00	0.000+00
29	32	1.723+03	0.000+00	0.000+00	0.000+00	0.000+00	0.000+00	9.085−12
29	34	1.653+03	0.000+00	0.000+00	0.000+00	1.782+02	0.000+00	0.000+00
29	35	1.653+03	0.000+00	0.000+00	0.000+00	5.441+01	5.916−10	0.000+00
29	37	1.622+03	0.000+00	0.000+00	0.000+00	0.000+00	0.000+00	5.794−04
29	38	1.622+03	8.627+06	2.429−03	9.079−02	0.000+00	0.000+00	1.106−03
29	39	1.622+03	8.680+05	3.422−04	1.279−02	0.000+00	0.000+00	2.672−04
29	40	1.620+03	0.000+00	0.000+00	0.000+00	2.445+02	1.216−05	0.000+00
29	41	1.620+03	0.000+00	0.000+00	0.000+00	9.661+00	1.774−06	0.000+00
29	42	1.620+03	0.000+00	0.000+00	0.000+00	1.415+02	4.827−10	0.000+00
29	43	1.620+03	7.288+07	2.868−02	1.071+00	0.000+00	0.000+00	7.562−05
29	44	1.620+03	4.774+07	2.415−02	9.017−01	0.000+00	0.000+00	8.887−04
29	45	1.620+03	0.000+00	0.000+00	0.000+00	2.024+03	2.731−05	0.000+00
29	46	1.620+03	0.000+00	0.000+00	0.000+00	0.000+00	0.000+00	1.852−02
29	47	1.620+03	2.556+09	1.293+00	4.827+01	0.000+00	0.000+00	2.825−01
29	48	1.620+03	2.180+07	6.121−03	2.284−01	0.000+00	0.000+00	1.154−03
29	49	1.603+03	0.000+00	0.000+00	0.000+00	4.797+02	0.000+00	0.000+00
30	31	8.968+04	3.201+04	2.315−02	3.418+01	0.000+00	0.000+00	1.248−10
30	32	1.724+03	0.000+00	0.000+00	0.000+00	3.538+00	6.369−09	0.000+00
30	33	1.654+03	0.000+00	0.000+00	0.000+00	0.000+00	0.000+00	2.559−03
30	34	1.654+03	1.544+05	3.802−05	1.035−03	0.000+00	0.000+00	2.010−03
30	35	1.654+03	4.203+04	1.724−05	4.695−04	0.000+00	0.000+00	9.252−04
30	36	1.642+03	0.000+00	0.000+00	0.000+00	5.644+03	0.000+00	0.000+00
30	37	1.623+03	0.000+00	0.000+00	0.000+00	4.480+00	7.359−05	0.000+00
30	38	1.623+03	0.000+00	0.000+00	0.000+00	1.286+00	1.329−05	0.000+00
30	39	1.623+03	0.000+00	0.000+00	0.000+00	2.194+00	9.297−06	0.000+00
30	40	1.621+03	4.652+05	1.833−04	4.891−03	0.000+00	0.000+00	1.622−03
30	41	1.621+03	4.036+08	2.226−01	5.941+00	0.000+00	0.000+00	9.963−04
30	42	1.621+03	0.000+00	0.000+00	0.000+00	0.000+00	0.000+00	2.649−02
30	43	1.621+03	0.000+00	0.000+00	0.000+00	6.179+00	3.208−07	0.000+00
30	44	1.621+03	0.000+00	0.000+00	0.000+00	6.542+03	0.000+00	0.000+00
30	45	1.621+03	1.214+09	6.693−01	1.786+01	0.000+00	0.000+00	6.084−02
30	47	1.621+03	0.000+00	0.000+00	0.000+00	9.042+03	0.000+00	0.000+00

Table 2: Transition wavelengths (λ_{ij} in $\mathring{A}$), radiative rates (A_{ji} in s^{-1}), oscillator strengths (f_{ij}, dimensionless), and line strengths (S, in atomic units) for electric dipole (E1), and A_{ji} for E2, M1, and M2 transitions of C V. ($a{\pm}b \equiv a{\times}10^{\pm b}$).

i	j	λ_{ij}	A^{E1}_{ji}	f^{E1}_{ij}	S^{E1}	A^{E2}_{ji}	A^{M1}_{ij}	A^{M2}_{ji}
30	48	1.621+03	0.000+00	0.000+00	0.000+00	4.167+03	1.651−05	0.000+00
30	49	1.604+03	1.088+08	2.520−02	6.656−01	0.000+00	0.000+00	1.325−03
31	32	1.758+03	6.664+03	3.088−06	5.362−05	0.000+00	0.000+00	6.298−03
31	33	1.686+03	0.000+00	0.000+00	0.000+00	0.000+00	7.129−04	0.000+00
31	34	1.686+03	0.000+00	0.000+00	0.000+00	4.647−01	2.193−04	0.000+00
31	35	1.685+03	0.000+00	0.000+00	0.000+00	8.762−02	6.337−05	0.000+00
31	36	1.673+03	6.216+08	8.693−02	1.436+00	0.000+00	0.000+00	0.000+00
31	37	1.653+03	1.110+04	4.545−06	7.418−05	0.000+00	0.000+00	4.339−04
31	38	1.653+03	1.171+06	7.990−04	1.304−02	0.000+00	0.000+00	3.541−03
31	39	1.653+03	0.000+00	0.000+00	0.000+00	0.000+00	0.000+00	1.582−02
31	40	1.651+03	0.000+00	0.000+00	0.000+00	1.818−01	2.098−07	0.000+00
31	41	1.651+03	0.000+00	0.000+00	0.000+00	4.004+03	0.000+00	0.000+00
31	43	1.651+03	0.000+00	0.000+00	0.000+00	0.000+00	0.000+00	2.938−12
31	45	1.651+03	0.000+00	0.000+00	0.000+00	1.022+04	0.000+00	0.000+00
31	48	1.650+03	9.779+08	6.655−01	1.085+01	0.000+00	0.000+00	1.120−02
31	49	1.634+03	0.000+00	0.000+00	0.000+00	7.909+03	8.379−06	0.000+00
32	33	4.079+04	5.286+05	4.396−02	1.771+01	0.000+00	0.000+00	0.000+00
32	34	4.079+04	5.286+05	1.318−01	5.311+01	0.000+00	0.000+00	1.152−08
32	35	4.065+04	5.343+05	2.206−01	8.855+01	0.000+00	0.000+00	2.142−08
32	36	3.449+04	0.000+00	0.000+00	0.000+00	0.000+00	7.476−07	0.000+00
32	37	2.755+04	0.000+00	0.000+00	0.000+00	4.403−02	4.801−08	0.000+00
32	38	2.755+04	0.000+00	0.000+00	0.000+00	4.397−02	1.076−08	0.000+00
32	39	2.753+04	0.000+00	0.000+00	0.000+00	4.419−02	0.000+00	0.000+00
32	40	2.711+04	6.775−03	1.244−09	3.330−07	0.000+00	0.000+00	1.104−16
32	41	2.711+04	0.000+00	0.000+00	0.000+00	0.000+00	0.000+00	1.557−17
32	43	2.709+04	0.000+00	0.000+00	0.000+00	1.158−10	0.000+00	0.000+00
32	45	2.709+04	0.000+00	0.000+00	0.000+00	0.000+00	0.000+00	5.744−16
32	48	2.692+04	0.000+00	0.000+00	0.000+00	7.544−05	4.303−13	0.000+00
32	49	2.306+04	8.070+01	6.434−06	1.465−03	0.000+00	0.000+00	4.011−07
33	34	7.754+08	0.000+00	0.000+00	0.000+00	0.000+00	3.853−14	0.000+00
33	35	1.142+07	0.000+00	0.000+00	0.000+00	1.625−15	0.000+00	0.000+00
33	37	8.489+04	3.512+04	1.138−01	3.181+01	0.000+00	0.000+00	0.000+00
33	38	8.487+04	0.000+00	0.000+00	0.000+00	0.000+00	0.000+00	1.760−11
33	40	8.081+04	0.000+00	0.000+00	0.000+00	8.321−05	0.000+00	0.000+00
33	48	7.912+04	0.000+00	0.000+00	0.000+00	0.000+00	0.000+00	1.892−10
33	49	5.306+04	0.000+00	0.000+00	0.000+00	0.000+00	3.831−06	0.000+00
34	35	1.159+07	0.000+00	0.000+00	0.000+00	3.395−15	8.651−09	0.000+00
34	36	2.231+05	2.480−01	6.168−07	1.359−03	0.000+00	0.000+00	0.000+00
34	37	8.490+04	2.634+04	2.847−02	2.387+01	0.000+00	0.000+00	2.168−11
34	38	8.488+04	4.739+04	8.530−02	7.151+01	0.000+00	0.000+00	3.182−10
34	39	8.471+04	0.000+00	0.000+00	0.000+00	0.000+00	0.000+00	2.272−11
34	40	8.082+04	0.000+00	0.000+00	0.000+00	8.318−05	9.099−12	0.000+00
34	41	8.086+04	0.000+00	0.000+00	0.000+00	8.534−05	0.000+00	0.000+00
34	43	8.062+04	0.000+00	0.000+00	0.000+00	0.000+00	0.000+00	2.609−22
34	45	8.062+04	0.000+00	0.000+00	0.000+00	3.366−05	0.000+00	0.000+00
34	48	7.913+04	6.406+01	1.002−04	7.830−02	0.000+00	0.000+00	4.437−10
34	49	5.306+04	0.000+00	0.000+00	0.000+00	2.218−07	3.349−06	0.000+00
35	36	2.275+05	0.000+00	0.000+00	0.000+00	0.000+00	0.000+00	1.260−11
35	37	8.553+04	1.716+03	1.129−03	1.589+00	0.000+00	0.000+00	5.612−18
35	38	8.551+04	1.544+04	1.693−02	2.383+01	0.000+00	0.000+00	1.316−10

Table 2: Transition wavelengths (λ_{ij} in Å), radiative rates (A_{ji} in s^{-1}), oscillator strengths (f_{ij}, dimensionless), and line strengths (S, in atomic units) for electric dipole (E1), and A_{ji} for E2, M1, and M2 transitions of C V. ($a{\pm}b \equiv a{\times}10^{\pm b}$).

i	j	λ_{ij}	A^{E1}_{ji}	f^{E1}_{ij}	S^{E1}	A^{E2}_{ji}	A^{M1}_{ij}	A^{M2}_{ji}
35	39	8.534+04	6.225+04	9.514−02	1.336+02	0.000+00	0.000+00	1.048−09
35	40	8.138+04	0.000+00	0.000+00	0.000+00	1.147−05	8.946−11	0.000+00
35	41	8.143+04	0.000+00	0.000+00	0.000+00	4.088−05	2.085−11	0.000+00
35	42	8.129+04	0.000+00	0.000+00	0.000+00	1.731−04	0.000+00	0.000+00
35	43	8.119+04	4.804−06	6.646−12	8.881−09	0.000+00	0.000+00	2.388−20
35	44	8.123+04	0.000+00	0.000+00	0.000+00	0.000+00	0.000+00	6.496−21
35	45	8.118+04	0.000+00	0.000+00	0.000+00	1.658−05	5.668−12	0.000+00
35	47	8.110+04	0.000+00	0.000+00	0.000+00	0.000+00	0.000+00	7.443−20
35	48	7.967+04	2.915+01	2.773−05	3.637−02	0.000+00	0.000+00	3.299−10
35	49	5.330+04	0.000+00	0.000+00	0.000+00	7.670−08	2.791−06	0.000+00
36	37	1.370+05	0.000+00	0.000+00	0.000+00	0.000+00	1.226−13	0.000+00
36	38	1.370+05	0.000+00	0.000+00	0.000+00	2.104−08	0.000+00	0.000+00
36	40	1.267+05	0.000+00	0.000+00	0.000+00	0.000+00	0.000+00	2.437−20
36	48	1.226+05	0.000+00	0.000+00	0.000+00	2.408−05	0.000+00	0.000+00
36	49	6.961+04	1.016+05	2.215−01	5.077+01	0.000+00	0.000+00	0.000+00
37	38	3.816+08	0.000+00	0.000+00	0.000+00	4.024−23	4.356−13	0.000+00
37	39	3.848+07	0.000+00	0.000+00	0.000+00	3.152−19	0.000+00	0.000+00
37	40	1.680+06	5.545+00	3.909−03	6.485+01	0.000+00	0.000+00	4.017−17
37	41	1.700+06	0.000+00	0.000+00	0.000+00	0.000+00	0.000+00	2.552−18
37	43	1.600+06	0.000+00	0.000+00	0.000+00	2.119−11	0.000+00	0.000+00
37	45	1.598+06	0.000+00	0.000+00	0.000+00	0.000+00	0.000+00	8.785−17
37	48	1.164+06	0.000+00	0.000+00	0.000+00	2.328−13	2.402−08	0.000+00
37	49	1.415+05	1.529−01	4.587−07	6.409−04	0.000+00	0.000+00	7.985−13
38	39	4.280+07	0.000+00	0.000+00	0.000+00	1.852−18	2.288−10	0.000+00
38	40	1.687+06	1.012+00	4.318−04	1.199+01	0.000+00	0.000+00	1.074−17
38	41	1.707+06	4.200+00	2.569−03	7.218+01	0.000+00	0.000+00	5.612−17
38	42	1.648+06	0.000+00	0.000+00	0.000+00	0.000+00	0.000+00	1.098−17
38	43	1.607+06	0.000+00	0.000+00	0.000+00	5.756−12	1.087−16	0.000+00
38	44	1.624+06	0.000+00	0.000+00	0.000+00	1.241−11	0.000+00	0.000+00
38	45	1.605+06	1.675+00	9.055−04	2.392+01	0.000+00	0.000+00	2.503−16
38	47	1.572+06	0.000+00	0.000+00	0.000+00	1.042−11	0.000+00	0.000+00
38	48	1.167+06	0.000+00	0.000+00	0.000+00	1.623−13	4.633−09	0.000+00
38	49	1.415+05	2.613+01	4.708−05	1.097−01	0.000+00	0.000+00	1.086−11
39	40	1.756+06	2.565−02	8.472−06	3.429−01	0.000+00	0.000+00	1.279−25
39	41	1.778+06	4.419−01	2.094−04	8.582+00	0.000+00	0.000+00	1.216−18
39	42	1.714+06	6.209+00	3.518−03	1.390+02	0.000+00	0.000+00	4.232−16
39	43	1.670+06	0.000+00	0.000+00	0.000+00	3.173−13	8.249−16	0.000+00
39	44	1.688+06	0.000+00	0.000+00	0.000+00	1.896−12	1.922−16	0.000+00
39	45	1.667+06	2.141−01	8.924−05	3.429+00	0.000+00	0.000+00	7.338−17
39	46	1.646+06	0.000+00	0.000+00	0.000+00	2.385−11	0.000+00	0.000+00
39	47	1.632+06	0.000+00	0.000+00	0.000+00	1.904−12	1.029−16	0.000+00
39	48	1.200+06	0.000+00	0.000+00	0.000+00	2.282−13	2.129−08	0.000+00
39	49	1.420+05	0.000+00	0.000+00	0.000+00	0.000+00	0.000+00	6.678−11
40	42	7.167+07	0.000+00	0.000+00	0.000+00	2.537−21	0.000+00	0.000+00
40	43	3.385+07	4.318−04	1.038−04	5.785+01	0.000+00	0.000+00	2.265−23
40	44	4.353+07	0.000+00	0.000+00	0.000+00	0.000+00	0.000+00	5.981−25
40	45	3.285+07	0.000+00	0.000+00	0.000+00	9.671−19	2.070−10	0.000+00
40	47	2.306+07	0.000+00	0.000+00	0.000+00	0.000+00	0.000+00	8.611−23
40	48	3.789+06	1.360−04	2.927−07	1.826−02	0.000+00	0.000+00	1.066−19
40	49	1.545+05	0.000+00	0.000+00	0.000+00	1.449−10	4.544−14	0.000+00

Table 2: Transition wavelengths (λ_{ij} in Å), radiative rates (A_{ji} in s^{-1}), oscillator strengths (f_{ij}, dimensionless), and line strengths (S, in atomic units) for electric dipole (E1), and A_{ji} for E2, M1, and M2 transitions of C V. ($a{\pm}b \equiv a{\times}10^{\pm b}$).

i	j	λ_{ij}	A^{E1}_{ji}	f^{E1}_{ij}	S^{E1}	A^{E2}_{ji}	A^{M1}_{ij}	A^{M2}_{ji}
41	42	4.794+07	0.000+00	0.000+00	0.000+00	2.962−19	1.311−10	0.000+00
41	43	2.744+07	5.070−05	5.722−06	3.617+00	0.000+00	0.000+00	1.055−23
41	44	3.347+07	4.520−04	9.759−05	7.527+01	0.000+00	0.000+00	2.491−23
41	45	2.678+07	0.000+00	0.000+00	0.000+00	5.600−19	2.395−11	0.000+00
41	46	2.223+07	0.000+00	0.000+00	0.000+00	0.000+00	0.000+00	8.992−23
41	47	1.989+07	6.031−05	4.600−06	2.109+00	0.000+00	0.000+00	1.033−22
41	48	3.692+06	2.196−01	3.205−04	2.727+01	0.000+00	0.000+00	1.065−19
41	49	1.543+05	0.000+00	0.000+00	0.000+00	4.416−06	0.000+00	0.000+00
42	43	6.414+07	8.810−08	4.226−08	8.031−02	0.000+00	0.000+00	2.538−34
42	44	1.109+08	4.525−07	8.339−07	2.740+00	0.000+00	0.000+00	5.896−30
42	45	6.065+07	0.000+00	0.000+00	0.000+00	4.697−20	3.317−11	0.000+00
42	46	4.144+07	2.563−04	8.063−05	9.900+01	0.000+00	0.000+00	4.448−23
42	47	3.400+07	1.330−05	2.306−06	2.323+00	0.000+00	0.000+00	1.044−23
42	48	4.000+06	0.000+00	0.000+00	0.000+00	0.000+00	0.000+00	2.369−18
43	45	1.113+09	3.035−10	5.635−08	1.445+00	0.000+00	0.000+00	2.196−33
43	46	1.171+08	0.000+00	0.000+00	0.000+00	4.364−23	0.000+00	0.000+00
43	47	7.235+07	0.000+00	0.000+00	0.000+00	1.008−20	3.177−11	0.000+00
43	48	4.266+06	0.000+00	0.000+00	0.000+00	9.300−17	4.291−19	0.000+00
43	49	1.552+05	0.000+00	0.000+00	0.000+00	0.000+00	0.000+00	2.077−21
44	45	1.339+08	3.602−07	7.527−07	2.986+00	0.000+00	0.000+00	1.057−27
44	46	6.617+07	0.000+00	0.000+00	0.000+00	1.548−20	4.032−11	0.000+00
44	47	4.904+07	0.000+00	0.000+00	0.000+00	6.242−21	2.839−12	0.000+00
44	48	4.150+06	0.000+00	0.000+00	0.000+00	1.781−13	0.000+00	0.000+00
45	46	1.308+08	0.000+00	0.000+00	0.000+00	0.000+00	0.000+00	1.003−26
45	47	7.738+07	3.720−05	4.294−05	7.657+01	0.000+00	0.000+00	1.783−24
45	48	4.283+06	4.159−01	8.167−04	8.060+01	0.000+00	0.000+00	2.979−18
45	49	1.552+05	0.000+00	0.000+00	0.000+00	1.095−05	0.000+00	0.000+00
46	47	1.894+08	0.000+00	0.000+00	0.000+00	8.346−23	1.776−12	0.000+00
47	48	4.534+06	0.000+00	0.000+00	0.000+00	1.558−13	0.000+00	0.000+00
48	49	1.610+05	1.494+04	3.486−02	9.240+01	0.000+00	0.000+00	1.797−11

Table 3: Comparison of A- values for some transitions of C V. ($a{\pm}b \equiv a{\times}10^{\pm b}$).

i	j	f (GRASP)	A (GRASP)	A (FAC)	A (PD)
1	4	2.1089−05	2.7764+07	1.746+07	2.159+07
1	7	7.0814−01	9.5498+11	9.226+11	9.477+11
1	10	5.0467−06	8.9784+06	6.111+06	6.939+06
1	17	1.7855−01	3.1956+11	2.778+11	3.105+11
2	3	1.5174−02	6.0233+07	7.317+07	5.616+07
2	4	4.5512−02	6.0180+07	7.310+07	5.655+07
2	5	7.6109−02	6.0747+07	7.370+07	5.735+07
2	7	2.1971−06	8.0107+03	....	....
2	9	3.3944−02	1.3141+10	1.304+10	1.376+10
2	10	1.0182−01	1.3140+10	1.304+10	1.375+10
2	11	1.6950−01	1.3126+10	1.303+10	1.374+10
2	17	2.2359−06	2.9981+05	....	2.898+05
3	8	2.1559−02	7.0437+08	6.595+08	7.088+08
3	13	6.5802−01	2.3521+10	2.280+10	2.349+10
4	6	8.6815−08	1.7508+00	1.272−01	....
4	8	2.1518−02	2.1092+09	1.975+09	2.129+09
4	12	4.0427−07	1.2714+05	....	....
4	13	1.6450−01	1.7642+10	1.710+10	1.761+10
4	14	4.9227−01	3.1676+10	3.074+10	3.165+10
4	16	1.2286−03	7.9166+07	3.847+07	5.150+07
5	8	2.1563−02	3.5202+09	3.296+09	3.557+09
5	13	6.5812−03	1.1756+09	1.139+09	1.174+09
5	14	9.8422−02	1.0548+10	1.024+10	1.054+10
5	15	5.5286−01	4.2325+10	4.104+10	4.225+10
5	16	3.0905−04	3.3168+07	1.676+07	2.214+07
6	7	8.5486−02	1.3082+07	....	5.875+06
6	10	1.3083−05	4.4733+05	....	4.013+05
6	17	3.8220−01	1.3641+10	1.303+10	1.457+10
7	8	8.7332−07	7.2973+04	....	....
7	12	2.3527−02	6.3422+09	5.880+09	5.646+09
7	13	4.8143−06	4.4335+05	....	3.673+05
7	14	1.9010−03	1.0504+08	5.065+07	6.862+07
7	16	7.1443−01	3.9534+10	3.794+10	3.950+10

GRASP: Present calculations from the GRASP code
FAC: Present calculations from the FAC code
PD: Porquet and Dubau [12]

Table 4: Collision strengths for resonance transitions of C V. ($a\pm b \equiv a\times10^{\pm b}$).

Transition		Energy (Ryd)					
i	j	30	35	40	45	50	FAC
1	2	5.655−3	4.740−3	4.023−3	3.434−3	2.995−3	3.734−3
1	3	3.019−3	2.469−3	1.968−3	1.585−3	1.300−3	1.648−3
1	4	9.048−3	7.401−3	5.899−3	4.751−3	3.896−3	4.938−3
1	5	1.505−2	1.231−2	9.808−3	7.895−3	6.474−3	8.227−3
1	6	1.597−2	1.783−2	1.913−2	2.007−2	2.104−2	1.858−2
1	7	5.430−2	7.038−2	8.452−2	9.760−2	1.095−1	9.114−2
1	8	2.066−3	1.506−3	1.196−3	9.874−4	8.472−4	8.924−4
1	9	9.399−4	7.665−4	6.070−4	4.868−4	3.982−4	4.282−4
1	10	2.817−3	2.298−3	1.820−3	1.459−3	1.194−3	1.280−3
1	11	4.689−3	3.822−3	3.026−3	2.427−3	1.985−3	2.137−3
1	12	3.324−3	3.722−3	4.052−3	4.310−3	4.603−3	4.018−3
1	13	3.286−4	2.224−4	1.551−4	1.132−4	8.560−5	1.163−4
1	14	5.480−4	3.714−4	2.598−4	1.903−4	1.448−4	1.951−4
1	15	7.650−4	5.174−4	3.608−4	2.632−4	1.991−4	2.710−4
1	16	1.086−3	1.111−3	1.244−3	1.397−3	1.546−3	9.786−4
1	17	9.800−3	1.333−2	1.622−2	1.884−2	2.116−2	1.906−2
1	18	1.097−3	6.993−4	5.244−4	4.227−4	3.531−4	3.398−4
1	19	4.068−4	3.315−4	2.600−4	2.075−4	1.686−4	1.684−4
1	20	1.220−3	9.939−4	7.793−4	6.220−4	5.054−4	5.044−4
1	21	2.030−3	1.654−3	1.296−3	1.035−3	8.405−4	8.403−4
1	22	1.430−3	1.562−3	1.665−3	1.774−3	1.873−3	1.586−3
1	23	1.965−4	1.280−4	8.874−5	6.453−5	4.863−5	6.276−5
1	24	3.275−4	2.135−4	1.482−4	1.079−4	8.155−5	1.049−4
1	25	4.574−4	2.979−4	2.065−4	1.501−4	1.131−4	1.463−4
1	26	1.435−5	6.360−6	3.895−6	2.625−6	1.862−6	2.777−6
1	27	2.846−5	1.533−5	1.173−5	1.014−5	9.290−6	5.486−6
1	28	2.578−5	1.142−5	6.991−6	4.712−6	3.341−6	4.996−6
1	29	4.090−5	2.486−5	2.105−5	1.973−5	1.919−5	7.908−6
1	30	6.710−4	5.732−4	5.986−4	6.519−4	7.110−4	4.712−4
1	31	3.839−3	5.281−3	6.419−3	7.429−3	8.351−3	7.348−3
1	32	6.892−4	3.846−4	2.771−4	2.177−4	1.786−4	1.588−4
1	33	2.248−4	1.744−4	1.343−4	1.061−4	8.559−5	8.080−5
1	34	6.740−4	5.227−4	4.028−4	3.180−4	2.566−4	2.422−4
1	35	1.122−3	8.698−4	6.700−4	5.290−4	4.266−4	4.030−4
1	36	9.085−4	9.259−4	9.722−4	1.019−3	1.059−3	8.354−4
1	37	1.205−4	7.415−5	5.095−5	3.688−5	2.770−5	3.502−5
1	38	2.008−4	1.236−4	8.501−5	6.161−5	4.636−5	5.849−5
1	39	2.804−4	1.725−4	1.185−4	8.577−5	6.442−5	8.163−5
1	40	1.296−5	5.545−6	3.309−6	2.201−6	1.550−6	2.244−6
1	41	2.515−5	1.248−5	8.944−6	7.328−6	6.432−6	4.034−6
1	42	2.328−5	9.957−6	5.942−6	3.951−6	2.783−6	4.037−6
1	43	1.045−6	1.580−7	7.264−8	4.066−8	2.576−8	3.335−8
1	44	2.061−6	5.733−7	3.728−7	3.118−7	3.429−7	5.528−8
1	45	4.262−5	2.423−5	1.966−5	1.789−5	1.703−5	6.454−6
1	46	1.640−6	2.477−7	1.139−7	6.374−8	4.037−8	5.238−8
1	47	2.248−6	6.696−7	4.455−7	3.793−7	4.235−7	5.746−8
1	48	4.403−4	3.267−4	3.265−4	3.483−4	3.763−4	2.509−4
1	49	2.248−3	2.953−3	3.516−3	4.034−3	4.520−3	3.762−3

Table 5: Effective collision strengths for transitions in C V. ($a{\pm}b \equiv a{\times}10^{\pm b}$).

Transition		Temperature (log T_e, K)										
i	j	4.0	4.2	4.4	4.6	4.8	5.0	5.2	5.4	5.6	5.8	6.0
1	2	4.987−2	4.551−2	4.212−2	3.778−2	3.228−2	2.665−2	2.177−2	1.781−2	1.460−2	1.198−2	9.812−3
1	3	5.368−3	5.332−3	5.224−3	5.004−3	4.744−3	4.534−3	4.383−3	4.234−3	4.037−3	3.772−3	3.431−3
1	4	1.625−2	1.608−2	1.572−2	1.504−2	1.425−2	1.361−2	1.316−2	1.271−2	1.212−2	1.132−2	1.029−2
1	5	2.708−2	2.677−2	2.616−2	2.503−2	2.372−2	2.267−2	2.193−2	2.120−2	2.020−2	1.887−2	1.715−2
1	6	1.871−2	1.917−2	1.876−2	1.776−2	1.668−2	1.588−2	1.542−2	1.519−2	1.515−2	1.533−2	1.564−2
1	7	2.674−2	2.708−2	2.740−2	2.785−2	2.866−2	3.000−2	3.183−2	3.420−2	3.746−2	4.223−2	4.836−2
1	8	1.182−2	1.078−2	9.230−3	7.684−3	6.383−3	5.340−3	4.502−3	3.823−3	3.261−3	2.780−3	2.347−3
1	9	1.239−3	1.181−3	1.124−3	1.084−3	1.061−3	1.042−3	1.021−3	9.975−4	9.677−4	9.237−4	8.544−4
1	10	3.800−3	3.590−3	3.396−3	3.265−3	3.189−3	3.129−3	3.065−3	2.993−3	2.902−3	2.770−3	2.562−3
1	11	6.169−3	5.847−3	5.558−3	5.368−3	5.262−3	5.177−3	5.079−3	4.966−3	4.821−3	4.604−3	4.259−3
1	12	5.842−3	5.023−3	4.393−3	3.965−3	3.694−3	3.512−3	3.387−3	3.319−3	3.313−3	3.368−3	3.429−3
1	13	8.990−4	8.040−4	7.301−4	6.931−4	6.780−4	6.556−4	6.120−4	5.526−4	4.872−4	4.207−4	3.540−4
1	14	1.503−3	1.343−3	1.219−3	1.157−3	1.132−3	1.094−3	1.022−3	9.225−4	8.132−4	7.023−4	5.910−4
1	15	2.103−3	1.878−3	1.704−3	1.616−3	1.581−3	1.528−3	1.426−3	1.288−3	1.135−3	9.799−4	8.244−4
1	16	3.493−3	2.978−3	2.602−3	2.387−3	2.266−3	2.143−3	1.975−3	1.779−3	1.595−3	1.449−3	1.342−3
1	17	5.694−3	5.695−3	5.738−3	5.868−3	6.086−3	6.372−3	6.756−3	7.308−3	8.113−3	9.222−3	1.044−2
1	18	2.601−3	2.493−3	2.354−3	2.198−3	2.033−3	1.864−3	1.695−3	1.527−3	1.357−3	1.185−3	1.010−3
1	19	4.795−4	4.585−4	4.438−4	4.328−4	4.234−4	4.159−4	4.105−4	4.052−4	3.963−4	3.797−4	3.509−4
1	20	1.515−3	1.428−3	1.366−3	1.320−3	1.284−3	1.256−3	1.236−3	1.218−3	1.190−3	1.140−3	1.053−3
1	21	2.529−3	2.380−3	2.276−3	2.202−3	2.143−3	2.097−3	2.063−3	2.032−3	1.984−3	1.899−3	1.753−3
1	22	2.238−3	2.020−3	1.862−3	1.743−3	1.645−3	1.567−3	1.511−3	1.480−3	1.473−3	1.485−3	1.491−3
1	23	3.944−4	3.823−4	3.729−4	3.603−4	3.404−4	3.153−4	2.883−4	2.613−4	2.341−4	2.059−4	1.759−4
1	24	6.581−4	6.378−4	6.222−4	6.014−4	5.685−4	5.265−4	4.813−4	4.361−4	3.906−4	3.435−4	2.934−4
1	25	9.187−4	8.905−4	8.692−4	8.408−4	7.953−4	7.367−4	6.735−4	6.100−4	5.462−4	4.801−4	4.099−4
1	26	2.265−4	2.320−4	2.340−4	2.242−4	1.981−4	1.618−4	1.245−4	9.203−5	6.633−5	4.706−5	3.300−5
1	27	4.137−4	4.146−4	4.147−4	3.970−4	3.516−4	2.882−4	2.227−4	1.655−4	1.203−4	8.652−5	6.191−5
1	28	4.074−4	4.174−4	4.216−4	4.044−4	3.577−4	2.924−4	2.251−4	1.663−4	1.199−4	8.502−5	5.959−5
1	29	5.595−4	5.497−4	5.451−4	5.208−4	4.617−4	3.794−4	2.941−4	2.197−4	1.609−4	1.170−4	8.514−5
1	30	2.033−3	1.820−3	1.668−3	1.533−3	1.393−3	1.249−3	1.110−3	9.853−4	8.783−4	7.921−4	7.206−4
1	31	2.206−3	2.252−3	2.338−3	2.443−3	2.557−3	2.695−3	2.883−3	3.143−3	3.492−3	3.942−3	4.397−3
1	32	1.241−3	1.225−3	1.200−3	1.167−3	1.121−3	1.060−3	9.829−4	8.918−4	7.901−4	6.828−4	5.735−4
1	33	2.058−4	2.056−4	2.067−4	2.091−4	2.123−4	2.157−4	2.180−4	2.176−4	2.130−4	2.028−4	1.857−4
1	34	6.395−4	6.310−4	6.291−4	6.328−4	6.404−4	6.491−4	6.551−4	6.535−4	6.392−4	6.084−4	5.568−4
1	35	1.053−3	1.042−3	1.042−3	1.049−3	1.063−3	1.079−3	1.089−3	1.087−3	1.063−3	1.012−3	9.265−4
1	36	9.897−4	9.858−4	9.790−4	9.708−4	9.617−4	9.521−4	9.423−4	9.335−4	9.277−4	9.258−4	9.150−4
1	37	1.737−4	1.748−4	1.743−4	1.721−4	1.679−4	1.616−4	1.531−4	1.424−4	1.296−4	1.148−4	9.827−5
1	38	2.901−4	2.920−4	2.913−4	2.875−4	2.804−4	2.698−4	2.554−4	2.375−4	2.161−4	1.914−4	1.639−4
1	39	4.060−4	4.088−4	4.078−4	4.025−4	3.924−4	3.773−4	3.571−4	3.319−4	3.019−4	2.674−4	2.289−4
1	40	5.883−5	5.606−5	5.206−5	4.715−5	4.168−5	3.597−5	3.034−5	2.505−5	2.026−5	1.603−5	1.239−5
1	41	1.107−4	1.040−4	9.582−5	8.651−5	7.653−5	6.626−5	5.621−5	4.679−5	3.830−5	3.087−5	2.447−5
1	42	1.058−4	1.007−4	9.346−5	8.462−5	7.481−5	6.457−5	5.447−5	4.498−5	3.638−5	2.880−5	2.224−5
1	43	7.456−6	6.969−6	6.399−6	5.769−6	5.086−6	4.356−6	3.599−6	2.856−6	2.175−6	1.595−6	1.133−6
1	44	1.494−5	1.342−5	1.197−5	1.058−5	9.205−6	7.829−6	6.465−6	5.166−6	3.996−6	3.005−6	2.210−6
1	45	1.841−4	1.710−4	1.563−4	1.405−4	1.240−4	1.075−4	9.153−5	7.674−5	6.356−5	5.218−5	4.245−5
1	46	1.169−5	1.089−5	9.988−6	9.003−6	7.942−6	6.808−6	5.629−6	4.468−6	3.405−6	2.498−6	1.774−6
1	47	1.642−5	1.468−5	1.303−5	1.147−5	9.955−6	8.450−6	6.972−6	5.574−6	4.321−6	3.262−6	2.411−6
1	48	9.611−4	9.273−4	8.878−4	8.416−4	7.881−4	7.279−4	6.628−4	5.965−4	5.332−4	4.772−4	4.273−4
1	49	1.256−3	1.307−3	1.369−3	1.445−3	1.537−3	1.649−3	1.782−3	1.940−3	2.131−3	2.360−3	2.573−3
2	3	1.335+0	1.349+0	1.365+0	1.387+0	1.419+0	1.466+0	1.533+0	1.618+0	1.723+0	1.849+0	1.977+0

Table 5: Effective collision strengths for transitions in C V. ($a{\pm}b \equiv a{\times}10^{\pm b}$).

Transition		Temperature (log T_e, K)										
i	j	4.0	4.2	4.4	4.6	4.8	5.0	5.2	5.4	5.6	5.8	6.0
2	4	4.053+0	4.076+0	4.114+0	4.172+0	4.262+0	4.402+0	4.601+0	4.856+0	5.169+0	5.547+0	5.930+0
2	5	6.691+0	6.750+0	6.827+0	6.931+0	7.088+0	7.325+0	7.659+0	8.085+0	8.608+0	9.238+0	9.877+0
2	6	1.454−1	1.490−1	1.445−1	1.343−1	1.237−1	1.164−1	1.112−1	1.047−1	9.482−2	8.228−2	6.887−2
2	7	1.510−1	1.509−1	1.499−1	1.513−1	1.602−1	1.757−1	1.886−1	1.888−1	1.738−1	1.483−1	1.192−1
2	8	7.354−1	6.597−1	5.788−1	5.080−1	4.544−1	4.174−1	3.944−1	3.833−1	3.822−1	3.885−1	3.940−1
2	9	6.802−2	6.056−2	5.337−2	4.784−2	4.410−2	4.171−2	4.053−2	4.094−2	4.365−2	4.923−2	5.661−2
2	10	2.024−1	1.797−1	1.584−1	1.422−1	1.314−1	1.245−1	1.211−1	1.225−1	1.307−1	1.475−1	1.696−1
2	11	3.740−1	3.269−1	2.832−1	2.499−1	2.273−1	2.128−1	2.051−1	2.061−1	2.188−1	2.462−1	2.827−1
2	12	6.160−2	4.819−2	3.736−2	2.961−2	2.420−2	2.004−2	1.646−2	1.328−2	1.052−2	8.192−3	6.256−3
2	13	1.277−1	1.205−1	1.161−1	1.150−1	1.163−1	1.189−1	1.229−1	1.295−1	1.397−1	1.535−1	1.673−1
2	14	2.130−1	2.008−1	1.935−1	1.915−1	1.936−1	1.980−1	2.046−1	2.156−1	2.326−1	2.556−1	2.784−1
2	15	2.988−1	2.816−1	2.711−1	2.683−1	2.713−1	2.775−1	2.869−1	3.023−1	3.262−1	3.584−1	3.904−1
2	16	1.313−1	1.199−1	1.105−1	1.045−1	1.004−1	9.545−2	8.824−2	7.900−2	6.849−2	5.738−2	4.628−2
2	17	4.820−2	4.564−2	4.372−2	4.297−2	4.247−2	4.083−2	3.758−2	3.311−2	2.805−2	2.290−2	1.801−2
2	18	1.023−1	9.666−2	9.105−2	8.586−2	8.111−2	7.715−2	7.437−2	7.296−2	7.287−2	7.373−2	7.405−2
2	19	1.483−2	1.478−2	1.465−2	1.438−2	1.397−2	1.353−2	1.322−2	1.319−2	1.357−2	1.445−2	1.552−2
2	20	4.423−2	4.416−2	4.379−2	4.297−2	4.172−2	4.039−2	3.948−2	3.941−2	4.058−2	4.324−2	4.650−2
2	21	7.451−2	7.412−2	7.334−2	7.188−2	6.972−2	6.744−2	6.586−2	6.570−2	6.761−2	7.202−2	7.741−2
2	22	1.340−2	1.167−2	1.030−2	9.089−3	7.892−3	6.708−3	5.605−3	4.624−3	3.763−3	3.009−3	2.349−3
2	23	2.713−2	2.742−2	2.758−2	2.759−2	2.740−2	2.722−2	2.733−2	2.788−2	2.895−2	3.042−2	3.163−2
2	24	4.527−2	4.573−2	4.595−2	4.592−2	4.557−2	4.526−2	4.544−2	4.639−2	4.817−2	5.064−2	5.267−2
2	25	6.348−2	6.411−2	6.444−2	6.443−2	6.398−2	6.355−2	6.378−2	6.508−2	6.756−2	7.100−2	7.383−2
2	26	2.467−2	2.554−2	2.593−2	2.560−2	2.449−2	2.295−2	2.145−2	2.024−2	1.943−2	1.894−2	1.843−2
2	27	3.535−2	3.591−2	3.593−2	3.501−2	3.299−2	3.032−2	2.766−2	2.538−2	2.357−2	2.220−2	2.091−2
2	28	4.452−2	4.609−2	4.679−2	4.622−2	4.422−2	4.144−2	3.870−2	3.652−2	3.502−2	3.412−2	3.320−2
2	29	3.680−2	3.632−2	3.552−2	3.389−2	3.113−2	2.770−2	2.421−2	2.102−2	1.822−2	1.582−2	1.368−2
2	30	4.857−2	4.630−2	4.424−2	4.189−2	3.890−2	3.541−2	3.169−2	2.787−2	2.393−2	1.993−2	1.599−2
2	31	2.079−2	2.076−2	2.067−2	2.020−2	1.914−2	1.760−2	1.577−2	1.378−2	1.169−2	9.596−3	7.579−3
2	32	4.486−2	4.021−2	3.681−2	3.441−2	3.270−2	3.149−2	3.066−2	3.015−2	2.995−2	2.995−2	2.961−2
2	33	8.215−3	8.124−3	8.014−3	7.887−3	7.740−3	7.576−3	7.415−3	7.299−3	7.287−3	7.433−3	7.619−3
2	34	2.500−2	2.454−2	2.410−2	2.367−2	2.321−2	2.271−2	2.223−2	2.188−2	2.185−2	2.228−2	2.284−2
2	35	4.027−2	3.978−2	3.926−2	3.874−2	3.815−2	3.747−2	3.678−2	3.628−2	3.628−2	3.704−2	3.799−2
2	36	4.191−3	3.923−3	3.698−3	3.495−3	3.284−3	3.042−3	2.758−3	2.434−3	2.082−3	1.720−3	1.370−3
2	37	1.125−2	1.138−2	1.151−2	1.165−2	1.181−2	1.200−2	1.219−2	1.241−2	1.265−2	1.292−2	1.302−2
2	38	1.886−2	1.911−2	1.933−2	1.955−2	1.980−2	2.007−2	2.038−2	2.071−2	2.110−2	2.155−2	2.170−2
2	39	2.662−2	2.705−2	2.739−2	2.766−2	2.794−2	2.826−2	2.864−2	2.908−2	2.960−2	3.021−2	3.041−2
2	40	1.225−2	1.223−2	1.214−2	1.199−2	1.180−2	1.156−2	1.127−2	1.096−2	1.065−2	1.034−2	9.930−3
2	41	1.605−2	1.594−2	1.576−2	1.554−2	1.526−2	1.489−2	1.443−2	1.387−2	1.326−2	1.264−2	1.190−2
2	42	2.191−2	2.180−2	2.162−2	2.138−2	2.107−2	2.068−2	2.021−2	1.968−2	1.913−2	1.859−2	1.786−2
2	43	3.043−3	2.934−3	2.793−3	2.631−3	2.448−3	2.244−3	2.027−3	1.805−3	1.591−3	1.395−3	1.214−3
2	44	3.258−3	3.133−3	2.974−3	2.789−3	2.579−3	2.345−3	2.092−3	1.831−3	1.576−3	1.339−3	1.125−3
2	45	1.377−2	1.363−2	1.340−2	1.307−2	1.263−2	1.205−2	1.130−2	1.037−2	9.295−3	8.148−3	6.977−3
2	46	4.817−3	4.657−3	4.440−3	4.180−3	3.882−3	3.552−3	3.202−3	2.848−3	2.508−3	2.197−3	1.912−3
2	47	3.086−3	2.959−3	2.803−3	2.625−3	2.423−3	2.198−3	1.954−3	1.701−3	1.451−3	1.220−3	1.010−3
2	48	2.044−2	2.003−2	1.953−2	1.891−2	1.811−2	1.709−2	1.578−2	1.417−2	1.229−2	1.026−2	8.212−3
2	49	1.132−2	1.139−2	1.139−2	1.127−2	1.098−2	1.046−2	9.686−3	8.660−3	7.439−3	6.124−3	4.825−3
3	4	3.076−1	3.041−1	2.974−1	2.872−1	2.779−1	2.741−1	2.732−1	2.664−1	2.480−1	2.196−1	1.859−1
3	5	2.453−1	2.434−1	2.393−1	2.340−1	2.326−1	2.396−1	2.506−1	2.558−1	2.500−1	2.359−1	2.180−1
3	6	3.932−2	4.153−2	4.038−2	3.669−2	3.260−2	2.975−2	2.793−2	2.589−2	2.284−2	1.899−2	1.497−2

Table 5: Effective collision strengths for transitions in C V. ($a{\pm}b \equiv a{\times}10^{\pm b}$).

Transition		Temperature (log T_e, K)										
i	j	4.0	4.2	4.4	4.6	4.8	5.0	5.2	5.4	5.6	5.8	6.0
3	7	9.206−2	9.158−2	9.028−2	8.929−2	9.183−2	9.871−2	1.054−1	1.059−1	9.829−2	8.495−2	6.936−2
3	8	1.975−1	1.740−1	1.430−1	1.124−1	8.678−2	6.693−2	5.210−2	4.137−2	3.401−2	2.946−2	2.689−2
3	9	1.541−1	1.409−1	1.296−1	1.212−1	1.157−1	1.127−1	1.120−1	1.137−1	1.177−1	1.234−1	1.282−1
3	10	9.473−2	7.991−2	6.622−2	5.553−2	4.760−2	4.116−2	3.530−2	2.980−2	2.476−2	2.021−2	1.614−2
3	11	1.161−1	9.675−2	7.932−2	6.609−2	5.671−2	4.956−2	4.351−2	3.837−2	3.432−2	3.145−2	2.935−2
3	12	3.906−2	3.008−2	2.308−2	1.806−2	1.455−2	1.189−2	9.662−3	7.723−3	6.049−3	4.633−3	3.463−3
3	13	3.590−1	3.617−1	3.668−1	3.747−1	3.867−1	4.048−1	4.329−1	4.760−1	5.391−1	6.242−1	7.157−1
3	14	8.877−2	8.276−2	7.645−2	7.152−2	6.770−2	6.342−2	5.779−2	5.098−2	4.352−2	3.586−2	2.846−2
3	15	8.043−2	7.415−2	6.797−2	6.367−2	6.079−2	5.764−2	5.349−2	4.879−2	4.432−2	4.052−2	3.720−2
3	16	6.996−2	6.339−2	5.778−2	5.378−2	5.079−2	4.747−2	4.314−2	3.794−2	3.223−2	2.638−2	2.075−2
3	17	2.712−2	2.572−2	2.438−2	2.352−2	2.282−2	2.163−2	1.971−2	1.727−2	1.462−2	1.197−2	9.475−3
3	18	3.360−2	2.875−2	2.447−2	2.081−2	1.765−2	1.490−2	1.257−2	1.063−2	9.053−3	7.827−3	6.861−3
3	19	2.563−2	2.494−2	2.429−2	2.368−2	2.308−2	2.259−2	2.232−2	2.236−2	2.271−2	2.331−2	2.370−2
3	20	1.827−2	1.737−2	1.638−2	1.523−2	1.386−2	1.235−2	1.081−2	9.328−3	7.914−3	6.581−3	5.337−3
3	21	2.231−2	2.115−2	2.004−2	1.879−2	1.726−2	1.553−2	1.380−2	1.220−2	1.082−2	9.650−3	8.622−3
3	22	7.133−3	6.770−3	6.316−3	5.758−3	5.094−3	4.378−3	3.676−3	3.022−3	2.427−3	1.899−3	1.442−3
3	23	6.115−2	6.351−2	6.594−2	6.891−2	7.272−2	7.779−2	8.460−2	9.357−2	1.051−1	1.191−1	1.324−1
3	24	2.105−2	2.143−2	2.153−2	2.121−2	2.037−2	1.910−2	1.753−2	1.571−2	1.367−2	1.147−2	9.236−3
3	25	2.056−2	2.057−2	2.034−2	1.973−2	1.864−2	1.721−2	1.563−2	1.403−2	1.246−2	1.099−2	9.605−3
3	26	3.007−2	3.171−2	3.244−2	3.216−2	3.098−2	2.939−2	2.792−2	2.694−2	2.665−2	2.708−2	2.767−2
3	27	1.168−2	1.223−2	1.246−2	1.213−2	1.111−2	9.638−3	8.024−3	6.477−3	5.089−3	3.892−3	2.894−3
3	28	1.264−2	1.332−2	1.358−2	1.319−2	1.207−2	1.049−2	8.833−3	7.325−3	6.064−3	5.067−3	4.281−3
3	29	1.716−2	1.715−2	1.679−2	1.585−2	1.423−2	1.222−2	1.014−2	8.200−3	6.465−3	4.962−3	3.699−3
3	30	2.024−2	1.961−2	1.903−2	1.827−2	1.717−2	1.578−2	1.423−2	1.254−2	1.073−2	8.868−3	7.034−3
3	31	1.121−2	1.101−2	1.080−2	1.042−2	9.778−3	8.920−3	7.943−3	6.909−3	5.854−3	4.808−3	3.812−3
3	32	1.352−2	1.156−2	1.004−2	8.850−3	7.852−3	6.957−3	6.117−3	5.323−3	4.593−3	3.957−3	3.407−3
3	33	1.259−2	1.204−2	1.157−2	1.115−2	1.078−2	1.043−2	1.012−2	9.866−3	9.682−3	9.569−3	9.382−3
3	34	8.802−3	8.349−3	7.917−3	7.471−3	6.973−3	6.403−3	5.755−3	5.049−3	4.316−3	3.591−3	2.904−3
3	35	1.034−2	9.831−3	9.359−3	8.883−3	8.362−3	7.774−3	7.117−3	6.416−3	5.712−3	5.046−3	4.416−3
3	36	3.477−3	3.295−3	3.112−3	2.916−3	2.695−3	2.440−3	2.150−3	1.836−3	1.513−3	1.201−3	9.189−4
3	37	2.736−2	2.817−2	2.921−2	3.052−2	3.221−2	3.434−2	3.697−2	4.019−2	4.409−2	4.867−2	5.273−2
3	38	9.341−3	9.360−3	9.332−3	9.240−3	9.052−3	8.724−3	8.213−3	7.495−3	6.590−3	5.561−3	4.492−3
3	39	8.082−3	8.103−3	8.077−3	7.989−3	7.815−3	7.528−3	7.104−3	6.543−3	5.879−3	5.172−3	4.459−3
3	40	1.711−2	1.698−2	1.671−2	1.634−2	1.590−2	1.541−2	1.495−2	1.457−2	1.438−2	1.443−2	1.448−2
3	41	4.554−3	4.503−3	4.409−3	4.262−3	4.052−3	3.766−3	3.401−3	2.967−3	2.490−3	2.007−3	1.554−3
3	42	4.573−3	4.534−3	4.451−3	4.318−3	4.127−3	3.874−3	3.561−3	3.205−3	2.835−3	2.484−3	2.160−3
3	43	3.801−3	3.638−3	3.429−3	3.191−3	2.927−3	2.646−3	2.359−3	2.087−3	1.846−3	1.644−3	1.469−3
3	44	6.454−4	6.182−4	5.831−4	5.411−4	4.923−4	4.373−4	3.776−4	3.159−4	2.552−4	1.989−4	1.496−4
3	45	5.170−3	5.098−3	4.970−3	4.784−3	4.536−3	4.216−3	3.819−3	3.348−3	2.825−3	2.287−3	1.776−3
3	46	8.685−4	8.410−4	8.018−4	7.525−4	6.939−4	6.272−4	5.548−4	4.807−4	4.095−4	3.453−4	2.887−4
3	47	1.335−3	1.266−3	1.176−3	1.071−3	9.521−4	8.233−4	6.904−4	5.606−4	4.403−4	3.345−4	2.460−4
3	48	8.251−3	8.108−3	7.952−3	7.764−3	7.512−3	7.157−3	6.661−3	6.007−3	5.215−3	4.339−3	3.452−3
3	49	5.910−3	5.919−3	5.875−3	5.759−3	5.550−3	5.229−3	4.790−3	4.244−3	3.623−3	2.974−3	2.344−3
4	5	9.364−1	9.279−1	9.103−1	8.856−1	8.708−1	8.817−1	9.051−1	9.079−1	8.715−1	8.039−1	7.215−1
4	6	1.181−1	1.248−1	1.213−1	1.103−1	9.803−2	8.946−2	8.402−2	7.790−2	6.875−2	5.719−2	4.510−2
4	7	2.763−1	2.749−1	2.710−1	2.680−1	2.756−1	2.962−1	3.161−1	3.176−1	2.948−1	2.548−1	2.081−1
4	8	6.628−1	5.764−1	4.687−1	3.650−1	2.791−1	2.132−1	1.644−1	1.293−1	1.054−1	9.052−2	8.205−2
4	9	1.017−1	8.571−2	7.058−2	5.859−2	4.966−2	4.251−2	3.616−2	3.035−2	2.510−2	2.042−2	1.628−2
4	10	6.664−1	5.885−1	5.209−1	4.702−1	4.355−1	4.128−1	3.995−1	3.950−1	3.993−1	4.102−1	4.196−1

Table 5: Effective collision strengths for transitions in C V. ($a{\pm}b \equiv a{\times}10^{\pm b}$).

Transition		Temperature (log T_e, K)										
i	j	4.0	4.2	4.4	4.6	4.8	5.0	5.2	5.4	5.6	5.8	6.0
4	11	4.480−1	3.678−1	2.963−1	2.417−1	2.026−1	1.730−1	1.485−1	1.277−1	1.108−1	9.770−2	8.730−2
4	12	1.211−1	9.369−2	7.187−2	5.605−2	4.490−2	3.650−2	2.953−2	2.352−2	1.837−2	1.404−2	1.048−2
4	13	3.895−1	3.836−1	3.790−1	3.784−1	3.823−1	3.901−1	4.035−1	4.266−1	4.638−1	5.173−1	5.759−1
4	14	9.100−1	9.081−1	9.116−1	9.237−1	9.466−1	9.829−1	1.040+0	1.131+0	1.267+0	1.452+0	1.653+0
4	15	2.858−1	2.649−1	2.438−1	2.284−1	2.173−1	2.051−1	1.889−1	1.699−1	1.504−1	1.319−1	1.148−1
4	16	2.098−1	1.902−1	1.734−1	1.614−1	1.524−1	1.426−1	1.298−1	1.144−1	9.754−2	8.036−2	6.383−2
4	17	8.136−2	7.715−2	7.311−2	7.053−2	6.842−2	6.483−2	5.908−2	5.177−2	4.382−2	3.589−2	2.841−2
4	18	9.469−2	8.176−2	7.025−2	6.031−2	5.154−2	4.380−2	3.712−2	3.151−2	2.692−2	2.334−2	2.050−2
4	19	1.729−2	1.670−2	1.594−2	1.495−2	1.369−2	1.225−2	1.076−2	9.298−3	7.896−3	6.571−3	5.331−3
4	20	1.033−1	1.010−1	9.839−2	9.530−2	9.168−2	8.804−2	8.499−2	8.292−2	8.197−2	8.198−2	8.150−2
4	21	7.040−2	6.754−2	6.440−2	6.056−2	5.565−2	5.003−2	4.434−2	3.898−2	3.414−2	2.988−2	2.604−2
4	22	2.160−2	2.043−2	1.902−2	1.732−2	1.531−2	1.316−2	1.104−2	9.076−3	7.290−3	5.703−3	4.330−3
4	23	7.443−2	7.671−2	7.867−2	8.048−2	8.220−2	8.428−2	8.726−2	9.152−2	9.736−2	1.049−1	1.119−1
4	24	1.631−1	1.685−1	1.737−1	1.796−1	1.868−1	1.964−1	2.098−1	2.280−1	2.519−1	2.815−1	3.096−1
4	25	7.098−2	7.148−2	7.111−2	6.943−2	6.605−2	6.137−2	5.599−2	5.022−2	4.421−2	3.816−2	3.224−2
4	26	4.984−2	5.265−2	5.385−2	5.301−2	5.011−2	4.607−2	4.193−2	3.836−2	3.571−2	3.407−2	3.291−2
4	27	6.357−2	6.641−2	6.749−2	6.628−2	6.271−2	5.789−2	5.311−2	4.925−2	4.674−2	4.566−2	4.515−2
4	28	4.381−2	4.628−2	4.726−2	4.596−2	4.210−2	3.665−2	3.081−2	2.534−2	2.057−2	1.660−2	1.334−2
4	29	5.753−2	5.805−2	5.738−2	5.486−2	5.032−2	4.466−2	3.897−2	3.394−2	2.984−2	2.674−2	2.430−2
4	30	6.061−2	5.878−2	5.705−2	5.478−2	5.149−2	4.735−2	4.270−2	3.766−2	3.227−2	2.671−2	2.124−2
4	31	3.370−2	3.310−2	3.246−2	3.131−2	2.937−2	2.678−2	2.384−2	2.073−2	1.757−2	1.443−2	1.144−2
4	32	3.903−2	3.359−2	2.938−2	2.605−2	2.322−2	2.066−2	1.821−2	1.588−2	1.373−2	1.184−2	1.020−2
4	33	8.448−3	8.115−3	7.764−3	7.371−3	6.910−3	6.362−3	5.730−3	5.033−3	4.305−3	3.585−3	2.899−3
4	34	5.048−2	4.865−2	4.693−2	4.525−2	4.353−2	4.174−2	3.990−2	3.812−2	3.652−2	3.516−2	3.362−2
4	35	3.347−2	3.190−2	3.042−2	2.891−2	2.724−2	2.529−2	2.308−2	2.066−2	1.819−2	1.581−2	1.355−2
4	36	1.024−2	9.745−3	9.237−3	8.680−3	8.039−3	7.289−3	6.431−3	5.495−3	4.531−3	3.600−3	2.754−3
4	37	3.310−2	3.372−2	3.446−2	3.533−2	3.635−2	3.752−2	3.882−2	4.027−2	4.198−2	4.403−2	4.563−2
4	38	7.199−2	7.386−2	7.615−2	7.899−2	8.254−2	8.696−2	9.232−2	9.880−2	1.067−1	1.160−1	1.242−1
4	39	2.955−2	2.976−2	2.971−2	2.936−2	2.866−2	2.754−2	2.590−2	2.372−2	2.109−2	1.821−2	1.526−2
4	40	2.500−2	2.481−2	2.438−2	2.374−2	2.292−2	2.193−2	2.083−2	1.971−2	1.871−2	1.793−2	1.719−2
4	41	3.292−2	3.256−2	3.199−2	3.125−2	3.034−2	2.927−2	2.812−2	2.703−2	2.619−2	2.573−2	2.528−2
4	42	1.638−2	1.614−2	1.578−2	1.529−2	1.462−2	1.370−2	1.253−2	1.115−2	9.651−3	8.171−3	6.782−3
4	43	5.939−3	5.681−3	5.345−3	4.954−3	4.515−3	4.041−3	3.555−3	3.086−3	2.661−3	2.298−3	1.985−3
4	44	5.222−3	5.010−3	4.733−3	4.410−3	4.046−3	3.652−3	3.244−3	2.848−3	2.486−3	2.173−3	1.899−3
4	45	1.966−2	1.943−2	1.901−2	1.842−2	1.764−2	1.669−2	1.556−2	1.430−2	1.301−2	1.180−2	1.065−2
4	46	3.240−3	3.112−3	2.937−3	2.724−3	2.477−3	2.200−3	1.905−3	1.608−3	1.326−3	1.073−3	8.540−4
4	47	5.580−3	5.321−3	4.992−3	4.612−3	4.188−3	3.731−3	3.260−3	2.805−3	2.391−3	2.034−3	1.727−3
4	48	2.484−2	2.444−2	2.399−2	2.341−2	2.263−2	2.155−2	2.004−2	1.807−2	1.569−2	1.306−2	1.040−2
4	49	1.770−2	1.771−2	1.757−2	1.723−2	1.661−2	1.566−2	1.435−2	1.272−2	1.086−2	8.916−3	7.029−3
5	6	1.970−1	2.081−1	2.024−1	1.840−1	1.636−1	1.493−1	1.403−1	1.302−1	1.149−1	9.561−2	7.539−2
5	7	4.609−1	4.586−1	4.521−1	4.471−1	4.597−1	4.940−1	5.274−1	5.303−1	4.926−1	4.260−1	3.481−1
5	8	1.276+0	1.107+0	8.935−1	6.889−1	5.203−1	3.919−1	2.978−1	2.309−1	1.855−1	1.572−1	1.409−1
5	9	1.240−1	1.032−1	8.407−2	6.942−2	5.898−2	5.109−2	4.454−2	3.906−2	3.480−2	3.179−2	2.960−2
5	10	4.470−1	3.659−1	2.946−1	2.404−1	2.017−1	1.724−1	1.481−1	1.275−1	1.107−1	9.767−2	8.732−2
5	11	1.588+0	1.364+0	1.168+0	1.019+0	9.151−1	8.426−1	7.929−1	7.629−1	7.513−1	7.543−1	7.572−1
5	12	2.098−1	1.624−1	1.243−1	9.647−2	7.686−2	6.216−2	5.008−2	3.976−2	3.097−2	2.363−2	1.761−2
5	13	2.026−1	1.890−1	1.754−1	1.659−1	1.596−1	1.528−1	1.441−1	1.347−1	1.265−1	1.205−1	1.157−1
5	14	5.870−1	5.663−1	5.470−1	5.359−1	5.324−1	5.321−1	5.348−1	5.457−1	5.707−1	6.134−1	6.621−1
5	15	1.859+0	1.845+0	1.841+0	1.855+0	1.891+0	1.951+0	2.049+0	2.205+0	2.444+0	2.776+0	3.136+0

Table 5: Effective collision strengths for transitions in C V. ($a{\pm}b \equiv a{\times}10^{\pm b}$).

Transition		Temperature (log T_e, K)										
i	j	4.0	4.2	4.4	4.6	4.8	5.0	5.2	5.4	5.6	5.8	6.0
5	16	3.457−1	3.132−1	2.852−1	2.651−1	2.502−1	2.338−1	2.125−1	1.869−1	1.589−1	1.303−1	1.027−1
5	17	1.356−1	1.285−1	1.218−1	1.175−1	1.139−1	1.079−1	9.832−2	8.616−2	7.293−2	5.975−2	4.730−2
5	18	1.655−1	1.422−1	1.214−1	1.035−1	8.796−2	7.438−2	6.278−2	5.311−2	4.527−2	3.916−2	3.434−2
5	19	2.125−2	2.047−2	1.961−2	1.852−2	1.709−2	1.542−2	1.373−2	1.217−2	1.080−2	9.643−3	8.624−3
5	20	6.960−2	6.705−2	6.409−2	6.032−2	5.545−2	4.987−2	4.422−2	3.889−2	3.409−2	2.986−2	2.603−2
5	21	2.175−1	2.146−1	2.100−1	2.032−1	1.941−1	1.842−1	1.749−1	1.672−1	1.616−1	1.578−1	1.534−1
5	22	3.612−2	3.410−2	3.172−2	2.888−2	2.553−2	2.194−2	1.841−2	1.513−2	1.215−2	9.507−3	7.219−3
5	23	4.959−2	4.992−2	4.966−2	4.857−2	4.640−2	4.349−2	4.028−2	3.703−2	3.388−2	3.094−2	2.810−2
5	24	1.245−1	1.269−1	1.283−1	1.286−1	1.277−1	1.264−1	1.256−1	1.259−1	1.278−1	1.315−1	1.348−1
5	25	3.414−1	3.521−1	3.622−1	3.729−1	3.852−1	4.012−1	4.236−1	4.543−1	4.951−1	5.460−1	5.942−1
5	26	4.130−2	4.360−2	4.449−2	4.331−2	3.986−2	3.502−2	2.992−2	2.526−2	2.134−2	1.823−2	1.576−2
5	27	8.431−2	8.707−2	8.749−2	8.449−2	7.786−2	6.915−2	6.018−2	5.209−2	4.538−2	4.015−2	3.597−2
5	28	1.624−1	1.714−1	1.753−1	1.729−1	1.643−1	1.524−1	1.405−1	1.308−1	1.244−1	1.215−1	1.200−1
5	29	7.021−2	7.066−2	6.985−2	6.667−2	6.056−2	5.265−2	4.447−2	3.700−2	3.064−2	2.547−2	2.131−2
5	30	1.004−1	9.745−2	9.466−2	9.094−2	8.550−2	7.862−2	7.084−2	6.242−2	5.342−2	4.411−2	3.499−2
5	31	5.646−2	5.538−2	5.426−2	5.230−2	4.903−2	4.470−2	3.977−2	3.458−2	2.929−2	2.405−2	1.907−2
5	32	6.172−2	5.372−2	4.745−2	4.241−2	3.806−2	3.401−2	3.010−2	2.631−2	2.278−2	1.967−2	1.697−2
5	33	1.027−2	9.789−3	9.333−3	8.868−3	8.356−3	7.773−3	7.119−3	6.420−3	5.717−3	5.052−3	4.422−3
5	34	3.433−2	3.246−2	3.078−2	2.915−2	2.739−2	2.540−2	2.314−2	2.071−2	1.823−2	1.584−2	1.357−2
5	35	1.040−1	1.015−1	9.877−2	9.574−2	9.225−2	8.817−2	8.362−2	7.884−2	7.418−2	6.989−2	6.537−2
5	36	1.701−2	1.617−2	1.532−2	1.440−2	1.334−2	1.211−2	1.069−2	9.142−3	7.541−3	5.992−3	4.585−3
5	37	2.008−2	2.016−2	2.015−2	2.002−2	1.973−2	1.918−2	1.833−2	1.716−2	1.576−2	1.426−2	1.269−2
5	38	5.333−2	5.415−2	5.486−2	5.548−2	5.599−2	5.636−2	5.654−2	5.652−2	5.650−2	5.669−2	5.642−2
5	39	1.520−1	1.560−1	1.603−1	1.653−1	1.713−1	1.787−1	1.876−1	1.982−1	2.112−1	2.266−1	2.397−1
5	40	1.622−2	1.609−2	1.579−2	1.532−2	1.466−2	1.379−2	1.273−2	1.154−2	1.031−2	9.149−3	8.067−3
5	41	3.397−2	3.344−2	3.271−2	3.179−2	3.061−2	2.910−2	2.727−2	2.522−2	2.312−2	2.118−2	1.934−2
5	42	8.315−2	8.204−2	8.049−2	7.861−2	7.634−2	7.365−2	7.069−2	6.781−2	6.547−2	6.399−2	6.256−2
5	43	3.816−3	3.671−3	3.475−3	3.237−3	2.961−3	2.654−3	2.328−3	2.001−3	1.693−3	1.419−3	1.181−3
5	44	7.250−3	6.911−3	6.475−3	5.965−3	5.391−3	4.766−3	4.119−3	3.487−3	2.904−3	2.395−3	1.960−3
5	45	2.274−2	2.240−2	2.188−2	2.117−2	2.021−2	1.897−2	1.741−2	1.560−2	1.365−2	1.173−2	9.909−3
5	46	1.729−2	1.657−2	1.562−2	1.451−2	1.326−2	1.192−2	1.054−2	9.220−3	8.034−3	7.028−3	6.155−3
5	47	5.001−3	4.775−3	4.496−3	4.173−3	3.810−3	3.410−3	2.987−3	2.565−3	2.166−3	1.809−3	1.497−3
5	48	4.161−2	4.105−2	4.031−2	3.931−2	3.793−2	3.603−2	3.345−2	3.010−2	2.609−2	2.168−2	1.723−2
5	49	2.941−2	2.935−2	2.910−2	2.854−2	2.755−2	2.600−2	2.385−2	2.115−2	1.807−2	1.484−2	1.170−2
6	7	4.567+0	4.643+0	4.729+0	4.839+0	4.988+0	5.189+0	5.445+0	5.754+0	6.139+0	6.626+0	7.135+0
6	8	1.412−1	1.210−1	9.682−2	7.418−2	5.578−2	4.172−2	3.114−2	2.321−2	1.729−2	1.286−2	9.509−3
6	9	1.831−2	1.566−2	1.300−2	1.082−2	9.167−3	7.818−3	6.605−3	5.474−3	4.430−3	3.490−3	2.668−3
6	10	5.643−2	4.798−2	3.964−2	3.288−2	2.775−2	2.362−2	1.992−2	1.649−2	1.333−2	1.050−2	8.024−3
6	11	9.883−2	8.342−2	6.843−2	5.635−2	4.727−2	4.001−2	3.361−2	2.774−2	2.239−2	1.760−2	1.343−2
6	12	1.710−1	1.596−1	1.498−1	1.430−1	1.394−1	1.388−1	1.407−1	1.451−1	1.518−1	1.600−1	1.665−1
6	13	3.052−2	2.765−2	2.512−2	2.332−2	2.204−2	2.072−2	1.901−2	1.692−2	1.459−2	1.216−2	9.742−3
6	14	5.116−2	4.634−2	4.210−2	3.910−2	3.700−2	3.482−2	3.199−2	2.855−2	2.471−2	2.071−2	1.674−2
6	15	7.150−2	6.468−2	5.869−2	5.447−2	5.152−2	4.848−2	4.451−2	3.964−2	3.418−2	2.846−2	2.280−2
6	16	1.871−1	1.797−1	1.768−1	1.782−1	1.830−1	1.907−1	2.027−1	2.215−1	2.488−1	2.841−1	3.190−1
6	17	9.668−2	9.870−2	1.006−1	1.034−1	1.077−1	1.136−1	1.225−1	1.370−1	1.603−1	1.946−1	2.350−1
6	18	1.963−2	1.691−2	1.424−2	1.185−2	9.755−3	7.954−3	6.447−3	5.202−3	4.169−3	3.302−3	2.567−3
6	19	3.223−3	3.195−3	3.110−3	2.960−3	2.737−3	2.459−3	2.155−3	1.842−3	1.531−3	1.231−3	9.554−4
6	20	1.035−2	1.004−2	9.624−3	9.062−3	8.317−3	7.438−3	6.498−3	5.544−3	4.602−3	3.700−3	2.870−3
6	21	1.732−2	1.677−2	1.605−2	1.512−2	1.387−2	1.241−2	1.084−2	9.243−3	7.671−3	6.165−3	4.781−3

Table 5: Effective collision strengths for transitions in C V. ($a{\pm}b \equiv a{\times}10^{\pm b}$).

Transition		Temperature (log T_e, K)										
i	*j*	4.0	4.2	4.4	4.6	4.8	5.0	5.2	5.4	5.6	5.8	6.0
6	22	2.932−2	2.921−2	2.926−2	2.948−2	2.981−2	3.036−2	3.127−2	3.264−2	3.446−2	3.656−2	3.811−2
6	23	7.663−3	7.713−3	7.671−3	7.502−3	7.157−3	6.666−3	6.075−3	5.410−3	4.682−3	3.913−3	3.144−3
6	24	1.282−2	1.289−2	1.281−2	1.252−2	1.193−2	1.111−2	1.013−2	9.027−3	7.822−3	6.549−3	5.274−3
6	25	1.796−2	1.806−2	1.795−2	1.754−2	1.673−2	1.558−2	1.420−2	1.264−2	1.093−2	9.138−3	7.340−3
6	26	6.354−3	6.639−3	6.780−3	6.698−3	6.329−3	5.743−3	5.054−3	4.332−3	3.610−3	2.909−3	2.258−3
6	27	1.540−2	1.578−2	1.589−2	1.560−2	1.483−2	1.381−2	1.282−2	1.204−2	1.151−2	1.119−2	1.085−2
6	28	1.145−2	1.197−2	1.222−2	1.208−2	1.141−2	1.035−2	9.108−3	7.806−3	6.503−3	5.239−3	4.066−3
6	29	2.516−2	2.548−2	2.546−2	2.488−2	2.371−2	2.237−2	2.134−2	2.090−2	2.108−2	2.172−2	2.224−2
6	30	3.641−2	3.581−2	3.514−2	3.443−2	3.377−2	3.353−2	3.415−2	3.589−2	3.881−2	4.270−2	4.627−2
6	31	2.895−2	2.993−2	3.091−2	3.183−2	3.269−2	3.376−2	3.549−2	3.835−2	4.288−2	4.944−2	5.669−2
6	32	7.479−3	6.076−3	5.035−3	4.270−3	3.682−3	3.194−3	2.755−3	2.342−3	1.949−3	1.581−3	1.245−3
6	33	1.741−3	1.676−3	1.609−3	1.534−3	1.443−3	1.331−3	1.195−3	1.038−3	8.696−4	6.999−4	5.409−4
6	34	5.491−3	5.188−3	4.915−3	4.648−3	4.354−3	4.006−3	3.592−3	3.120−3	2.611−3	2.101−3	1.624−3
6	35	8.489−3	8.148−3	7.818−3	7.474−3	7.064−3	6.546−3	5.900−3	5.142−3	4.315−3	3.478−3	2.691−3
6	36	1.538−2	1.519−2	1.510−2	1.514−2	1.530−2	1.560−2	1.606−2	1.666−2	1.741−2	1.822−2	1.873−2
6	37	3.668−3	3.660−3	3.632−3	3.575−3	3.477−3	3.321−3	3.092−3	2.789−3	2.423−3	2.020−3	1.614−3
6	38	6.161−3	6.166−3	6.124−3	6.022−3	5.846−3	5.573−3	5.184−3	4.672−3	4.057−3	3.384−3	2.705−3
6	39	8.704−3	8.746−3	8.695−3	8.539−3	8.268−3	7.860−3	7.292−3	6.559−3	5.687−3	4.735−3	3.778−3
6	40	3.313−3	3.300−3	3.258−3	3.181−3	3.066−3	2.903−3	2.681−3	2.398−3	2.062−3	1.699−3	1.338−3
6	41	6.241−3	6.183−3	6.109−3	6.023−3	5.916−3	5.783−3	5.617−3	5.422−3	5.214−3	5.004−3	4.747−3
6	42	5.890−3	5.830−3	5.742−3	5.617−3	5.433−3	5.162−3	4.782−3	4.286−3	3.693−3	3.045−3	2.401−3
6	43	7.240−4	6.960−4	6.619−4	6.219−4	5.749−4	5.199−4	4.571−4	3.884−4	3.175−4	2.491−4	1.878−4
6	44	1.987−3	1.917−3	1.832−3	1.735−3	1.626−3	1.509−3	1.384−3	1.257−3	1.133−3	1.017−3	9.068−4
6	45	1.040−2	1.031−2	1.021−2	1.015−2	1.013−2	1.018−2	1.034−2	1.061−2	1.103−2	1.155−2	1.190−2
6	46	1.138−3	1.094−3	1.040−3	9.773−4	9.034−4	8.169−4	7.181−4	6.101−4	4.987−4	3.913−4	2.950−4
6	47	2.250−3	2.162−3	2.062−3	1.955−3	1.839−3	1.714−3	1.582−3	1.448−3	1.317−3	1.196−3	1.078−3
6	48	1.467−2	1.426−2	1.392−2	1.369−2	1.358−2	1.364−2	1.392−2	1.445−2	1.524−2	1.624−2	1.703−2
6	49	1.758−2	1.798−2	1.840−2	1.887−2	1.939−2	2.002−2	2.083−2	2.192−2	2.347−2	2.556−2	2.761−2
7	8	6.115−1	5.257−1	4.238−1	3.271−1	2.473−1	1.855−1	1.386−1	1.030−1	7.608−2	5.559−2	4.002−2
7	9	8.235−2	6.826−2	5.544−2	4.530−2	3.769−2	3.166−2	2.644−2	2.176−2	1.759−2	1.392−2	1.073−2
7	10	2.512−1	2.074−1	1.679−1	1.368−1	1.136−1	9.526−2	7.946−2	6.536−2	5.280−2	4.177−2	3.221−2
7	11	4.340−1	3.572−1	2.880−1	2.335−1	1.929−1	1.611−1	1.339−1	1.099−1	8.861−2	6.999−2	5.392−2
7	12	2.381−1	1.880−1	1.479−1	1.187−1	9.817−2	8.350−2	7.278−2	6.558−2	6.215−2	6.269−2	6.587−2
7	13	1.294−1	1.200−1	1.110−1	1.041−1	9.857−2	9.234−2	8.412−2	7.412−2	6.304−2	5.160−2	4.054−2
7	14	2.178−1	2.019−1	1.868−1	1.752−1	1.661−1	1.558−1	1.423−1	1.258−1	1.077−1	8.907−2	7.113−2
7	15	3.026−1	2.801−1	2.589−1	2.425−1	2.297−1	2.153−1	1.962−1	1.729−1	1.470−1	1.203−1	9.448−2
7	16	1.604+0	1.566+0	1.548+0	1.552+0	1.581+0	1.635+0	1.724+0	1.870+0	2.092+0	2.398+0	2.728+0
7	17	4.350−1	4.319−1	4.302−1	4.333−1	4.402−1	4.484−1	4.583−1	4.732−1	4.953−1	5.238−1	5.479−1
7	18	8.152−2	7.139−2	6.203−2	5.349−2	4.556−2	3.824−2	3.161−2	2.569−2	2.044−2	1.585−2	1.193−2
7	19	1.278−2	1.257−2	1.220−2	1.161−2	1.074−2	9.657−3	8.458−3	7.225−3	6.007−3	4.846−3	3.782−3
7	20	4.029−2	3.899−2	3.743−2	3.533−2	3.250−2	2.911−2	2.544−2	2.170−2	1.803−2	1.454−2	1.135−2
7	21	6.683−2	6.468−2	6.215−2	5.875−2	5.412−2	4.850−2	4.240−2	3.617−2	3.005−2	2.423−2	1.890−2
7	22	3.940−2	3.609−2	3.309−2	3.019−2	2.720−2	2.427−2	2.166−2	1.956−2	1.812−2	1.739−2	1.710−2
7	23	2.984−2	3.044−2	3.070−2	3.044−2	2.943−2	2.774−2	2.552−2	2.284−2	1.977−2	1.643−2	1.308−2
7	24	4.992−2	5.091−2	5.130−2	5.081−2	4.910−2	4.628−2	4.260−2	3.819−2	3.312−2	2.762−2	2.208−2
7	25	6.969−2	7.105−2	7.161−2	7.095−2	6.858−2	6.463−2	5.945−2	5.322−2	4.605−2	3.828−2	3.047−2
7	26	2.383−2	2.509−2	2.566−2	2.513−2	2.331−2	2.056−2	1.745−2	1.435−2	1.145−2	8.860−3	6.635−3
7	27	6.811−2	7.078−2	7.171−2	7.016−2	6.589−2	6.003−2	5.404−2	4.889−2	4.505−2	4.261−2	4.086−2
7	28	4.269−2	4.498−2	4.604−2	4.513−2	4.187−2	3.694−2	3.134−2	2.577−2	2.056−2	1.590−2	1.191−2

Table 5: Effective collision strengths for transitions in C V. ($a{\pm}b \equiv a{\times}10^{\pm b}$).

Transition		Temperature (log T_e, K)										
i	j	4.0	4.2	4.4	4.6	4.8	5.0	5.2	5.4	5.6	5.8	6.0
7	29	1.212−1	1.251−1	1.261−1	1.234−1	1.165−1	1.076−1	9.909−2	9.267−2	8.912−2	8.843−2	8.872−2
7	30	2.845−1	2.843−1	2.857−1	2.888−1	2.937−1	3.025−1	3.175−1	3.406−1	3.731−1	4.146−1	4.547−1
7	31	1.073−1	1.072−1	1.072−1	1.071−1	1.067−1	1.066−1	1.074−1	1.097−1	1.137−1	1.187−1	1.224−1
7	32	3.630−2	3.147−2	2.764−2	2.449−2	2.168−2	1.898−2	1.629−2	1.360−2	1.100−2	8.590−3	6.479−3
7	33	7.571−3	7.165−3	6.782−3	6.385−3	5.936−3	5.409−3	4.801−3	4.130−3	3.431−3	2.749−3	2.123−3
7	34	2.311−2	2.169−2	2.042−2	1.917−2	1.780−2	1.621−2	1.439−2	1.238−2	1.028−2	8.240−3	6.364−3
7	35	3.683−2	3.483−2	3.301−2	3.118−2	2.911−2	2.663−2	2.371−2	2.045−2	1.702−2	1.366−2	1.056−2
7	36	1.671−2	1.589−2	1.513−2	1.438−2	1.359−2	1.275−2	1.187−2	1.101−2	1.024−2	9.639−3	9.113−3
7	37	1.381−2	1.384−2	1.383−2	1.372−2	1.347−2	1.299−2	1.220−2	1.108−2	9.652−3	8.044−3	6.402−3
7	38	2.326−2	2.341−2	2.341−2	2.321−2	2.273−2	2.186−2	2.051−2	1.860−2	1.621−2	1.352−2	1.078−2
7	39	3.286−2	3.323−2	3.328−2	3.293−2	3.214−2	3.081−2	2.880−2	2.606−2	2.265−2	1.884−2	1.498−2
7	40	9.886−3	9.833−3	9.670−3	9.380−3	8.945−3	8.344−3	7.562−3	6.617−3	5.563−3	4.484−3	3.464−3
7	41	2.616−2	2.577−2	2.523−2	2.458−2	2.375−2	2.273−2	2.155−2	2.028−2	1.908−2	1.808−2	1.714−2
7	42	1.745−2	1.720−2	1.685−2	1.638−2	1.570−2	1.472−2	1.340−2	1.176−2	9.909−3	7.998−3	6.186−3
7	43	2.212−3	2.111−3	1.979−3	1.821−3	1.640−3	1.439−3	1.227−3	1.013−3	8.094−4	6.244−4	4.651−4
7	44	8.717−3	8.359−3	7.897−3	7.359−3	6.757−3	6.107−3	5.438−3	4.790−3	4.201−3	3.688−3	3.232−3
7	45	5.861−2	5.782−2	5.660−2	5.511−2	5.343−2	5.165−2	4.997−2	4.864−2	4.800−2	4.820−2	4.842−2
7	46	3.467−3	3.311−3	3.105−3	2.857−3	2.571−3	2.256−3	1.922−3	1.587−3	1.268−3	9.779−4	7.285−4
7	47	1.033−2	9.886−3	9.335−3	8.706−3	8.009−3	7.257−3	6.485−3	5.740−3	5.062−3	4.476−3	3.952−3
7	48	1.148−1	1.156−1	1.172−1	1.196−1	1.230−1	1.278−1	1.341−1	1.421−1	1.521−1	1.641−1	1.743−1
7	49	5.062−2	5.118−2	5.169−2	5.219−2	5.271−2	5.330−2	5.398−2	5.477−2	5.573−2	5.678−2	5.698−2
8	9	6.564+0	6.923+0	7.348+0	7.818+0	8.311+0	8.852+0	9.541+0	1.048+1	1.168+1	1.307+1	1.431+1
8	10	1.976+1	2.082+1	2.208+1	2.347+1	2.494+1	2.655+1	2.861+1	3.141+1	3.501+1	3.918+1	4.289+1
8	11	3.344+1	3.504+1	3.703+1	3.926+1	4.163+1	4.425+1	4.764+1	5.228+1	5.828+1	6.523+1	7.142+1
8	12	5.850−1	4.709−1	3.890−1	3.294−1	2.835−1	2.430−1	2.041−1	1.673−1	1.344−1	1.063−1	8.324−2
8	13	1.347+0	1.439+0	1.494+0	1.522+0	1.525+0	1.502+0	1.458+0	1.408+0	1.364+0	1.327+0	1.282+0
8	14	2.243+0	2.396+0	2.487+0	2.532+0	2.539+0	2.500+0	2.427+0	2.344+0	2.270+0	2.209+0	2.134+0
8	15	3.147+0	3.358+0	3.485+0	3.547+0	3.555+0	3.501+0	3.398+0	3.282+0	3.179+0	3.094+0	2.990+0
8	16	7.590−1	7.915−1	7.707−1	7.328−1	6.881−1	6.234−1	5.342−1	4.326−1	3.338−1	2.477−1	1.779−1
8	17	2.184−1	2.409−1	2.487−1	2.526−1	2.526−1	2.403−1	2.133−1	1.777−1	1.407−1	1.071−1	7.902−2
8	18	1.945+0	1.808+0	1.705+0	1.640+0	1.610+0	1.614+0	1.652+0	1.719+0	1.808+0	1.904+0	1.963+0
8	19	1.280−1	1.200−1	1.142−1	1.099−1	1.069−1	1.066−1	1.115−1	1.241−1	1.468−1	1.799−1	2.152−1
8	20	3.876−1	3.618−1	3.433−1	3.296−1	3.202−1	3.193−1	3.338−1	3.716−1	4.397−1	5.386−1	6.438−1
8	21	7.152−1	6.486−1	6.019−1	5.689−1	5.467−1	5.407−1	5.616−1	6.221−1	7.336−1	8.958−1	1.068+0
8	22	6.719−2	6.099−2	5.477−2	4.794−2	4.016−2	3.215−2	2.482−2	1.868−2	1.379−2	1.002−2	7.158−3
8	23	2.962−1	3.023−1	3.089−1	3.154−1	3.228−1	3.347−1	3.552−1	3.860−1	4.268−1	4.739−1	5.133−1
8	24	4.933−1	5.033−1	5.143−1	5.251−1	5.374−1	5.573−1	5.913−1	6.427−1	7.106−1	7.890−1	8.548−1
8	25	6.911−1	7.051−1	7.208−1	7.365−1	7.541−1	7.821−1	8.296−1	9.013−1	9.963−1	1.106+0	1.198+0
8	26	4.069−1	4.316−1	4.524−1	4.667−1	4.750−1	4.818−1	4.910−1	5.037−1	5.182−1	5.315−1	5.338−1
8	27	4.895−1	5.200−1	5.439−1	5.575−1	5.605−1	5.584−1	5.567−1	5.577−1	5.610−1	5.642−1	5.583−1
8	28	7.331−1	7.778−1	8.158−1	8.424−1	8.578−1	8.698−1	8.859−1	9.082−1	9.343−1	9.585−1	9.637−1
8	29	3.712−1	3.955−1	4.119−1	4.160−1	4.063−1	3.871−1	3.638−1	3.399−1	3.174−1	2.970−1	2.762−1
8	30	1.982−1	1.970−1	1.922−1	1.807−1	1.614−1	1.370−1	1.115−1	8.758−2	6.669−2	4.934−2	3.555−2
8	31	8.329−2	8.183−2	8.061−2	7.721−2	7.026−2	6.068−2	5.019−2	4.007−2	3.097−2	2.321−2	1.688−2
8	32	3.639−1	3.423−1	3.272−1	3.181−1	3.145−1	3.156−1	3.211−1	3.301−1	3.415−1	3.530−1	3.575−1
8	33	4.519−2	4.327−2	4.185−2	4.092−2	4.047−2	4.056−2	4.141−2	4.340−2	4.699−2	5.236−2	5.795−2
8	34	1.301−1	1.265−1	1.236−1	1.217−1	1.208−1	1.213−1	1.240−1	1.300−1	1.408−1	1.569−1	1.736−1
8	35	2.173−1	2.121−1	2.077−1	2.044−1	2.025−1	2.030−1	2.071−1	2.168−1	2.346−1	2.612−1	2.888−1
8	36	1.417−2	1.236−2	1.094−2	9.732−3	8.598−3	7.460−3	6.307−3	5.176−3	4.117−3	3.174−3	2.373−3

Table 5: Effective collision strengths for transitions in C V. ($a{\pm}b \equiv a{\times}10^{\pm b}$).

Transition		Temperature (log T_e, K)										
i	j	4.0	4.2	4.4	4.6	4.8	5.0	5.2	5.4	5.6	5.8	6.0
8	37	9.514−2	9.651−2	9.790−2	9.954−2	1.016−1	1.044−1	1.080−1	1.125−1	1.179−1	1.236−1	1.269−1
8	38	1.582−1	1.604−1	1.627−1	1.655−1	1.691−1	1.738−1	1.798−1	1.873−1	1.963−1	2.058−1	2.114−1
8	39	2.212−1	2.241−1	2.273−1	2.313−1	2.364−1	2.431−1	2.517−1	2.623−1	2.750−1	2.883−1	2.961−1
8	40	1.098−1	1.090−1	1.074−1	1.051−1	1.021−1	9.835−2	9.402−2	8.931−2	8.453−2	7.988−2	7.467−2
8	41	1.438−1	1.424−1	1.398−1	1.361−1	1.312−1	1.251−1	1.180−1	1.102−1	1.024−1	9.491−2	8.716−2
8	42	1.970−1	1.956−1	1.928−1	1.888−1	1.834−1	1.768−1	1.691−1	1.607−1	1.521−1	1.438−1	1.345−1
8	43	1.169−1	1.173−1	1.174−1	1.171−1	1.164−1	1.151−1	1.135−1	1.117−1	1.101−1	1.087−1	1.061−1
8	44	1.216−1	1.213−1	1.203−1	1.185−1	1.156−1	1.116−1	1.065−1	1.010−1	9.551−2	9.057−2	8.531−2
8	45	1.202−1	1.178−1	1.141−1	1.090−1	1.023−1	9.398−2	8.422−2	7.358−2	6.288−2	5.290−2	4.392−2
8	46	1.838−1	1.844−1	1.845−1	1.841−1	1.830−1	1.810−1	1.785−1	1.756−1	1.731−1	1.709−1	1.668−1
8	47	1.144−1	1.138−1	1.126−1	1.103−1	1.069−1	1.022−1	9.635−2	8.992−2	8.357−2	7.780−2	7.204−2
8	48	6.971−2	6.742−2	6.439−2	6.049−2	5.551−2	4.941−2	4.238−2	3.491−2	2.758−2	2.094−2	1.533−2
8	49	2.448−2	2.444−2	2.409−2	2.337−2	2.219−2	2.048−2	1.824−2	1.558−2	1.273−2	9.943−3	7.445−3
9	10	1.204+0	1.008+0	8.541−1	7.373−1	6.451−1	5.609−1	4.766−1	3.941−1	3.178−1	2.511−1	1.945−1
9	11	1.723+0	1.614+0	1.525+0	1.460+0	1.415+0	1.375+0	1.335+0	1.298+0	1.269+0	1.246+0	1.213+0
9	12	1.732−1	1.285−1	9.563−2	7.281−2	5.727−2	4.574−2	3.610−2	2.776−2	2.076−2	1.515−2	1.081−2
9	13	1.053+1	1.157+1	1.249+1	1.329+1	1.394+1	1.452+1	1.534+1	1.667+1	1.856+1	2.085+1	2.294+1
9	14	4.551−1	4.485−1	4.217−1	3.938−1	3.671−1	3.318−1	2.841−1	2.301−1	1.776−1	1.320−1	9.516−2
9	15	5.192−1	4.965−1	4.620−1	4.335−1	4.107−1	3.822−1	3.444−1	3.036−1	2.680−1	2.411−1	2.209−1
9	16	3.438−1	3.298−1	3.044−1	2.794−1	2.564−1	2.287−1	1.936−1	1.551−1	1.184−1	8.701−2	6.195−2
9	17	1.771−1	1.751−1	1.675−1	1.597−1	1.517−1	1.396−1	1.222−1	1.018−1	8.137−2	6.311−2	4.786−2
9	18	4.563−1	3.553−1	2.777−1	2.209−1	1.801−1	1.517−1	1.338−1	1.256−1	1.267−1	1.356−1	1.469−1
9	19	4.127−1	4.089−1	4.118−1	4.222−1	4.401−1	4.653−1	4.978−1	5.366−1	5.796−1	6.225−1	6.513−1
9	20	9.461−2	8.578−2	7.813−2	7.046−2	6.192−2	5.291−2	4.425−2	3.644−2	2.962−2	2.374−2	1.868−2
9	21	1.355−1	1.235−1	1.154−1	1.089−1	1.026−1	9.725−2	9.441−2	9.525−2	9.998−2	1.078−1	1.153−1
9	22	1.681−2	1.555−2	1.448−2	1.324−2	1.159−2	9.665−3	7.734−3	5.992−3	4.517−3	3.319−3	2.379−3
9	23	5.705−1	5.911−1	6.107−1	6.332−1	6.651−1	7.169−1	8.014−1	9.324−1	1.121+0	1.363+0	1.600+0
9	24	8.077−2	8.386−2	8.432−2	8.107−2	7.374−2	6.369−2	5.277−2	4.228−2	3.289−2	2.491−2	1.838−2
9	25	1.252−1	1.277−1	1.286−1	1.269−1	1.224−1	1.168−1	1.122−1	1.098−1	1.098−1	1.112−1	1.117−1
9	26	5.149−1	5.395−1	5.684−1	6.017−1	6.429−1	6.991−1	7.767−1	8.780−1	1.000+0	1.133+0	1.242+0
9	27	9.501−2	1.042−1	1.091−1	1.085−1	1.019−1	9.084−2	7.768−2	6.406−2	5.103−2	3.930−2	2.928−2
9	28	1.204−1	1.296−1	1.347−1	1.346−1	1.294−1	1.217−1	1.149−1	1.108−1	1.097−1	1.110−1	1.119−1
9	29	1.091−1	1.188−1	1.239−1	1.227−1	1.146−1	1.016−1	8.624−2	7.059−2	5.579−2	4.261−2	3.147−2
9	30	7.236−2	7.407−2	7.393−2	7.075−2	6.399−2	5.477−2	4.472−2	3.510−2	2.659−2	1.949−2	1.387−2
9	31	3.291−2	3.307−2	3.288−2	3.152−2	2.862−2	2.465−2	2.035−2	1.623−2	1.257−2	9.453−3	6.914−3
9	32	7.942−2	6.718−2	5.764−2	5.041−2	4.486−2	4.049−2	3.703−2	3.446−2	3.287−2	3.232−2	3.214−2
9	33	8.984−2	8.713−2	8.599−2	8.636−2	8.826−2	9.171−2	9.661−2	1.026−1	1.093−1	1.157−1	1.193−1
9	34	2.700−2	2.497−2	2.314−2	2.139−2	1.958−2	1.764−2	1.555−2	1.340−2	1.128−2	9.277−3	7.438−3
9	35	4.487−2	4.123−2	3.839−2	3.611−2	3.422−2	3.264−2	3.139−2	3.053−2	3.012−2	3.011−2	2.990−2
9	36	6.467−3	5.656−3	5.020−3	4.480−3	3.974−3	3.464−3	2.941−3	2.416−3	1.914−3	1.461−3	1.077−3
9	37	1.960−1	1.994−1	2.036−1	2.094−1	2.177−1	2.293−1	2.455−1	2.680−1	2.984−1	3.368−1	3.730−1
9	38	2.830−2	2.758−2	2.653−2	2.512−2	2.328−2	2.096−2	1.823−2	1.525−2	1.227−2	9.505−3	7.111−3
9	39	4.248−2	4.235−2	4.196−2	4.130−2	4.036−2	3.912−2	3.762−2	3.597−2	3.432−2	3.275−2	3.094−2
9	40	1.118−1	1.128−1	1.138−1	1.152−1	1.172−1	1.201−1	1.240−1	1.289−1	1.346−1	1.403−1	1.430−1
9	41	3.567−2	3.516−2	3.417−2	3.260−2	3.037−2	2.748−2	2.402−2	2.019−2	1.631−2	1.267−2	9.492−3
9	42	3.733−2	3.689−2	3.603−2	3.474−2	3.304−2	3.098−2	2.869−2	2.640−2	2.431−2	2.254−2	2.089−2
9	43	1.334−1	1.347−1	1.363−1	1.386−1	1.421−1	1.468−1	1.528−1	1.598−1	1.670−1	1.733−1	1.753−1
9	44	2.784−2	2.743−2	2.672−2	2.562−2	2.401−2	2.184−2	1.915−2	1.609−2	1.294−2	9.967−3	7.381−3
9	45	3.427−2	3.359−2	3.250−2	3.095−2	2.884−2	2.613−2	2.289−2	1.928−2	1.558−2	1.209−2	9.022−3

Table 5: Effective collision strengths for transitions in C V. ($a{\pm}b \equiv a{\times}10^{\pm b}$).

Transition		Temperature (log T_e, K)										
i	j	4.0	4.2	4.4	4.6	4.8	5.0	5.2	5.4	5.6	5.8	6.0
9	46	3.241−2	3.227−2	3.200−2	3.161−2	3.111−2	3.051−2	2.986−2	2.921−2	2.861−2	2.803−2	2.711−2
9	47	3.130−2	3.080−2	2.994−2	2.864−2	2.677−2	2.429−2	2.124−2	1.782−2	1.432−2	1.102−2	8.162−3
9	48	2.992−2	2.868−2	2.715−2	2.528−2	2.300−2	2.028−2	1.723−2	1.405−2	1.098−2	8.242−3	5.965−3
9	49	1.296−2	1.274−2	1.237−2	1.180−2	1.100−2	9.934−3	8.651−3	7.239−3	5.814−3	4.488−3	3.336−3
10	11	5.302+0	4.840+0	4.464+0	4.185+0	3.974+0	3.785+0	3.593+0	3.409+0	3.249+0	3.115+0	2.971+0
10	12	4.450−1	3.398−1	2.589−1	2.014−1	1.615−1	1.311−1	1.048−1	8.133−2	6.129−2	4.502−2	3.233−2
10	13	8.512+0	9.286+0	9.948+0	1.051+1	1.097+1	1.136+1	1.191+1	1.284+1	1.418+1	1.583+1	1.735+1
10	14	2.435+1	2.666+1	2.869+1	3.043+1	3.182+1	3.307+1	3.485+1	3.778+1	4.198+1	4.710+1	5.178+1
10	15	1.686+0	1.632+0	1.525+0	1.427+0	1.343+0	1.235+0	1.092+0	9.331−1	7.873−1	6.690−1	5.762−1
10	16	1.052+0	1.013+0	9.392−1	8.672−1	8.009−1	7.214−1	6.227−1	5.170−1	4.181−1	3.334−1	2.639−1
10	17	5.314−1	5.253−1	5.025−1	4.790−1	4.551−1	4.190−1	3.670−1	3.056−1	2.444−1	1.896−1	1.439−1
10	18	1.137+0	9.127−1	7.336−1	5.989−1	4.997−1	4.293−1	3.852−1	3.667−1	3.739−1	4.035−1	4.393−1
10	19	9.277−2	8.452−2	7.731−2	6.995−2	6.162−2	5.275−2	4.416−2	3.639−2	2.959−2	2.372−2	1.867−2
10	20	1.371+0	1.356+0	1.361+0	1.388+0	1.434+0	1.502+0	1.593+0	1.706+0	1.834+0	1.965+0	2.054+0
10	21	4.496−1	4.023−1	3.684−1	3.404−1	3.130−1	2.880−1	2.697−1	2.612−1	2.629−1	2.728−1	2.833−1
10	22	5.375−2	4.884−2	4.490−2	4.071−2	3.545−2	2.945−2	2.351−2	1.818−2	1.369−2	1.005−2	7.196−3
10	23	5.381−1	5.578−1	5.732−1	5.857−1	5.997−1	6.249−1	6.735−1	7.574−1	8.863−1	1.057+0	1.228+0
10	24	1.426+0	1.476+0	1.521+0	1.569+0	1.635+0	1.744+0	1.927+0	2.217+0	2.638+0	3.180+0	3.710+0
10	25	3.652−1	3.745−1	3.770−1	3.692−1	3.498−1	3.243−1	2.996−1	2.799−1	2.664−1	2.579−1	2.495−1
10	26	6.825−1	7.228−1	7.595−1	7.906−1	8.193−1	8.556−1	9.100−1	9.876−1	1.087+0	1.200+0	1.292+0
10	27	9.005−1	9.496−1	9.990−1	1.047+0	1.098+0	1.165+0	1.262+0	1.395+0	1.560+0	1.743+0	1.893+0
10	28	3.960−1	4.292−1	4.469−1	4.447−1	4.222−1	3.877−1	3.511−1	3.191−1	2.942−1	2.762−1	2.606−1
10	29	5.416−1	5.771−1	6.056−1	6.229−1	6.294−1	6.337−1	6.457−1	6.710−1	7.108−1	7.605−1	8.004−1
10	30	2.166−1	2.218−1	2.216−1	2.123−1	1.923−1	1.649−1	1.350−1	1.065−1	8.130−2	6.046−2	4.402−2
10	31	9.870−2	9.923−2	9.869−2	9.469−2	8.603−2	7.413−2	6.119−2	4.881−2	3.778−2	2.841−2	2.078−2
10	32	2.162−1	1.858−1	1.622−1	1.441−1	1.299−1	1.185−1	1.092−1	1.022−1	9.788−2	9.651−2	9.619−2
10	33	2.761−2	2.537−2	2.340−2	2.156−2	1.969−2	1.771−2	1.560−2	1.343−2	1.130−2	9.289−3	7.445−3
10	34	3.115−1	3.035−1	2.995−1	2.995−1	3.035−1	3.119−1	3.244−1	3.405−1	3.588−1	3.767−1	3.859−1
10	35	1.308−1	1.216−1	1.140−1	1.073−1	1.011−1	9.532−2	8.999−2	8.542−2	8.189−2	7.935−2	7.659−2
10	36	1.850−2	1.641−2	1.473−2	1.324−2	1.180−2	1.032−2	8.779−3	7.221−3	5.726−3	4.374−3	3.224−3
10	37	1.857−1	1.874−1	1.891−1	1.916−1	1.952−1	2.007−1	2.092−1	2.219−1	2.407−1	2.658−1	2.897−1
10	38	4.893−1	4.968−1	5.057−1	5.180−1	5.353−1	5.598−1	5.943−1	6.425−1	7.086−1	7.927−1	8.715−1
10	39	1.257−1	1.246−1	1.224−1	1.190−1	1.143−1	1.084−1	1.014−1	9.373−2	8.613−2	7.903−2	7.198−2
10	40	1.644−1	1.646−1	1.641−1	1.633−1	1.621−1	1.609−1	1.599−1	1.592−1	1.591−1	1.594−1	1.575−1
10	41	2.323−1	2.331−1	2.332−1	2.331−1	2.331−1	2.337−1	2.353−1	2.382−1	2.425−1	2.472−1	2.479−1
10	42	1.230−1	1.213−1	1.182−1	1.136−1	1.073−1	9.926−2	8.996−2	8.007−2	7.042−2	6.168−2	5.378−2
10	43	1.971−1	1.978−1	1.984−1	1.990−1	2.001−1	2.018−1	2.041−1	2.068−1	2.097−1	2.119−1	2.098−1
10	44	1.959−1	1.968−1	1.974−1	1.984−1	1.997−1	2.017−1	2.044−1	2.076−1	2.109−1	2.135−1	2.118−1
10	45	1.373−1	1.359−1	1.336−1	1.302−1	1.257−1	1.201−1	1.137−1	1.069−1	1.003−1	9.437−2	8.817−2
10	46	1.057−1	1.047−1	1.030−1	1.004−1	9.667−2	9.189−2	8.615−2	7.983−2	7.348−2	6.747−2	6.146−2
10	47	1.758−1	1.761−1	1.759−1	1.756−1	1.752−1	1.749−1	1.747−1	1.746−1	1.746−1	1.743−1	1.709−1
10	48	8.958−2	8.599−2	8.147−2	7.590−2	6.907−2	6.095−2	5.183−2	4.234−2	3.321−2	2.507−2	1.831−2
10	49	3.896−2	3.832−2	3.721−2	3.551−2	3.307−2	2.985−2	2.599−2	2.174−2	1.746−2	1.347−2	1.002−2
11	12	7.103−1	5.439−1	4.159−1	3.249−1	2.620−1	2.138−1	1.716−1	1.335−1	1.006−1	7.381−2	5.286−2
11	13	1.665+0	1.675+0	1.648+0	1.625+0	1.605+0	1.567+0	1.517+0	1.482+0	1.485+0	1.527+0	1.576+0
11	14	9.757+0	1.048+1	1.106+1	1.156+1	1.195+1	1.226+1	1.272+1	1.353+1	1.477+1	1.635+1	1.781+1
11	15	4.645+1	5.075+1	5.447+1	5.764+1	6.014+1	6.235+1	6.556+1	7.093+1	7.871+1	8.824+1	9.695+1
11	16	1.690+0	1.620+0	1.495+0	1.374+0	1.264+0	1.132+0	9.683−1	7.914−1	6.242−1	4.788−1	3.587−1
11	17	8.850−1	8.747−1	8.365−1	7.975−1	7.579−1	6.985−1	6.121−1	5.101−1	4.081−1	3.167−1	2.404−1

Table 5: Effective collision strengths for transitions in C V. ($a{\pm}b \equiv a{\times}10^{\pm b}$).

Transition		Temperature (log T_e, K)										
i	j	4.0	4.2	4.4	4.6	4.8	5.0	5.2	5.4	5.6	5.8	6.0
11	18	1.975+0	1.580+0	1.264+0	1.027+0	8.528−1	7.291−1	6.512−1	6.176−1	6.281−1	6.770−1	7.375−1
11	19	1.323−1	1.217−1	1.145−1	1.085−1	1.026−1	9.736−2	9.461−2	9.552−2	1.003−1	1.081−1	1.157−1
11	20	4.303−1	3.899−1	3.606−1	3.354−1	3.099−1	2.861−1	2.687−1	2.607−1	2.628−1	2.730−1	2.836−1
11	21	2.907+0	2.749+0	2.661+0	2.635+0	2.655+0	2.722+0	2.837+0	2.997+0	3.191+0	3.395+0	3.531+0
11	22	8.980−2	8.164−2	7.515−2	6.827−2	5.955−2	4.953−2	3.954−2	3.057−2	2.299−2	1.687−2	1.207−2
11	23	2.902−1	2.973−1	3.003−1	2.971−1	2.873−1	2.752−1	2.662−1	2.638−1	2.689−1	2.799−1	2.892−1
11	24	8.233−1	8.494−1	8.669−1	8.747−1	8.766−1	8.861−1	9.208−1	9.956−1	1.120+0	1.291+0	1.458+0
11	25	2.776+0	2.875+0	2.961+0	3.046+0	3.156+0	3.339+0	3.658+0	4.176+0	4.940+0	5.930+0	6.898+0
11	26	4.154−1	4.465−1	4.655−1	4.688−1	4.571−1	4.388−1	4.237−1	4.175−1	4.216−1	4.334−1	4.424−1
11	27	8.437−1	9.020−1	9.442−1	9.641−1	9.627−1	9.547−1	9.567−1	9.783−1	1.021+0	1.080+0	1.127+0
11	28	2.396+0	2.526+0	2.656+0	2.782+0	2.915+0	3.089+0	3.341+0	3.687+0	4.119+0	4.599+0	4.991+0
11	29	5.524−1	5.966−1	6.266−1	6.359−1	6.226−1	5.956−1	5.666−1	5.437−1	5.305−1	5.263−1	5.214−1
11	30	3.554−1	3.644−1	3.647−1	3.500−1	3.172−1	2.719−1	2.223−1	1.747−1	1.327−1	9.770−2	7.003−2
11	31	1.645−1	1.654−1	1.647−1	1.583−1	1.441−1	1.242−1	1.025−1	8.177−2	6.326−2	4.755−2	3.476−2
11	32	4.053−1	3.399−1	2.901−1	2.529−1	2.247−1	2.027−1	1.854−1	1.725−1	1.646−1	1.619−1	1.612−1
11	33	4.827−2	4.351−2	3.991−2	3.713−2	3.490−2	3.310−2	3.170−2	3.076−2	3.029−2	3.024−2	3.001−2
11	34	1.418−1	1.288−1	1.186−1	1.103−1	1.031−1	9.660−2	9.084−2	8.599−2	8.229−2	7.965−2	7.682−2
11	35	6.253−1	6.012−1	5.857−1	5.777−1	5.769−1	5.836−1	5.976−1	6.178−1	6.422−1	6.666−1	6.772−1
11	36	3.133−2	2.774−2	2.485−2	2.230−2	1.984−2	1.732−2	1.471−2	1.209−2	9.575−3	7.310−3	5.385−3
11	37	9.895−2	9.860−2	9.767−2	9.618−2	9.409−2	9.141−2	8.829−2	8.511−2	8.231−2	8.016−2	7.764−2
11	38	2.831−1	2.843−1	2.849−1	2.854−1	2.863−1	2.882−1	2.924−1	3.005−1	3.147−1	3.354−1	3.547−1
11	39	9.536−1	9.664−1	9.812−1	1.001+0	1.030+0	1.071+0	1.130+0	1.214+0	1.331+0	1.483+0	1.625+0
11	40	1.219−1	1.206−1	1.182−1	1.146−1	1.097−1	1.037−1	9.697−2	9.003−2	8.355−2	7.791−2	7.239−2
11	41	2.320−1	2.304−1	2.272−1	2.225−1	2.162−1	2.085−1	1.997−1	1.906−1	1.822−1	1.747−1	1.662−1
11	42	5.565−1	5.590−1	5.599−1	5.602−1	5.610−1	5.632−1	5.675−1	5.747−1	5.847−1	5.957−1	5.967−1
11	43	1.318−1	1.314−1	1.304−1	1.288−1	1.266−1	1.240−1	1.210−1	1.178−1	1.147−1	1.117−1	1.073−1
11	44	2.153−1	2.144−1	2.125−1	2.095−1	2.053−1	1.998−1	1.933−1	1.862−1	1.789−1	1.719−1	1.631−1
11	45	1.837−1	1.808−1	1.760−1	1.691−1	1.598−1	1.479−1	1.339−1	1.187−1	1.036−1	8.955−2	7.685−2
11	46	5.870−1	5.907−1	5.947−1	6.003−1	6.085−1	6.201−1	6.350−1	6.524−1	6.706−1	6.859−1	6.859−1
11	47	1.896−1	1.887−1	1.867−1	1.837−1	1.794−1	1.737−1	1.667−1	1.589−1	1.510−1	1.432−1	1.344−1
11	48	1.478−1	1.422−1	1.349−1	1.257−1	1.143−1	1.007−1	8.556−2	6.977−2	5.459−2	4.106−2	2.980−2
11	49	6.514−2	6.418−2	6.237−2	5.949−2	5.535−2	4.991−2	4.341−2	3.629−2	2.913−2	2.247−2	1.670−2
12	13	2.100−1	2.028−1	1.881−1	1.725−1	1.580−1	1.408−1	1.192−1	9.546−2	7.281−2	5.334−2	3.781−2
12	14	3.546−1	3.422−1	3.173−1	2.913−1	2.670−1	2.384−1	2.024−1	1.628−1	1.249−1	9.236−2	6.636−2
12	15	4.911−1	4.739−1	4.392−1	4.029−1	3.690−1	3.290−1	2.786−1	2.231−1	1.702−1	1.247−1	8.839−2
12	16	3.267+0	2.953+0	2.747+0	2.607+0	2.500+0	2.399+0	2.299+0	2.211+0	2.143+0	2.092+0	2.028+0
12	17	2.549+1	2.639+1	2.746+1	2.865+1	2.982+1	3.104+1	3.269+1	3.517+1	3.863+1	4.286+1	4.677+1
12	18	2.500−1	1.925−1	1.437−1	1.056−1	7.669−2	5.506−2	3.919−2	2.773−2	1.956−2	1.375−2	9.619−3
12	19	1.766−2	1.545−2	1.378−2	1.231−2	1.072−2	9.014−3	7.323−3	5.762−3	4.396−3	3.253−3	2.338−3
12	20	6.460−2	5.408−2	4.638−2	4.013−2	3.418−2	2.830−2	2.276−2	1.778−2	1.350−2	9.968−3	7.158−3
12	21	9.444−2	8.099−2	7.123−2	6.295−2	5.447−2	4.561−2	3.695−2	2.901−2	2.210−2	1.634−2	1.174−2
12	22	5.107−1	5.129−1	5.194−1	5.314−1	5.496−1	5.755−1	6.103−1	6.535−1	7.027−1	7.524−1	7.852−1
12	23	3.154−2	3.329−2	3.395−2	3.301−2	3.026−2	2.624−2	2.173−2	1.729−2	1.328−2	9.854−3	7.088−3
12	24	5.310−2	5.603−2	5.713−2	5.559−2	5.104−2	4.437−2	3.690−2	2.959−2	2.300−2	1.742−2	1.290−2
12	25	7.372−2	7.780−2	7.935−2	7.718−2	7.078−2	6.138−2	5.080−2	4.042−2	3.103−2	2.303−2	1.656−2
12	26	7.038−2	7.684−2	8.020−2	7.969−2	7.509−2	6.734−2	5.780−2	4.760−2	3.763−2	2.858−2	2.092−2
12	27	2.072−1	2.196−1	2.287−1	2.334−1	2.341−1	2.333−1	2.334−1	2.353−1	2.386−1	2.419−1	2.411−1
12	28	1.267−1	1.383−1	1.445−1	1.437−1	1.355−1	1.216−1	1.044−1	8.594−2	6.791−2	5.156−2	3.773−2
12	29	3.690−1	3.861−1	4.017−1	4.144−1	4.255−1	4.394−1	4.595−1	4.853−1	5.140−1	5.409−1	5.548−1

Table 5: Effective collision strengths for transitions in C V. ($a{\pm}b \equiv a{\times}10^{\pm b}$).

Transition		Temperature (log T_e, K)										
i	j	4.0	4.2	4.4	4.6	4.8	5.0	5.2	5.4	5.6	5.8	6.0
12	30	5.894−1	5.950−1	6.049−1	6.197−1	6.430−1	6.815−1	7.408−1	8.229−1	9.253−1	1.039+0	1.133+0
12	31	3.121−1	3.187−1	3.269−1	3.376−1	3.533−1	3.803−1	4.275−1	5.051−1	6.217−1	7.760−1	9.316−1
12	32	2.822−2	2.195−2	1.716−2	1.359−2	1.087−2	8.720−3	6.945−3	5.457−3	4.213−3	3.188−3	2.361−3
12	33	4.699−3	4.205−3	3.803−3	3.452−3	3.113−3	2.757−3	2.373−3	1.971−3	1.573−3	1.205−3	8.881−4
12	34	1.484−2	1.312−2	1.175−2	1.059−2	9.492−3	8.371−3	7.186−3	5.957−3	4.748−3	3.635−3	2.680−3
12	35	2.420−2	2.158−2	1.946−2	1.760−2	1.581−2	1.395−2	1.198−2	9.929−3	7.911−3	6.054−3	4.459−3
12	36	1.374−1	1.359−1	1.361−1	1.381−1	1.422−1	1.484−1	1.568−1	1.670−1	1.783−1	1.894−1	1.961−1
12	37	1.322−2	1.296−2	1.252−2	1.187−2	1.099−2	9.847−3	8.490−3	7.015−3	5.551−3	4.214−3	3.079−3
12	38	2.219−2	2.178−2	2.105−2	1.998−2	1.849−2	1.658−2	1.431−2	1.186−2	9.423−3	7.201−3	5.315−3
12	39	3.100−2	3.044−2	2.943−2	2.790−2	2.579−2	2.309−2	1.988−2	1.642−2	1.299−2	9.852−3	7.198−3
12	40	2.661−2	2.599−2	2.501−2	2.363−2	2.180−2	1.950−2	1.682−2	1.393−2	1.106−2	8.422−3	6.177−3
12	41	4.977−2	4.876−2	4.734−2	4.550−2	4.323−2	4.053−2	3.746−2	3.422−2	3.101−2	2.802−2	2.513−2
12	42	4.797−2	4.691−2	4.517−2	4.268−2	3.935−2	3.518−2	3.033−2	2.510−2	1.992−2	1.518−2	1.113−2
12	43	2.465−2	2.426−2	2.357−2	2.247−2	2.088−2	1.876−2	1.621−2	1.342−2	1.063−2	8.078−3	5.911−3
12	44	6.734−2	6.783−2	6.829−2	6.876−2	6.922−2	6.966−2	7.009−2	7.056−2	7.118−2	7.184−2	7.138−2
12	45	8.122−2	7.984−2	7.824−2	7.658−2	7.500−2	7.351−2	7.213−2	7.085−2	6.964−2	6.836−2	6.608−2
12	46	3.870−2	3.805−2	3.695−2	3.524−2	3.275−2	2.944−2	2.544−2	2.106−2	1.669−2	1.268−2	9.282−3
12	47	7.664−2	7.733−2	7.812−2	7.907−2	8.021−2	8.148−2	8.288−2	8.442−2	8.613−2	8.781−2	8.796−2
12	48	1.764−1	1.761−1	1.764−1	1.778−1	1.805−1	1.852−1	1.919−1	2.009−1	2.118−1	2.234−1	2.306−1
12	49	1.192−1	1.213−1	1.239−1	1.272−1	1.318−1	1.382−1	1.477−1	1.619−1	1.829−1	2.114−1	2.405−1
13	14	3.963+0	3.977+0	3.770+0	3.535+0	3.327+0	3.085+0	2.778+0	2.443+0	2.128+0	1.862+0	1.636+0
13	15	2.827+0	2.758+0	2.519+0	2.272+0	2.061+0	1.834+0	1.563+0	1.276+0	1.013+0	7.972−1	6.298−1
13	16	1.826+0	1.816+0	1.696+0	1.551+0	1.412+0	1.256+0	1.070+0	8.684−1	6.759−1	5.081−1	3.714−1
13	17	6.314−1	5.934−1	5.375−1	4.910−1	4.537−1	4.087−1	3.483−1	2.797−1	2.135−1	1.566−1	1.113−1
13	18	1.189+0	8.905−1	6.618−1	4.930−1	3.688−1	2.772−1	2.110−1	1.645−1	1.330−1	1.125−1	9.854−2
13	19	4.183−1	3.615−1	3.169−1	2.803−1	2.485−1	2.204−1	1.966−1	1.780−1	1.652−1	1.580−1	1.531−1
13	20	5.861−1	5.021−1	4.358−1	3.796−1	3.279−1	2.799−1	2.375−1	2.023−1	1.753−1	1.560−1	1.415−1
13	21	4.721−1	4.079−1	3.570−1	3.117−1	2.665−1	2.222−1	1.822−1	1.492−1	1.235−1	1.043−1	8.961−2
13	22	8.964−2	8.223−2	7.563−2	6.806−2	5.848−2	4.773−2	3.729−2	2.814−2	2.064−2	1.476−2	1.031−2
13	23	1.304+0	1.363+0	1.415+0	1.462+0	1.510+0	1.566+0	1.638+0	1.727+0	1.828+0	1.929+0	1.988+0
13	24	4.229−1	4.415−1	4.469−1	4.352−1	4.058−1	3.660−1	3.253−1	2.896−1	2.612−1	2.400−1	2.223−1
13	25	3.688−1	3.896−1	3.938−1	3.789−1	3.452−1	3.003−1	2.532−1	2.102−1	1.739−1	1.447−1	1.215−1
13	26	5.568+0	5.790+0	6.065+0	6.396+0	6.819+0	7.400+0	8.213+0	9.326+0	1.078+1	1.253+1	1.411+1
13	27	5.001−1	5.462−1	5.741−1	5.752−1	5.461−1	4.957−1	4.368−1	3.790−1	3.275−1	2.842−1	2.474−1
13	28	4.624−1	5.104−1	5.344−1	5.280−1	4.900−1	4.309−1	3.648−1	3.019−1	2.477−1	2.043−1	1.700−1
13	29	5.240−1	5.722−1	5.982−1	5.935−1	5.555−1	4.942−1	4.230−1	3.517−1	2.863−1	2.300−1	1.832−1
13	30	2.633−1	2.803−1	2.868−1	2.787−1	2.544−1	2.190−1	1.797−1	1.419−1	1.084−1	8.024−2	5.772−2
13	31	1.326−1	1.376−1	1.385−1	1.330−1	1.202−1	1.024−1	8.303−2	6.476−2	4.884−2	3.574−2	2.544−2
13	32	1.954−1	1.530−1	1.205−1	9.620−2	7.775−2	6.335−2	5.188−2	4.271−2	3.552−2	3.000−2	2.565−2
13	33	1.108−1	1.028−1	9.560−2	8.870−2	8.173−2	7.453−2	6.721−2	6.008−2	5.358−2	4.803−2	4.313−2
13	34	1.468−1	1.341−1	1.229−1	1.124−1	1.019−1	9.098−2	7.987−2	6.901−2	5.902−2	5.038−2	4.297−2
13	35	1.409−1	1.214−1	1.062−1	9.354−2	8.223−2	7.156−2	6.139−2	5.194−2	4.356−2	3.647−2	3.050−2
13	36	3.030−2	2.728−2	2.458−2	2.197−2	1.931−2	1.652−2	1.368−2	1.092−2	8.401−3	6.235−3	4.477−3
13	37	4.044−1	4.018−1	3.977−1	3.932−1	3.892−1	3.863−1	3.850−1	3.854−1	3.875−1	3.900−1	3.862−1
13	38	1.527−1	1.492−1	1.439−1	1.371−1	1.287−1	1.188−1	1.080−1	9.677−2	8.601−2	7.619−2	6.703−2
13	39	1.297−1	1.264−1	1.213−1	1.146−1	1.061−1	9.585−2	8.440−2	7.250−2	6.103−2	5.074−2	4.180−2
13	40	1.204+0	1.240+0	1.285+0	1.342+0	1.413+0	1.503+0	1.614+0	1.749+0	1.913+0	2.099+0	2.255+0
13	41	1.698−1	1.680−1	1.645−1	1.588−1	1.505−1	1.393−1	1.257−1	1.104−1	9.498−2	8.048−2	6.737−2
13	42	1.573−1	1.551−1	1.508−1	1.439−1	1.339−1	1.208−1	1.055−1	8.915−2	7.342−2	5.950−2	4.781−2

Table 5: Effective collision strengths for transitions in C V. ($a{\pm}b \equiv a{\times}10^{\pm b}$).

Transition		Temperature (log T_e, K)										
i	j	4.0	4.2	4.4	4.6	4.8	5.0	5.2	5.4	5.6	5.8	6.0
13	43	7.651−1	7.572−1	7.461−1	7.343−1	7.232−1	7.145−1	7.112−1	7.167−1	7.335−1	7.603−1	7.801−1
13	44	8.350−2	8.167−2	7.884−2	7.481−2	6.949−2	6.298−2	5.571−2	4.831−2	4.141−2	3.540−2	3.023−2
13	45	1.479−1	1.471−1	1.442−1	1.389−1	1.309−1	1.200−1	1.066−1	9.126−2	7.542−2	6.038−2	4.706−2
13	46	8.298−2	8.100−2	7.789−2	7.350−2	6.775−2	6.083−2	5.327−2	4.580−2	3.909−2	3.351−2	2.890−2
13	47	1.037−1	1.007−1	9.655−2	9.115−2	8.419−2	7.569−2	6.613−2	5.626−2	4.692−2	3.869−2	3.170−2
13	48	1.156−1	1.101−1	1.037−1	9.601−2	8.696−2	7.646−2	6.489−2	5.296−2	4.154−2	3.136−2	2.284−2
13	49	5.413−2	5.297−2	5.103−2	4.818−2	4.429−2	3.936−2	3.365−2	2.758−2	2.167−2	1.635−2	1.189−2
14	15	6.805+0	6.760+0	6.321+0	5.842+0	5.423+0	4.951+0	4.371+0	3.746+0	3.166+0	2.682+0	2.286+0
14	16	3.018+0	2.995+0	2.796+0	2.556+0	2.328+0	2.074+0	1.769+0	1.438+0	1.120+0	8.431−1	6.170−1
14	17	1.109+0	1.047+0	9.557−1	8.796−1	8.190−1	7.461−1	6.509−1	5.459−1	4.471−1	3.632−1	2.946−1
14	18	1.665+0	1.272+0	9.632−1	7.309−1	5.562−1	4.248−1	3.280−1	2.591−1	2.121−1	1.814−1	1.603−1
14	19	1.779−1	1.544−1	1.355−1	1.183−1	1.005−1	8.226−2	6.509−2	5.003−2	3.748−2	2.744−2	1.965−2
14	20	9.354−1	8.514−1	7.824−1	7.169−1	6.485−1	5.796−1	5.164−1	4.643−1	4.266−1	4.032−1	3.863−1
14	21	9.409−1	8.297−1	7.415−1	6.606−1	5.767−1	4.920−1	4.138−1	3.478−1	2.962−1	2.582−1	2.292−1
14	22	1.756−1	1.543−1	1.374−1	1.211−1	1.027−1	8.315−2	6.459−2	4.855−2	3.552−2	2.537−2	1.774−2
14	23	4.212−1	4.400−1	4.457−1	4.343−1	4.052−1	3.657−1	3.251−1	2.894−1	2.611−1	2.399−1	2.221−1
14	24	2.286+0	2.393+0	2.480+0	2.552+0	2.616+0	2.691+0	2.792+0	2.923+0	3.076+0	3.232+0	3.321+0
14	25	7.884−1	8.270−1	8.362−1	8.096−1	7.468−1	6.627−1	5.757−1	4.978−1	4.339−1	3.843−1	3.439−1
14	26	1.701+0	1.802+0	1.887+0	1.945+0	1.982+0	2.021+0	2.095+0	2.229+0	2.435+0	2.706+0	2.957+0
14	27	6.387+0	6.657+0	6.975+0	7.343+0	7.798+0	8.416+0	9.287+0	1.049+1	1.208+1	1.398+1	1.571+1
14	28	1.082+0	1.184+0	1.239+0	1.232+0	1.156+0	1.036+0	9.007−1	7.718−1	6.600−1	5.685−1	4.927−1
14	29	2.592+0	2.726+0	2.856+0	2.974+0	3.089+0	3.234+0	3.453+0	3.780+0	4.240+0	4.815+0	5.343+0
14	30	4.368−1	4.657−1	4.777−1	4.656−1	4.258−1	3.668−1	3.012−1	2.379−1	1.817−1	1.346−1	9.698−2
14	31	2.219−1	2.304−1	2.322−1	2.235−1	2.022−1	1.724−1	1.399−1	1.092−1	8.247−2	6.049−2	4.322−2
14	32	3.078−1	2.420−1	1.918−1	1.542−1	1.256−1	1.030−1	8.478−2	7.010−2	5.849−2	4.955−2	4.245−2
14	33	4.967−2	4.399−2	3.917−2	3.481−2	3.058−2	2.630−2	2.201−2	1.784−2	1.401−2	1.067−2	7.891−3
14	34	3.044−1	2.818−1	2.617−1	2.424−1	2.228−1	2.024−1	1.814−1	1.610−1	1.423−1	1.264−1	1.124−1
14	35	2.793−1	2.505−1	2.263−1	2.046−1	1.836−1	1.625−1	1.414−1	1.212−1	1.028−1	8.699−2	7.355−2
14	36	5.565−2	4.881−2	4.311−2	3.801−2	3.307−2	2.812−2	2.318−2	1.846−2	1.418−2	1.052−2	7.560−3
14	37	1.525−1	1.490−1	1.438−1	1.370−1	1.286−1	1.187−1	1.079−1	9.670−2	8.595−2	7.613−2	6.699−2
14	38	7.156−1	7.108−1	7.023−1	6.920−1	6.816−1	6.723−1	6.652−1	6.609−1	6.596−1	6.596−1	6.499−1
14	39	2.794−1	2.729−1	2.628−1	2.493−1	2.325−1	2.126−1	1.905−1	1.678−1	1.459−1	1.261−1	1.083−1
14	40	4.124−1	4.179−1	4.231−1	4.280−1	4.329−1	4.381−1	4.445−1	4.535−1	4.673−1	4.862−1	5.006−1
14	41	1.529+0	1.569+0	1.620+0	1.684+0	1.764+0	1.864+0	1.989+0	2.141+0	2.328+0	2.544+0	2.724+0
14	42	3.213−1	3.174−1	3.105−1	2.994−1	2.833−1	2.617−1	2.353−1	2.060−1	1.765−1	1.491−1	1.247−1
14	43	3.343−1	3.294−1	3.222−1	3.134−1	3.031−1	2.919−1	2.814−1	2.731−1	2.687−1	2.683−1	2.668−1
14	44	6.949−1	6.876−1	6.763−1	6.629−1	6.486−1	6.355−1	6.263−1	6.243−1	6.323−1	6.496−1	6.620−1
14	45	5.298−1	5.376−1	5.454−1	5.530−1	5.609−1	5.699−1	5.812−1	5.971−1	6.205−1	6.521−1	6.779−1
14	46	1.905−1	1.863−1	1.798−1	1.705−1	1.584−1	1.438−1	1.278−1	1.118−1	9.712−2	8.459−2	7.381−2
14	47	5.093−1	5.021−1	4.922−1	4.805−1	4.676−1	4.546−1	4.436−1	4.372−1	4.377−1	4.448−1	4.494−1
14	48	1.931−1	1.842−1	1.736−1	1.608−1	1.455−1	1.279−1	1.085−1	8.856−2	6.948−2	5.248−2	3.827−2
14	49	9.063−2	8.871−2	8.547−2	8.068−2	7.415−2	6.590−2	5.634−2	4.621−2	3.634−2	2.746−2	2.001−2
15	16	4.145+0	4.112+0	3.839+0	3.509+0	3.192+0	2.839+0	2.419+0	1.967+0	1.534+0	1.158+0	8.498−1
15	17	1.470+0	1.381+0	1.251+0	1.143+0	1.056+0	9.512−1	8.106−1	6.510−1	4.969−1	3.644−1	2.588−1
15	18	2.533+0	1.932+0	1.456+0	1.097+0	8.283−1	6.278−1	4.809−1	3.770−1	3.062−1	2.600−1	2.284−1
15	19	1.722−1	1.548−1	1.406−1	1.266−1	1.107−1	9.368−2	7.777−2	6.442−2	5.408−2	4.645−2	4.061−2
15	20	5.665−1	5.062−1	4.578−1	4.105−1	3.568−1	2.993−1	2.447−1	1.977−1	1.599−1	1.309−1	1.085−1
15	21	2.274+0	1.998+0	1.786+0	1.601+0	1.421+0	1.247+0	1.088+0	9.571−1	8.589−1	7.933−1	7.453−1
15	22	1.897−1	1.789−1	1.687−1	1.548−1	1.349−1	1.110−1	8.712−2	6.590−2	4.838−2	3.461−2	2.418−2

Table 5: Effective collision strengths for transitions in C V. ($a{\pm}b \equiv a{\times}10^{\pm b}$).

Transition		Temperature (log T_e, K)										
i	j	4.0	4.2	4.4	4.6	4.8	5.0	5.2	5.4	5.6	5.8	6.0
15	23	3.682−1	3.895−1	3.944−1	3.802−1	3.469−1	3.019−1	2.546−1	2.113−1	1.746−1	1.453−1	1.219−1
15	24	7.857−1	8.249−1	8.349−1	8.091−1	7.469−1	6.630−1	5.761−1	4.981−1	4.342−1	3.845−1	3.441−1
15	25	3.749+0	3.920+0	4.051+0	4.144+0	4.204+0	4.264+0	4.357+0	4.499+0	4.681+0	4.876+0	4.981+0
15	26	6.646−1	7.306−1	7.651−1	7.588−1	7.104−1	6.345−1	5.504−1	4.722−1	4.074−1	3.584−1	3.204−1
15	27	1.886+0	2.024+0	2.117+0	2.150+0	2.121+0	2.064+0	2.020+0	2.020+0	2.082+0	2.203+0	2.323+0
15	28	1.277+1	1.333+1	1.396+1	1.467+1	1.552+1	1.668+1	1.832+1	2.061+1	2.364+1	2.728+1	3.058+1
15	29	1.148+0	1.245+0	1.311+0	1.331+0	1.298+0	1.230+0	1.153+0	1.089+0	1.052+0	1.047+0	1.051+0
15	30	6.044−1	6.458−1	6.644−1	6.495−1	5.952−1	5.132−1	4.213−1	3.325−1	2.537−1	1.877−1	1.349−1
15	31	3.096−1	3.216−1	3.246−1	3.130−1	2.834−1	2.416−1	1.960−1	1.527−1	1.151−1	8.414−2	5.984−2
15	32	4.513−1	3.541−1	2.793−1	2.232−1	1.806−1	1.473−1	1.207−1	9.946−2	8.275−2	6.994−2	5.982−2
15	33	6.109−2	5.265−2	4.601−2	4.049−2	3.559−2	3.101−2	2.667−2	2.269−2	1.919−2	1.625−2	1.377−2
15	34	1.893−1	1.652−1	1.458−1	1.292−1	1.137−1	9.872−2	8.413−2	7.038−2	5.802−2	4.746−2	3.862−2
15	35	6.746−1	6.140−1	5.624−1	5.154−1	4.693−1	4.223−1	3.749−1	3.289−1	2.869−1	2.508−1	2.196−1
15	36	7.241−2	6.474−2	5.804−2	5.172−2	4.535−2	3.874−2	3.204−2	2.556−2	1.965−2	1.458−2	1.047−2
15	37	1.295−1	1.262−1	1.212−1	1.145−1	1.060−1	9.579−2	8.437−2	7.248−2	6.103−2	5.074−2	4.180−2
15	38	2.792−1	2.727−1	2.627−1	2.492−1	2.324−1	2.125−1	1.905−1	1.678−1	1.459−1	1.261−1	1.083−1
15	39	1.203+0	1.194+0	1.176+0	1.152+0	1.126+0	1.100+0	1.077+0	1.057+0	1.042+0	1.031+0	1.006+0
15	40	2.173−1	2.149−1	2.097−1	2.010−1	1.884−1	1.719−1	1.525−1	1.318−1	1.118−1	9.426−2	7.935−2
15	41	5.012−1	5.024−1	5.020−1	4.992−1	4.934−1	4.843−1	4.729−1	4.614−1	4.532−1	4.503−1	4.461−1
15	42	2.806+0	2.875+0	2.966+0	3.082+0	3.228+0	3.410+0	3.632+0	3.903+0	4.233+0	4.614+0	4.928+0
15	43	1.464−1	1.432−1	1.382−1	1.311−1	1.220−1	1.111−1	9.926−2	8.769−2	7.745−2	6.911−2	6.209−2
15	44	3.246−1	3.182−1	3.086−1	2.958−1	2.797−1	2.610−1	2.411−1	2.221−1	2.061−1	1.941−1	1.835−1
15	45	3.738−1	3.704−1	3.637−1	3.525−1	3.360−1	3.137−1	2.867−1	2.574−1	2.290−1	2.043−1	1.828−1
15	46	1.698+0	1.682+0	1.656+0	1.624+0	1.591+0	1.561+0	1.542+0	1.541+0	1.564+0	1.610+0	1.643+0
15	47	2.574−1	2.523−1	2.448−1	2.348−1	2.222−1	2.073−1	1.915−1	1.763−1	1.636−1	1.540−1	1.456−1
15	48	2.709−1	2.590−1	2.442−1	2.262−1	2.046−1	1.796−1	1.522−1	1.241−1	9.722−2	7.332−2	5.336−2
15	49	1.269−1	1.243−1	1.197−1	1.130−1	1.037−1	9.211−2	7.868−2	6.446−2	5.062−2	3.818−2	2.775−2
16	17	4.403+1	4.543+1	4.667+1	4.760+1	4.802+1	4.829+1	4.955+1	5.274+1	5.803+1	6.481+1	7.111+1
16	18	1.207+0	9.387−1	7.209−1	5.516−1	4.188−1	3.133−1	2.304−1	1.667−1	1.186−1	8.292−2	5.703−2
16	19	1.284−1	1.140−1	1.029−1	9.238−2	8.016−2	6.657−2	5.304−2	4.077−2	3.037−2	2.198−2	1.550−2
16	20	4.821−1	4.057−1	3.496−1	3.026−1	2.561−1	2.092−1	1.649−1	1.259−1	9.339−2	6.749−2	4.761−2
16	21	7.586−1	6.432−1	5.589−1	4.874−1	4.148−1	3.401−1	2.687−1	2.055−1	1.526−1	1.103−1	7.769−2
16	22	3.457−1	2.992−1	2.634−1	2.324−1	2.024−1	1.742−1	1.508−1	1.338−1	1.229−1	1.168−1	1.124−1
16	23	2.286−1	2.463−1	2.539−1	2.483−1	2.282−1	1.980−1	1.639−1	1.305−1	1.005−1	7.493−2	5.423−2
16	24	3.777−1	4.071−1	4.196−1	4.104−1	3.773−1	3.275−1	2.712−1	2.161−1	1.665−1	1.242−1	8.995−2
16	25	5.209−1	5.617−1	5.792−1	5.668−1	5.214−1	4.529−1	3.754−1	2.993−1	2.306−1	1.721−1	1.246−1
16	26	4.523−1	4.993−1	5.276−1	5.291−1	4.994−1	4.453−1	3.780−1	3.072−1	2.400−1	1.809−1	1.323−1
16	27	3.066+0	3.221+0	3.371+0	3.507+0	3.639+0	3.809+0	4.065+0	4.452+0	4.993+0	5.666+0	6.280+0
16	28	7.889−1	8.716−1	9.219−1	9.253−1	8.737−1	7.789−1	6.605−1	5.356−1	4.166−1	3.117−1	2.253−1
16	29	7.737+0	8.065+0	8.428+0	8.828+0	9.306+0	9.960+0	1.090+1	1.223+1	1.401+1	1.614+1	1.808+1
16	30	2.993+0	3.102+0	3.187+0	3.243+0	3.271+0	3.299+0	3.356+0	3.455+0	3.590+0	3.736+0	3.814+0
16	31	8.099−1	8.331−1	8.349−1	8.108−1	7.608−1	6.963−1	6.319−1	5.775−1	5.380−1	5.130−1	4.930−1
16	32	2.351−1	1.901−1	1.544−1	1.262−1	1.031−1	8.333−2	6.605−2	5.102−2	3.829−2	2.790−2	1.977−2
16	33	4.492−2	4.005−2	3.585−2	3.193−2	2.802−2	2.399−2	1.989−2	1.589−2	1.223−2	9.077−3	6.514−3
16	34	1.439−1	1.259−1	1.111−1	9.802−2	8.544−2	7.282−2	6.020−2	4.803−2	3.694−2	2.741−2	1.969−2
16	35	2.349−1	2.060−1	1.822−1	1.610−1	1.405−1	1.199−1	9.916−2	7.916−2	6.089−2	4.517−2	3.243−2
16	36	7.040−2	6.361−2	5.810−2	5.343−2	4.925−2	4.540−2	4.194−2	3.900−2	3.667−2	3.492−2	3.317−2
16	37	9.975−2	9.672−2	9.238−2	8.668−2	7.938−2	7.047−2	6.029−2	4.955−2	3.909−2	2.964−2	2.168−2
16	38	1.667−1	1.619−1	1.548−1	1.452−1	1.328−1	1.178−1	1.007−1	8.269−2	6.520−2	4.944−2	3.616−2

Table 5: Effective collision strengths for transitions in C V. ($a{\pm}b \equiv a{\times}10^{\pm b}$).

Transition		Temperature (log T_e, K)										
i	j	4.0	4.2	4.4	4.6	4.8	5.0	5.2	5.4	5.6	5.8	6.0
16	39	2.347−1	2.284−1	2.185−1	2.049−1	1.872−1	1.658−1	1.415−1	1.161−1	9.142−2	6.924−2	5.058−2
16	40	1.646−1	1.636−1	1.603−1	1.539−1	1.442−1	1.308−1	1.143−1	9.567−2	7.666−2	5.891−2	4.359−2
16	41	5.990−1	6.071−1	6.161−1	6.262−1	6.375−1	6.508−1	6.673−1	6.895−1	7.204−1	7.603−1	7.926−1
16	42	2.929−1	2.895−1	2.829−1	2.717−1	2.548−1	2.315−1	2.023−1	1.692−1	1.353−1	1.036−1	7.624−2
16	43	9.855−2	9.574−2	9.163−2	8.598−2	7.848−2	6.919−2	5.864−2	4.769−2	3.725−2	2.803−2	2.040−2
16	44	6.488−1	6.413−1	6.298−1	6.159−1	6.007−1	5.856−1	5.734−1	5.672−1	5.696−1	5.800−1	5.866−1
16	45	1.788+0	1.832+0	1.887+0	1.957+0	2.045+0	2.158+0	2.298+0	2.472+0	2.684+0	2.929+0	3.131+0
16	46	1.517−1	1.478−1	1.416−1	1.328−1	1.210−1	1.065−1	9.003−2	7.304−2	5.688−2	4.262−2	3.086−2
16	47	8.844−1	8.735−1	8.586−1	8.418−1	8.244−1	8.084−1	7.971−1	7.946−1	8.040−1	8.244−1	8.383−1
16	48	9.050−1	8.902−1	8.727−1	8.550−1	8.383−1	8.238−1	8.125−1	8.046−1	8.001−1	7.968−1	7.817−1
16	49	2.909−1	2.862−1	2.788−1	2.687−1	2.559−1	2.407−1	2.238−1	2.064−1	1.898−1	1.749−1	1.605−1
17	18	5.955−1	4.570−1	3.449−1	2.592−1	1.942−1	1.445−1	1.065−1	7.775−2	5.603−2	3.976−2	2.773−2
17	19	6.160−2	5.305−2	4.652−2	4.076−2	3.488−2	2.889−2	2.321−2	1.816−2	1.386−2	1.031−2	7.490−3
17	20	2.348−1	1.924−1	1.612−1	1.362−1	1.134−1	9.224−2	7.315−2	5.669−2	4.296−2	3.182−2	2.303−2
17	21	3.561−1	2.962−1	2.523−1	2.164−1	1.824−1	1.495−1	1.193−1	9.282−2	7.055−2	5.237−2	3.796−2
17	22	5.070−1	4.486−1	4.060−1	3.739−1	3.491−1	3.322−1	3.261−1	3.347−1	3.616−1	4.056−1	4.517−1
17	23	1.083−1	1.158−1	1.188−1	1.159−1	1.066−1	9.275−2	7.696−2	6.127−2	4.698−2	3.479−2	2.495−2
17	24	1.823−1	1.949−1	2.000−1	1.953−1	1.799−1	1.570−1	1.310−1	1.053−1	8.209−2	6.251−2	4.682−2
17	25	2.522−1	2.698−1	2.767−1	2.701−1	2.485−1	2.163−1	1.794−1	1.428−1	1.095−1	8.105−2	5.809−2
17	26	1.853−1	2.052−1	2.161−1	2.154−1	2.024−1	1.804−1	1.539−1	1.264−1	1.001−1	7.636−2	5.624−2
17	27	7.432−1	7.881−1	8.240−1	8.482−1	8.642−1	8.852−1	9.252−1	9.913−1	1.083+0	1.190+0	1.279+0
17	28	3.330−1	3.688−1	3.885−1	3.875−1	3.643−1	3.248−1	2.773−1	2.277−1	1.802−1	1.374−1	1.012−1
17	29	1.479+0	1.549+0	1.616+0	1.678+0	1.746+0	1.845+0	2.002+0	2.226+0	2.512+0	2.832+0	3.097+0
17	30	2.775+0	2.808+0	2.858+0	2.934+0	3.059+0	3.276+0	3.636+0	4.188+0	4.966+0	5.937+0	6.855+0
17	31	1.321+0	1.369+0	1.432+0	1.513+0	1.610+0	1.730+0	1.880+0	2.058+0	2.259+0	2.465+0	2.615+0
17	32	1.008−1	8.026−2	6.433−2	5.220−2	4.273−2	3.495−2	2.824−2	2.234−2	1.718−2	1.281−2	9.264−3
17	33	1.937−2	1.725−2	1.548−2	1.388−2	1.230−2	1.067−2	8.989−3	7.323−3	5.760−3	4.375−3	3.215−3
17	34	6.173−2	5.415−2	4.801−2	4.265−2	3.755−2	3.242−2	2.723−2	2.213−2	1.738−2	1.319−2	9.688−3
17	35	1.017−1	8.956−2	7.965−2	7.090−2	6.249−2	5.397−2	4.533−2	3.685−2	2.894−2	2.196−2	1.613−2
17	36	1.610−1	1.531−1	1.459−1	1.391−1	1.325−1	1.259−1	1.198−1	1.152−1	1.133−1	1.147−1	1.172−1
17	37	4.931−2	4.808−2	4.619−2	4.357−2	4.009−2	3.571−2	3.060−2	2.513−2	1.976−2	1.491−2	1.083−2
17	38	8.284−2	8.088−2	7.776−2	7.337−2	6.752−2	6.019−2	5.167−2	4.257−2	3.367−2	2.565−2	1.892−2
17	39	1.157−1	1.131−1	1.088−1	1.025−1	9.419−2	8.376−2	7.167−2	5.880−2	4.620−2	3.483−2	2.529−2
17	40	7.143−2	7.009−2	6.785−2	6.452−2	5.992−2	5.400−2	4.694−2	3.919−2	3.137−2	2.410−2	1.781−2
17	41	1.757−1	1.731−1	1.693−1	1.645−1	1.587−1	1.521−1	1.450−1	1.380−1	1.316−1	1.259−1	1.196−1
17	42	1.285−1	1.262−1	1.221−1	1.162−1	1.079−1	9.720−2	8.448−2	7.053−2	5.645−2	4.336−2	3.205−2
17	43	6.678−2	6.582−2	6.410−2	6.139−2	5.746−2	5.216−2	4.559−2	3.816−2	3.053−2	2.337−2	1.719−2
17	44	2.510−1	2.527−1	2.548−1	2.579−1	2.627−1	2.694−1	2.780−1	2.880−1	2.985−1	3.077−1	3.097−1
17	45	3.688−1	3.640−1	3.584−1	3.530−1	3.489−1	3.465−1	3.466−1	3.492−1	3.542−1	3.599−1	3.597−1
17	46	1.048−1	1.032−1	1.004−1	9.617−2	9.003−2	8.176−2	7.148−2	5.985−2	4.788−2	3.666−2	2.696−2
17	47	2.977−1	3.003−1	3.035−1	3.083−1	3.155−1	3.256−1	3.386−1	3.538−1	3.697−1	3.839−1	3.885−1
17	48	8.080−1	8.156−1	8.285−1	8.487−1	8.785−1	9.207−1	9.789−1	1.058+0	1.164+0	1.296+0	1.416+0
17	49	3.543−1	3.651−1	3.781−1	3.945−1	4.158−1	4.429−1	4.762−1	5.145−1	5.557−1	5.957−1	6.204−1
18	19	1.949+1	2.171+1	2.362+1	2.527+1	2.703+1	2.926+1	3.209+1	3.557+1	3.986+1	4.497+1	4.970+1
18	20	5.807+1	6.488+1	7.070+1	7.567+1	8.096+1	8.765+1	9.612+1	1.066+2	1.195+2	1.348+2	1.490+2
18	21	9.760+1	1.087+2	1.182+2	1.262+2	1.349+2	1.459+2	1.599+2	1.773+2	1.988+2	2.244+2	2.481+2
18	22	3.867−1	3.641−1	3.485−1	3.277−1	2.947−1	2.521−1	2.069−1	1.648−1	1.287−1	9.974−2	7.712−2
18	23	5.709+0	5.829+0	5.896+0	5.898+0	5.848+0	5.775+0	5.704+0	5.639+0	5.574+0	5.489+0	5.308+0
18	24	9.514+0	9.709+0	9.821+0	9.830+0	9.749+0	9.628+0	9.507+0	9.395+0	9.283+0	9.139+0	8.837+0

Table 5: Effective collision strengths for transitions in C V. ($a{\pm}b \equiv a{\times}10^{\pm b}$).

Transition		Temperature (log T_e, K)										
i	j	4.0	4.2	4.4	4.6	4.8	5.0	5.2	5.4	5.6	5.8	6.0
18	25	1.336+1	1.364+1	1.382+1	1.387+1	1.378+1	1.360+1	1.341+1	1.323+1	1.305+1	1.283+1	1.240+1
18	26	1.669+0	1.716+0	1.738+0	1.698+0	1.581+0	1.416+0	1.249+0	1.108+0	1.001+0	9.244−1	8.591−1
18	27	1.992+0	2.063+0	2.107+0	2.072+0	1.925+0	1.706+0	1.474+0	1.274+0	1.119+0	1.005+0	9.150−1
18	28	3.012+0	3.234+0	3.635+0	3.978+0	3.974+0	3.631+0	3.136+0	2.656+0	2.266+0	1.978+0	1.756+0
18	29	1.485+0	1.548+0	1.573+0	1.520+0	1.377+0	1.178+0	9.718−1	7.913−1	6.485−1	5.420−1	4.614−1
18	30	7.928−1	8.024−1	8.105−1	7.849−1	7.089−1	5.967−1	4.739−1	3.598−1	2.640−1	1.886−1	1.322−1
18	31	4.048−1	4.247−1	4.389−1	4.287−1	3.871−1	3.243−1	2.563−1	1.939−1	1.422−1	1.019−1	7.159−2
18	32	4.674+0	4.517+0	4.450+0	4.476+0	4.594+0	4.798+0	5.076+0	5.402+0	5.745+0	6.060+0	6.220+0
18	33	2.992−1	2.812−1	2.666−1	2.565−1	2.558−1	2.708−1	3.074−1	3.709−1	4.652−1	5.888−1	7.145−1
18	34	8.342−1	8.009−1	7.716−1	7.513−1	7.557−1	8.048−1	9.173−1	1.109+0	1.393+0	1.765+0	2.142+0
18	35	1.373+0	1.324+0	1.279+0	1.247+0	1.255+0	1.338+0	1.525+0	1.845+0	2.318+0	2.935+0	3.563+0
18	36	4.299−2	3.597−2	3.063−2	2.627−2	2.236−2	1.864−2	1.509−2	1.183−2	8.999−3	6.674−3	4.842−3
18	37	6.532−1	6.705−1	6.917−1	7.204−1	7.598−1	8.130−1	8.819−1	9.665−1	1.066+0	1.176+0	1.269+0
18	38	1.086+0	1.115+0	1.150+0	1.198+0	1.263+0	1.352+0	1.467+0	1.609+0	1.775+0	1.958+0	2.115+0
18	39	1.520+0	1.561+0	1.609+0	1.675+0	1.767+0	1.893+0	2.055+0	2.254+0	2.487+0	2.745+0	2.967+0
18	40	1.109+0	1.129+0	1.151+0	1.176+0	1.204+0	1.233+0	1.260+0	1.280+0	1.290+0	1.285+0	1.247+0
18	41	1.275+0	1.294+0	1.314+0	1.336+0	1.360+0	1.385+0	1.406+0	1.421+0	1.431+0	1.436+0	1.423+0
18	42	1.995+0	2.031+0	2.070+0	2.115+0	2.167+0	2.220+0	2.269+0	2.307+0	2.334+0	2.353+0	2.341+0
18	43	7.977−1	8.019−1	8.054−1	8.091−1	8.132−1	8.180−1	8.241−1	8.319−1	8.413−1	8.508−1	8.475−1
18	44	7.830−1	7.793−1	7.714−1	7.594−1	7.434−1	7.244−1	7.043−1	6.858−1	6.706−1	6.591−1	6.424−1
18	45	5.857−1	5.827−1	5.761−1	5.660−1	5.523−1	5.353−1	5.158−1	4.954−1	4.760−1	4.593−1	4.414−1
18	46	1.260+0	1.266+0	1.271+0	1.276+0	1.281+0	1.288+0	1.297+0	1.309+0	1.323+0	1.338+0	1.333+0
18	47	7.187−1	7.132−1	7.025−1	6.864−1	6.649−1	6.393−1	6.120−1	5.860−1	5.638−1	5.461−1	5.260−1
18	48	1.582−1	1.514−1	1.418−1	1.293−1	1.141−1	9.686−2	7.883−2	6.161−2	4.644−2	3.399−2	2.433−2
18	49	6.780−2	6.601−2	6.299−2	5.859−2	5.276−2	4.573−2	3.804−2	3.036−2	2.330−2	1.723−2	1.234−2
19	20	2.102+0	1.941+0	1.783+0	1.600+0	1.389+0	1.165+0	9.484−1	7.521−1	5.830−1	4.427−1	3.294−1
19	21	4.857+0	4.618+0	4.472+0	4.377+0	4.307+0	4.260+0	4.236+0	4.228+0	4.224+0	4.201+0	4.096+0
19	22	8.015−2	7.372−2	6.997−2	6.541−2	5.766−2	4.742−2	3.677−2	2.727−2	1.959−2	1.374−2	9.463−3
19	23	4.545+1	4.867+1	5.080+1	5.201+1	5.327+1	5.560+1	5.942+1	6.482+1	7.193+1	8.056+1	8.844+1
19	24	5.315−1	5.505−1	5.540−1	5.307−1	4.757−1	4.001−1	3.196−1	2.455−1	1.829−1	1.329−1	9.447−2
19	25	9.643−1	9.906−1	1.014+0	1.018+0	9.931−1	9.518−1	9.118−1	8.840−1	8.703−1	8.662−1	8.546−1
19	26	3.382+0	3.418+0	3.426+0	3.385+0	3.296+0	3.188+0	3.088+0	3.009+0	2.944+0	2.879+0	2.771+0
19	27	4.375−1	4.815−1	5.036−1	4.925−1	4.428−1	3.672−1	2.855−1	2.115−1	1.511−1	1.050−1	7.141−2
19	28	6.604−1	7.062−1	7.458−1	7.548−1	7.106−1	6.262−1	5.311−1	4.466−1	3.806−1	3.322−1	2.943−1
19	29	5.079−1	5.558−1	5.729−1	5.500−1	4.864−1	3.985−1	3.070−1	2.259−1	1.604−1	1.108−1	7.498−2
19	30	2.695−1	2.826−1	2.912−1	2.843−1	2.561−1	2.134−1	1.670−1	1.246−1	8.978−2	6.296−2	4.320−2
19	31	1.431−1	1.555−1	1.659−1	1.675−1	1.566−1	1.362−1	1.120−1	8.841−2	6.782−2	5.113−2	3.816−2
19	32	6.812−1	5.654−1	4.713−1	3.966−1	3.425−1	3.131−1	3.117−1	3.404−1	4.003−1	4.885−1	5.823−1
19	33	1.151+0	1.148+0	1.174+0	1.227+0	1.309+0	1.420+0	1.556+0	1.707+0	1.862+0	2.005+0	2.089+0
19	34	8.953−2	7.827−2	6.999−2	6.357−2	5.814−2	5.306−2	4.793−2	4.260−2	3.707−2	3.151−2	2.606−2
19	35	2.541−1	2.401−1	2.325−1	2.307−1	2.348−1	2.452−1	2.624−1	2.867−1	3.180−1	3.558−1	3.915−1
19	36	1.504−2	1.290−2	1.116−2	9.636−3	8.200−3	6.806−3	5.475−3	4.258−3	3.204−3	2.336−3	1.655−3
19	37	1.119+0	1.147+0	1.181+0	1.237+0	1.334+0	1.493+0	1.740+0	2.106+0	2.619+0	3.280+0	3.951+0
19	38	7.666−2	7.519−2	7.247−2	6.846−2	6.308−2	5.644−2	4.887−2	4.093−2	3.317−2	2.607−2	1.990−2
19	39	2.208−1	2.248−1	2.295−1	2.357−1	2.439−1	2.539−1	2.651−1	2.767−1	2.885−1	3.008−1	3.100−1
19	40	1.401+0	1.442+0	1.497+0	1.576+0	1.689+0	1.844+0	2.043+0	2.282+0	2.552+0	2.838+0	3.072+0
19	41	9.800−2	9.468−2	8.982−2	8.336−2	7.519−2	6.550−2	5.494−2	4.434−2	3.450−2	2.597−2	1.898−2
19	42	2.504−1	2.524−1	2.548−1	2.584−1	2.635−1	2.702−1	2.782−1	2.866−1	2.949−1	3.023−1	3.049−1
19	43	1.161+0	1.184+0	1.214+0	1.252+0	1.298+0	1.350+0	1.402+0	1.448+0	1.487+0	1.516+0	1.518+0

Table 5: Effective collision strengths for transitions in C V. ($a{\pm}b \equiv a{\times}10^{\pm b}$).

Transition		Temperature (log T_e, K)										
i	j	4.0	4.2	4.4	4.6	4.8	5.0	5.2	5.4	5.6	5.8	6.0
19	44	1.769−1	1.716−1	1.632−1	1.513−1	1.358−1	1.173−1	9.700−2	7.687−2	5.852−2	4.300−2	3.066−2
19	45	1.015−1	9.753−2	9.178−2	8.416−2	7.472−2	6.383−2	5.233−2	4.118−2	3.119−2	2.283−2	1.623−2
19	46	2.613−1	2.610−1	2.599−1	2.584−1	2.566−1	2.545−1	2.521−1	2.496−1	2.470−1	2.441−1	2.381−1
19	47	1.687−1	1.640−1	1.568−1	1.464−1	1.324−1	1.152−1	9.606−2	7.665−2	5.870−2	4.333−2	3.099−2
19	48	5.602−2	5.391−2	5.076−2	4.651−2	4.118−2	3.501−2	2.849−2	2.219−2	1.660−2	1.197−2	8.376−3
19	49	2.222−2	2.190−2	2.120−2	2.002−2	1.833−2	1.615−2	1.364−2	1.103−2	8.567−3	6.408−3	4.640−3
20	21	1.466+1	1.356+1	1.278+1	1.217+1	1.164+1	1.119+1	1.081+1	1.052+1	1.027+1	1.003+1	9.641+0
20	22	3.056−1	2.648−1	2.394−1	2.170−1	1.889−1	1.562−1	1.241−1	9.625−2	7.370−2	5.593−2	4.202−2
20	23	3.481+1	3.727+1	3.891+1	3.980+1	4.069+1	4.233+1	4.506+1	4.900+1	5.423+1	6.062+1	6.648+1
20	24	1.034+2	1.106+2	1.154+2	1.179+2	1.207+2	1.258+2	1.343+2	1.464+2	1.624+2	1.818+2	1.996+2
20	25	2.678+0	2.759+0	2.814+0	2.793+0	2.669+0	2.480+0	2.284+0	2.122+0	2.004+0	1.923+0	1.844+0
20	26	4.214+0	4.330+0	4.375+0	4.310+0	4.124+0	3.871+0	3.617+0	3.398+0	3.221+0	3.070+0	2.900+0
20	27	5.610+0	5.735+0	5.814+0	5.784+0	5.609+0	5.345+0	5.071+0	4.835+0	4.643+0	4.475+0	4.263+0
20	28	2.083+0	2.254+0	2.377+0	2.381+0	2.206+0	1.900+0	1.559+0	1.252+0	1.008+0	8.265−1	6.897−1
20	29	3.050+0	3.177+0	3.234+0	3.180+0	3.004+0	2.755+0	2.499+0	2.274+0	2.093+0	1.946+0	1.804+0
20	30	8.752−1	9.190−1	9.484−1	9.308−1	8.504−1	7.292−1	6.006−1	4.861−1	3.932−1	3.211−1	2.647−1
20	31	4.288−1	4.668−1	4.998−1	5.070−1	4.758−1	4.148−1	3.413−1	2.694−1	2.066−1	1.557−1	1.163−1
20	32	1.704+0	1.452+0	1.247+0	1.080+0	9.562−1	8.934−1	9.056−1	1.002+0	1.189+0	1.457+0	1.741+0
20	33	8.730−2	7.689−2	6.913−2	6.303−2	5.781−2	5.286−2	4.782−2	4.253−2	3.704−2	3.150−2	2.605−2
20	34	3.683+0	3.668+0	3.739+0	3.896+0	4.143+0	4.482+0	4.899+0	5.368+0	5.853+0	6.305+0	6.580+0
20	35	6.673−1	6.269−1	6.031−1	5.937−1	5.978−1	6.160−1	6.492−1	6.977−1	7.616−1	8.400−1	9.137−1
20	36	5.134−2	4.272−2	3.608−2	3.057−2	2.567−2	2.110−2	1.687−2	1.306−2	9.799−3	7.134−3	5.053−3
20	37	9.421−1	9.594−1	9.782−1	1.010+0	1.071+0	1.180+0	1.356+0	1.622+0	1.999+0	2.488+0	2.984+0
20	38	2.748+0	2.814+0	2.897+0	3.032+0	3.259+0	3.628+0	4.197+0	5.032+0	6.197+0	7.694+0	9.206+0
20	39	5.499−1	5.560−1	5.618−1	5.686−1	5.773−1	5.877−1	5.994−1	6.114−1	6.240−1	6.385−1	6.482−1
20	40	1.561+0	1.597+0	1.645+0	1.713+0	1.813+0	1.952+0	2.133+0	2.355+0	2.609+0	2.881+0	3.103+0
20	41	2.467+0	2.528+0	2.612+0	2.734+0	2.911+0	3.153+0	3.466+0	3.841+0	4.265+0	4.715+0	5.081+0
20	42	6.309−1	6.298−1	6.267−1	6.226−1	6.185−1	6.150−1	6.123−1	6.107−1	6.101−1	6.101−1	6.035−1
20	43	1.576+0	1.595+0	1.617+0	1.643+0	1.672+0	1.702+0	1.730+0	1.752+0	1.767+0	1.776+0	1.759+0
20	44	1.626+0	1.643+0	1.663+0	1.686+0	1.713+0	1.741+0	1.768+0	1.789+0	1.804+0	1.814+0	1.798+0
20	45	8.995−1	9.081−1	9.194−1	9.378−1	9.677−1	1.013+0	1.077+0	1.160+0	1.258+0	1.367+0	1.457+0
20	46	7.432−1	7.348−1	7.208−1	7.008−1	6.747−1	6.431−1	6.082−1	5.728−1	5.396−1	5.100−1	4.795−1
20	47	1.364+0	1.375+0	1.387+0	1.400+0	1.414+0	1.427+0	1.437+0	1.442+0	1.444+0	1.442+0	1.421+0
20	48	1.686−1	1.623−1	1.530−1	1.404−1	1.247−1	1.065−1	8.731−2	6.893−2	5.272−2	3.941−2	2.900−2
20	49	6.664−2	6.567−2	6.357−2	6.005−2	5.497−2	4.845−2	4.093−2	3.312−2	2.573−2	1.926−2	1.396−2
21	22	4.373−1	3.922−1	3.649−1	3.369−1	2.950−1	2.418−1	1.871−1	1.386−1	9.940−2	6.966−2	4.794−2
21	23	4.246+0	4.467+0	4.619+0	4.668+0	4.631+0	4.582+0	4.588+0	4.700+0	4.947+0	5.326+0	5.701+0
21	24	3.699+1	3.951+1	4.120+1	4.209+1	4.286+1	4.432+1	4.685+1	5.063+1	5.575+1	6.210+1	6.795+1
21	25	1.944+2	2.078+2	2.168+2	2.217+2	2.267+2	2.361+2	2.517+2	2.742+2	3.039+2	3.400+2	3.731+2
21	26	2.306+0	2.431+0	2.485+0	2.428+0	2.244+0	1.984+0	1.717+0	1.487+0	1.309+0	1.174+0	1.062+0
21	27	4.791+0	5.024+0	5.145+0	5.076+0	4.774+0	4.323+0	3.849+0	3.431+0	3.096+0	2.833+0	2.595+0
21	28	1.512+1	1.593+1	1.732+1	1.858+1	1.876+1	1.785+1	1.644+1	1.502+1	1.382+1	1.284+1	1.191+1
21	29	2.734+0	2.915+0	3.015+0	2.975+0	2.767+0	2.448+0	2.106+0	1.797+0	1.546+0	1.350+0	1.188+0
21	30	1.364+0	1.431+0	1.474+0	1.443+0	1.310+0	1.111+0	8.994−1	7.092−1	5.515−1	4.252−1	3.249−1
21	31	7.108−1	7.739−1	8.278−1	8.386−1	7.862−1	6.851−1	5.638−1	4.451−1	3.415−1	2.576−1	1.925−1
21	32	3.518+0	2.884+0	2.391+0	2.007+0	1.730+0	1.578+0	1.567+0	1.709+0	2.007+0	2.448+0	2.917+0
21	33	2.495−1	2.363−1	2.295−1	2.286−1	2.335−1	2.445−1	2.621−1	2.867−1	3.181−1	3.560−1	3.916−1
21	34	6.504−1	6.145−1	5.943−1	5.877−1	5.941−1	6.139−1	6.481−1	6.973−1	7.616−1	8.401−1	9.139−1
21	35	6.451+0	6.404+0	6.504+0	6.753+0	7.159+0	7.718+0	8.412+0	9.194+0	1.001+1	1.077+1	1.123+1

Table 5: Effective collision strengths for transitions in C V. ($a{\pm}b \equiv a{\times}10^{\pm b}$).

Transition		Temperature (log T_e, K)										
i	j	4.0	4.2	4.4	4.6	4.8	5.0	5.2	5.4	5.6	5.8	6.0
21	36	8.495−2	7.085−2	5.995−2	5.087−2	4.274−2	3.515−2	2.809−2	2.175−2	1.631−2	1.186−2	8.391−3
21	37	4.901−1	5.004−1	5.125−1	5.284−1	5.484−1	5.729−1	6.031−1	6.406−1	6.863−1	7.375−1	7.755−1
21	38	1.414+0	1.441+0	1.472+0	1.521+0	1.600+0	1.729+0	1.926+0	2.215+0	2.615+0	3.125+0	3.627+0
21	39	5.149+0	5.263+0	5.403+0	5.635+0	6.038+0	6.705+0	7.746+0	9.286+0	1.144+1	1.422+1	1.703+1
21	40	8.145−1	8.222−1	8.317−1	8.458−1	8.666−1	8.956−1	9.326−1	9.765−1	1.025+0	1.075+0	1.108+0
21	41	1.735+0	1.760+0	1.791+0	1.838+0	1.908+0	2.009+0	2.144+0	2.312+0	2.506+0	2.717+0	2.884+0
21	42	5.931+0	6.075+0	6.272+0	6.561+0	6.981+0	7.561+0	8.311+0	9.217+0	1.024+1	1.134+1	1.224+1
21	43	1.013+0	1.013+0	1.011+0	1.005+0	9.968−1	9.859−1	9.727−1	9.578−1	9.416−1	9.226−1	8.888−1
21	44	1.542+0	1.541+0	1.534+0	1.521+0	1.502+0	1.475+0	1.442+0	1.405+0	1.369+0	1.335+0	1.291+0
21	45	7.867−1	7.822−1	7.750−1	7.670−1	7.606−1	7.586−1	7.645−1	7.805−1	8.074−1	8.437−1	8.729−1
21	46	4.903+0	4.978+0	5.069+0	5.181+0	5.313+0	5.457+0	5.598+0	5.719+0	5.815+0	5.885+0	5.863+0
21	47	1.399+0	1.392+0	1.377+0	1.353+0	1.321+0	1.280+0	1.233+0	1.184+0	1.137+0	1.095+0	1.049+0
21	48	2.764−1	2.660−1	2.506−1	2.299−1	2.039−1	1.738−1	1.419−1	1.112−1	8.386−2	6.130−2	4.369−2
21	49	1.108−1	1.092−1	1.057−1	9.987−2	9.145−2	8.060−2	6.810−2	5.511−2	4.280−2	3.202−2	2.320−2
22	23	1.329−1	1.436−1	1.524−1	1.531−1	1.414−1	1.202−1	9.556−2	7.218−2	5.239−2	3.686−2	2.529−2
22	24	2.316−1	2.491−1	2.636−1	2.646−1	2.449−1	2.095−1	1.683−1	1.292−1	9.608−2	7.003−2	5.044−2
22	25	3.096−1	3.342−1	3.543−1	3.550−1	3.272−1	2.780−1	2.210−1	1.669−1	1.212−1	8.531−2	5.855−2
22	26	2.689−1	3.020−1	3.241−1	3.232−1	2.931−1	2.432−1	1.880−1	1.379−1	9.742−2	6.689−2	4.494−2
22	27	8.684−1	8.768−1	8.738−1	8.389−1	7.635−1	6.647−1	5.667−1	4.844−1	4.221−1	3.775−1	3.424−1
22	28	4.857−1	5.444−1	5.819−1	5.767−1	5.202−1	4.298−1	3.315−1	2.430−1	1.716−1	1.178−1	7.920−2
22	29	1.608+0	1.558+0	1.502+0	1.415+0	1.289+0	1.146+0	1.017+0	9.161−1	8.454−1	7.980−1	7.563−1
22	30	1.176+1	1.122+1	1.079+1	1.040+1	1.005+1	9.746+0	9.508+0	9.319+0	9.153+0	8.969+0	8.640+0
22	31	8.415+1	8.693+1	8.918+1	9.110+1	9.454+1	1.011+2	1.112+2	1.244+2	1.406+2	1.589+2	1.746+2
22	32	1.644−1	1.188−1	8.537−2	6.161−2	4.476−2	3.261−2	2.370−2	1.711−2	1.227−2	8.735−3	6.179−3
22	33	1.807−2	1.504−2	1.265−2	1.067−2	8.921−3	7.304−3	5.810−3	4.476−3	3.337−3	2.413−3	1.696−3
22	34	7.527−2	5.901−2	4.698−2	3.783−2	3.049−2	2.429−2	1.895−2	1.441−2	1.066−2	7.671−3	5.387−3
22	35	1.076−1	8.658−2	7.068−2	5.816−2	4.767−2	3.847−2	3.029−2	2.316−2	1.718−2	1.237−2	8.677−3
22	36	1.589+0	1.606+0	1.646+0	1.714+0	1.813+0	1.945+0	2.106+0	2.286+0	2.470+0	2.638+0	2.733+0
22	37	3.093−2	2.989−2	2.825−2	2.596−2	2.304−2	1.963−2	1.599−2	1.247−2	9.339−3	6.743−3	4.719−3
22	38	5.275−2	5.100−2	4.827−2	4.451−2	3.972−2	3.415−2	2.824−2	2.255−2	1.753−2	1.343−2	1.025−2
22	39	7.233−2	6.979−2	6.587−2	6.050−2	5.370−2	4.574−2	3.728−2	2.908−2	2.177−2	1.572−2	1.100−2
22	40	7.785−2	7.495−2	7.068−2	6.491−2	5.760−2	4.903−2	3.990−2	3.107−2	2.321−2	1.673−2	1.170−2
22	41	4.509−1	4.546−1	4.584−1	4.628−1	4.679−1	4.730−1	4.774−1	4.803−1	4.821−1	4.836−1	4.805−1
22	42	1.416−1	1.365−1	1.287−1	1.181−1	1.046−1	8.891−2	7.227−2	5.621−2	4.198−2	3.024−2	2.114−2
22	43	1.257−1	1.218−1	1.156−1	1.067−1	9.513−2	8.149−2	6.680−2	5.241−2	3.946−2	2.864−2	2.014−2
22	44	4.187−1	4.213−1	4.244−1	4.288−1	4.350−1	4.431−1	4.529−1	4.640−1	4.758−1	4.869−1	4.900−1
22	45	1.300+0	1.323+0	1.351+0	1.387+0	1.430+0	1.478+0	1.525+0	1.566+0	1.599+0	1.627+0	1.634+0
22	46	1.985−1	1.919−1	1.816−1	1.674−1	1.492−1	1.278−1	1.048−1	8.225−2	6.194−2	4.496−2	3.162−2
22	47	4.849−1	4.892−1	4.951−1	5.038−1	5.156−1	5.306−1	5.480−1	5.670−1	5.861−1	6.038−1	6.105−1
22	48	1.567+0	1.593+0	1.629+0	1.686+0	1.772+0	1.896+0	2.061+0	2.267+0	2.510+0	2.779+0	3.013+0
22	49	9.564−1	9.609−1	9.589−1	9.607−1	9.919−1	1.083+0	1.263+0	1.557+0	1.986+0	2.545+0	3.115+0
23	24	5.809+0	6.015+0	6.114+0	6.073+0	5.895+0	5.643+0	5.386+0	5.164+0	4.981+0	4.819+0	4.606+0
23	25	2.350+0	2.500+0	2.581+0	2.554+0	2.405+0	2.185+0	1.956+0	1.758+0	1.605+0	1.490+0	1.386+0
23	26	7.056+1	7.383+1	7.590+1	7.774+1	8.192+1	9.048+1	1.035+2	1.204+2	1.407+2	1.635+2	1.837+2
23	27	1.927+0	2.129+0	2.248+0	2.230+0	2.050+0	1.766+0	1.460+0	1.189+0	9.734−1	8.134−1	6.928−1
23	28	1.904+0	2.156+0	2.303+0	2.289+0	2.083+0	1.753+0	1.398+0	1.087+0	8.451−1	6.698−1	5.441−1
23	29	1.877+0	2.103+0	2.210+0	2.158+0	1.940+0	1.622+0	1.287+0	9.897−1	7.528−1	5.755−1	4.458−1
23	30	1.009+0	1.117+0	1.182+0	1.174+0	1.075+0	9.139−1	7.321−1	5.612−1	4.170−1	3.034−1	2.178−1
23	31	3.938−1	4.279−1	4.530−1	4.512−1	4.141−1	3.535−1	2.871−1	2.260−1	1.742−1	1.315−1	9.672−2

Table 5: Effective collision strengths for transitions in C V. ($a{\pm}b \equiv a{\times}10^{\pm b}$).

Transition		Temperature (log T_e, K)										
i	j	4.0	4.2	4.4	4.6	4.8	5.0	5.2	5.4	5.6	5.8	6.0
23	32	1.098+0	8.623−1	6.846−1	5.581−1	4.713−1	4.140−1	3.786−1	3.598−1	3.541−1	3.589−1	3.663−1
23	33	1.036+0	9.326−1	8.254−1	7.104−1	6.012−1	5.156−1	4.648−1	4.526−1	4.782−1	5.367−1	6.047−1
23	34	9.940−1	8.716−1	7.564−1	6.418−1	5.366−1	4.539−1	4.014−1	3.810−1	3.912−1	4.275−1	4.721−1
23	35	6.546−1	5.480−1	4.722−1	4.185−1	3.798−1	3.511−1	3.294−1	3.128−1	2.997−1	2.874−1	2.711−1
23	36	7.750−2	6.047−2	4.832−2	3.924−2	3.195−2	2.572−2	2.024−2	1.547−2	1.146−2	8.227−3	5.746−3
23	37	3.457+0	3.588+0	3.766+0	4.004+0	4.316+0	4.707+0	5.166+0	5.662+0	6.158+0	6.602+0	6.852+0
23	38	5.767−1	5.715−1	5.627−1	5.531−1	5.451−1	5.410−1	5.425−1	5.505−1	5.656−1	5.877−1	6.067−1
23	39	3.835−1	3.799−1	3.731−1	3.638−1	3.528−1	3.404−1	3.276−1	3.155−1	3.052−1	2.977−1	2.903−1
23	40	9.205+0	9.490+0	9.966+0	1.073+1	1.179+1	1.320+1	1.505+1	1.748+1	2.068+1	2.464+1	2.848+1
23	41	6.229−1	6.165−1	6.056−1	5.908−1	5.727−1	5.523−1	5.309−1	5.101−1	4.917−1	4.774−1	4.627−1
23	42	5.245−1	5.162−1	5.028−1	4.843−1	4.613−1	4.349−1	4.073−1	3.808−1	3.573−1	3.381−1	3.200−1
23	43	5.819+0	5.958+0	6.156+0	6.449+0	6.873+0	7.453+0	8.197+0	9.080+0	1.006+1	1.108+1	1.187+1
23	44	6.068−1	5.966−1	5.797−1	5.557−1	5.250−1	4.890−1	4.508−1	4.137−1	3.808−1	3.532−1	3.276−1
23	45	4.584−1	4.443−1	4.230−1	3.948−1	3.605−1	3.223−1	2.833−1	2.467−1	2.151−1	1.897−1	1.693−1
23	46	5.585−1	5.461−1	5.274−1	5.031−1	4.743−1	4.432−1	4.130−1	3.865−1	3.655−1	3.497−1	3.338−1
23	47	5.924−1	5.816−1	5.642−1	5.393−1	5.067−1	4.675−1	4.250−1	3.829−1	3.447−1	3.122−1	2.831−1
23	48	2.037−1	1.940−1	1.809−1	1.646−1	1.452−1	1.234−1	1.009−1	7.920−2	5.994−2	4.390−2	3.126−2
23	49	8.848−2	8.538−2	8.082−2	7.465−2	6.682−2	5.758−2	4.759−2	3.768−2	2.864−2	2.097−2	1.487−2
24	25	8.264+0	8.624+0	8.815+0	8.759+0	8.437+0	7.959+0	7.462+0	7.030+0	6.683+0	6.397+0	6.071+0
24	26	1.585+1	1.674+1	1.727+1	1.756+1	1.807+1	1.925+1	2.125+1	2.403+1	2.752+1	3.154+1	3.512+1
24	27	7.731+1	8.111+1	8.359+1	8.575+1	9.041+1	9.982+1	1.141+2	1.327+2	1.549+2	1.799+2	2.021+2
24	28	4.389+0	4.935+0	5.337+0	5.417+0	5.041+0	4.335+0	3.537+0	2.818+0	2.249+0	1.832+0	1.525+0
24	29	2.865+1	3.014+1	3.106+1	3.172+1	3.312+1	3.609+1	4.076+1	4.693+1	5.444+1	6.297+1	7.053+1
24	30	1.677+0	1.854+0	1.965+0	1.954+0	1.793+0	1.525+0	1.222+0	9.374−1	6.966−1	5.071−1	3.644−1
24	31	7.830−1	8.425−1	8.870−1	8.856−1	8.242−1	7.251−1	6.214−1	5.341−1	4.704−1	4.285−1	3.981−1
24	32	1.687+0	1.327+0	1.062+0	8.765−1	7.501−1	6.669−1	6.161−1	5.900−1	5.838−1	5.939−1	6.076−1
24	33	1.530−1	1.241−1	1.026−1	8.593−2	7.215−2	6.009−2	4.925−2	3.956−2	3.107−2	2.388−2	1.795−2
24	34	2.262+0	2.104+0	1.913+0	1.685+0	1.455+0	1.271+0	1.161+0	1.136+0	1.196+0	1.329+0	1.481+0
24	35	1.433+0	1.270+0	1.121+0	9.763−1	8.447−1	7.408−1	6.730−1	6.428−1	6.477−1	6.812−1	7.207−1
24	36	1.374−1	1.062−1	8.417−2	6.787−2	5.500−2	4.415−2	3.472−2	2.658−2	1.979−2	1.434−2	1.017−2
24	37	5.774−1	5.731−1	5.647−1	5.550−1	5.468−1	5.422−1	5.432−1	5.509−1	5.657−1	5.875−1	6.061−1
24	38	5.835+0	6.053+0	6.349+0	6.741+0	7.255+0	7.900+0	8.655+0	9.470+0	1.028+1	1.101+1	1.141+1
24	39	9.598−1	9.504−1	9.341−1	9.146−1	8.952−1	8.787−1	8.677−1	8.643−1	8.700−1	8.859−1	8.989−1
24	40	2.482+0	2.527+0	2.600+0	2.721+0	2.896+0	3.135+0	3.458+0	3.892+0	4.468+0	5.183+0	5.870+0
24	41	1.115+1	1.148+1	1.204+1	1.295+1	1.423+1	1.592+1	1.813+1	2.106+1	2.490+1	2.966+1	3.427+1
24	42	1.238+0	1.223+0	1.199+0	1.168+0	1.129+0	1.085+0	1.039+0	9.956−1	9.570−1	9.265−1	8.954−1
24	43	2.407+0	2.438+0	2.480+0	2.543+0	2.637+0	2.770+0	2.947+0	3.163+0	3.410+0	3.671+0	3.866+0
24	44	5.179+0	5.275+0	5.415+0	5.625+0	5.937+0	6.372+0	6.938+0	7.620+0	8.388+0	9.194+0	9.821+0
24	45	3.153+0	3.209+0	3.303+0	3.462+0	3.701+0	4.036+0	4.499+0	5.130+0	5.974+0	7.031+0	8.059+0
24	46	1.240+0	1.223+0	1.195+0	1.156+0	1.109+0	1.055+0	1.001+0	9.510−1	9.089−1	8.752−1	8.382−1
24	47	3.814+0	3.874+0	3.959+0	4.090+0	4.286+0	4.563+0	4.929+0	5.377+0	5.886+0	6.424+0	6.843+0
24	48	3.406−1	3.248−1	3.031−1	2.758−1	2.432−1	2.068−1	1.690−1	1.329−1	1.007−1	7.394−2	5.283−2
24	49	1.498−1	1.446−1	1.369−1	1.265−1	1.133−1	9.781−2	8.106−2	6.449−2	4.938−2	3.657−2	2.634−2
25	26	2.983+0	3.327+0	3.510+0	3.471+0	3.204+0	2.813+0	2.428+0	2.128+0	1.933+0	1.832+0	1.771+0
25	27	1.374+1	1.472+1	1.529+1	1.548+1	1.557+1	1.600+1	1.700+1	1.860+1	2.078+1	2.342+1	2.580+1
25	28	1.514+2	1.595+2	1.657+2	1.714+2	1.812+2	1.993+2	2.265+2	2.617+2	3.044+2	3.526+2	3.955+2
25	29	6.729+0	7.263+0	7.576+0	7.634+0	7.540+0	7.504+0	7.674+0	8.103+0	8.798+0	9.704+0	1.053+1
25	30	2.308+0	2.554+0	2.706+0	2.689+0	2.465+0	2.097+0	1.681+0	1.290+0	9.597−1	6.999−1	5.040−1
25	31	9.205−1	1.000+0	1.060+0	1.056+0	9.649−1	8.112−1	6.386−1	4.788−1	3.461−1	2.434−1	1.674−1

Table 5: Effective collision strengths for transitions in C V. ($a{\pm}b \equiv a{\times}10^{\pm b}$).

Transition		Temperature (log T_e, K)										
i	j	4.0	4.2	4.4	4.6	4.8	5.0	5.2	5.4	5.6	5.8	6.0
25	32	2.410+0	1.893+0	1.513+0	1.245+0	1.062+0	9.423−1	8.684−1	8.302−1	8.203−1	8.335−1	8.520−1
25	33	2.717−1	2.307−1	2.020−1	1.820−1	1.680−1	1.580−1	1.509−1	1.458−1	1.423−1	1.406−1	1.392−1
25	34	7.771−1	6.468−1	5.547−1	4.887−1	4.398−1	4.020−1	3.719−1	3.477−1	3.287−1	3.151−1	3.038−1
25	35	4.587+0	4.189+0	3.757+0	3.271+0	2.797+0	2.418+0	2.185+0	2.117+0	2.211+0	2.444+0	2.717+0
25	36	1.535−1	1.234−1	1.014−1	8.426−2	6.991−2	5.707−2	4.536−2	3.491−2	2.598−2	1.872−2	1.311−2
25	37	3.842−1	3.806−1	3.738−1	3.645−1	3.533−1	3.408−1	3.280−1	3.158−1	3.053−1	2.976−1	2.900−1
25	38	9.611−1	9.529−1	9.372−1	9.177−1	8.978−1	8.806−1	8.690−1	8.651−1	8.704−1	8.857−1	8.979−1
25	39	8.993+0	9.293+0	9.693+0	1.023+1	1.094+1	1.184+1	1.290+1	1.406+1	1.523+1	1.630+1	1.691+1
25	40	7.683−1	7.580−1	7.420−1	7.209−1	6.954−1	6.676−1	6.405−1	6.175−1	6.001−1	5.861−1	5.649−1
25	41	2.536+0	2.551+0	2.583+0	2.648+0	2.757+0	2.917+0	3.144+0	3.460+0	3.886+0	4.422+0	4.932+0
25	42	2.070+1	2.129+1	2.228+1	2.388+1	2.613+1	2.911+1	3.304+1	3.825+1	4.508+1	5.353+1	6.174+1
25	43	9.887−1	9.738−1	9.508−1	9.213−1	8.874−1	8.526−1	8.214−1	7.979−1	7.839−1	7.780−1	7.670−1
25	44	2.112+0	2.108+0	2.100+0	2.092+0	2.089+0	2.098+0	2.126+0	2.179+0	2.256+0	2.350+0	2.416+0
25	45	1.225+0	1.204+0	1.174+0	1.143+0	1.120+0	1.113+0	1.129+0	1.171+0	1.245+0	1.349+0	1.448+0
25	46	1.275+1	1.300+1	1.338+1	1.395+1	1.479+1	1.594+1	1.742+1	1.919+1	2.116+1	2.322+1	2.482+1
25	47	1.870+0	1.858+0	1.840+0	1.818+0	1.797+0	1.783+0	1.783+0	1.803+0	1.845+0	1.904+0	1.945+0
25	48	4.762−1	4.546−1	4.246−1	3.861−1	3.401−1	2.887−1	2.356−1	1.848−1	1.397−1	1.022−1	7.266−2
25	49	2.083−1	2.012−1	1.904−1	1.756−1	1.570−1	1.351−1	1.115−1	8.822−2	6.702−2	4.905−2	3.475−2
26	27	6.135+0	6.867+0	7.320+0	7.345+0	6.890+0	6.124+0	5.279+0	4.512+0	3.886+0	3.397+0	2.993+0
26	28	4.158+0	4.937+0	5.398+0	5.408+0	4.933+0	4.145+0	3.280+0	2.501+0	1.876+0	1.410+0	1.072+0
26	29	5.162+0	5.979+0	6.458+0	6.450+0	5.931+0	5.091+0	4.169+0	3.328+0	2.637+0	2.101+0	1.691+0
26	30	1.597+0	1.829+0	1.959+0	1.938+0	1.755+0	1.476+0	1.179+0	9.149−1	6.967−1	5.223−1	3.847−1
26	31	7.502−1	8.430−1	8.969−1	8.851−1	7.980−1	6.618−1	5.137−1	3.795−1	2.700−1	1.867−1	1.262−1
26	32	1.239+0	9.221−1	6.798−1	5.008−1	3.726−1	2.847−1	2.280−1	1.940−1	1.751−1	1.639−1	1.531−1
26	33	4.348−1	3.712−1	3.219−1	2.824−1	2.497−1	2.218−1	1.983−1	1.791−1	1.641−1	1.532−1	1.441−1
26	34	7.496−1	6.180−1	5.185−1	4.407−1	3.771−1	3.233−1	2.775−1	2.394−1	2.089−1	1.857−1	1.671−1
26	35	7.998−1	6.290−1	5.047−1	4.122−1	3.405−1	2.827−1	2.352−1	1.965−1	1.659−1	1.423−1	1.240−1
26	36	1.283−1	1.037−1	8.496−2	7.000−2	5.727−2	4.596−2	3.586−2	2.710−2	1.983−2	1.407−2	9.728−3
26	37	2.380+0	2.308+0	2.198+0	2.061+0	1.905+0	1.737+0	1.569+0	1.411+0	1.274+0	1.158+0	1.048+0
26	38	8.728−1	8.461−1	8.059−1	7.550−1	6.956−1	6.304−1	5.634−1	4.993−1	4.416−1	3.913−1	3.449−1
26	39	5.251−1	5.048−1	4.747−1	4.364−1	3.917−1	3.431−1	2.942−1	2.486−1	2.089−1	1.759−1	1.482−1
26	40	7.789+0	7.861+0	7.959+0	8.105+0	8.319+0	8.608+0	8.964+0	9.358+0	9.753+0	1.009+1	1.019+1
26	41	1.090+0	1.057+0	1.012+0	9.569−1	8.932−1	8.238−1	7.534−1	6.872−1	6.293−1	5.819−1	5.398−1
26	42	8.224−1	7.899−1	7.446−1	6.870−1	6.182−1	5.412−1	4.619−1	3.866−1	3.205−1	2.661−1	2.223−1
26	43	3.593+1	3.729+1	3.946+1	4.261+1	4.662+1	5.137+1	5.705+1	6.406+1	7.288+1	8.355+1	9.354+1
26	44	1.429+0	1.402+0	1.356+0	1.291+0	1.204+0	1.101+0	9.895−1	8.794−1	7.793−1	6.942−1	6.196−1
26	45	7.167−1	6.901−1	6.532−1	6.062−1	5.500−1	4.866−1	4.206−1	3.574−1	3.011−1	2.545−1	2.165−1
26	46	1.257+0	1.213+0	1.146+0	1.057+0	9.464−1	8.214−1	6.934−1	5.747−1	4.735−1	3.927−1	3.289−1
26	47	1.477+0	1.442+0	1.388+0	1.313+0	1.215+0	1.098+0	9.704−1	8.445−1	7.299−1	6.323−1	5.492−1
26	48	3.927−1	3.714−1	3.433−1	3.088−1	2.688−1	2.251−1	1.808−1	1.393−1	1.033−1	7.403−2	5.153−2
26	49	1.417−1	1.373−1	1.299−1	1.193−1	1.059−1	9.037−2	7.396−2	5.801−2	4.369−2	3.172−2	2.230−2
27	28	1.030+1	1.188+1	1.286+1	1.293+1	1.197+1	1.035+1	8.563+0	6.943+0	5.627+0	4.618+0	3.841+0
27	29	5.208+0	6.086+0	6.616+0	6.614+0	6.023+0	5.052+0	3.987+0	3.027+0	2.254+0	1.675+0	1.254+0
27	30	3.158+1	3.357+1	3.498+1	3.599+1	3.757+1	4.061+1	4.531+1	5.153+1	5.922+1	6.814+1	7.622+1
27	31	4.196+0	4.277+0	4.307+0	4.217+0	3.992+0	3.693+0	3.396+0	3.144+0	2.943+0	2.777+0	2.603+0
27	32	1.533+0	1.142+0	8.430−1	6.219−1	4.624−1	3.515−1	2.781−1	2.319−1	2.038−1	1.854−1	1.689−1
27	33	1.884−1	1.504−1	1.218−1	9.945−2	8.094−2	6.491−2	5.084−2	3.874−2	2.869−2	2.069−2	1.457−2
27	34	1.014+0	8.368−1	7.037−1	6.007−1	5.175−1	4.479−1	3.894−1	3.414−1	3.036−1	2.752−1	2.524−1
27	35	1.232+0	9.859−1	8.037−1	6.647−1	5.539−1	4.620−1	3.848−1	3.207−1	2.694−1	2.299−1	1.990−1

Table 5: Effective collision strengths for transitions in C V. ($a{\pm}b \equiv a{\times}10^{\pm b}$).

Transition		Temperature (log T_e, K)										
i	j	4.0	4.2	4.4	4.6	4.8	5.0	5.2	5.4	5.6	5.8	6.0
27	36	3.141−1	2.434−1	1.933−1	1.565−1	1.284−1	1.059−1	8.747−2	7.257−2	6.079−2	5.182−2	4.487−2
27	37	3.835−1	3.707−1	3.512−1	3.257−1	2.954−1	2.616−1	2.268−1	1.933−1	1.632−1	1.378−1	1.168−1
27	38	2.837+0	2.745+0	2.607+0	2.437+0	2.242+0	2.033+0	1.822+0	1.626+0	1.456+0	1.312+0	1.181+0
27	39	1.051+0	1.013+0	9.580−1	8.889−1	8.081−1	7.191−1	6.280−1	5.413−1	4.641−1	3.983−1	3.411−1
27	40	1.050+0	1.019+0	9.756−1	9.210−1	8.573−1	7.876−1	7.168−1	6.502−1	5.919−1	5.440−1	5.020−1
27	41	1.109+1	1.118+1	1.129+1	1.147+1	1.174+1	1.211+1	1.257+1	1.309+1	1.361+1	1.406+1	1.419+1
27	42	1.487+0	1.439+0	1.373+0	1.290+0	1.192+0	1.082+0	9.697−1	8.622−1	7.670−1	6.882−1	6.211−1
27	43	3.829+0	3.872+0	3.924+0	4.000+0	4.114+0	4.281+0	4.525+0	4.872+0	5.350+0	5.956+0	6.522+0
27	44	4.751+1	4.925+1	5.201+1	5.603+1	6.113+1	6.722+1	7.451+1	8.356+1	9.498+1	1.088+2	1.218+2
27	45	1.017+0	9.774−1	9.241−1	8.578−1	7.798−1	6.938−1	6.059−1	5.232−1	4.509−1	3.915−1	3.422−1
27	46	2.456+0	2.400+0	2.310+0	2.183+0	2.021+0	1.829+0	1.625+0	1.425+0	1.245+0	1.093+0	9.629−1
27	47	2.403+0	2.393+0	2.391+0	2.413+0	2.466+0	2.553+0	2.682+0	2.865+0	3.117+0	3.437+0	3.735+0
27	48	1.602+0	1.536+0	1.449+0	1.347+0	1.231+0	1.107+0	9.829−1	8.661−1	7.637−1	6.771−1	5.992−1
27	49	3.990−1	3.855−1	3.665−1	3.428−1	3.152−1	2.854−1	2.555−1	2.276−1	2.033−1	1.836−1	1.667−1
28	29	6.003+0	6.932+0	7.529+0	7.605+0	7.088+0	6.164+0	5.106+0	4.116+0	3.286+0	2.635+0	2.131+0
28	30	2.800+0	3.217+0	3.465+0	3.443+0	3.113+0	2.582+0	2.001+0	1.475+0	1.048+0	7.240−1	4.896−1
28	31	1.350+0	1.519+0	1.621+0	1.604+0	1.449+0	1.203+0	9.337−1	6.896−1	4.905−1	3.390−1	2.291−1
28	32	2.174+0	1.620+0	1.197+0	8.847−1	6.603−1	5.061−1	4.064−1	3.467−1	3.136−1	2.940−1	2.750−1
28	33	2.555−1	2.016−1	1.622−1	1.329−1	1.102−1	9.202−2	7.718−2	6.517−2	5.568−2	4.844−2	4.276−2
28	34	7.678−1	6.081−1	4.908−1	4.017−1	3.310−1	2.724−1	2.232−1	1.822−1	1.490−1	1.232−1	1.031−1
28	35	3.061+0	2.440+0	1.987+0	1.650+0	1.390+0	1.183+0	1.016+0	8.825−1	7.797−1	7.035−1	6.428−1
28	36	2.477−1	1.980−1	1.607−1	1.313−1	1.066−1	8.506−2	6.606−2	4.975−2	3.631−2	2.573−2	1.776−2
28	37	3.860−1	3.709−1	3.482−1	3.192−1	2.853−1	2.486−1	2.119−1	1.779−1	1.485−1	1.247−1	1.055−1
28	38	7.600−1	7.333−1	6.939−1	6.436−1	5.845−1	5.194−1	4.527−1	3.892−1	3.326−1	2.852−1	2.457−1
28	39	5.656+0	5.470+0	5.201+0	4.874+0	4.501+0	4.100+0	3.695+0	3.315+0	2.981+0	2.698+0	2.433+0
28	40	8.226−1	7.905−1	7.455−1	6.878−1	6.188−1	5.417−1	4.622−1	3.868−1	3.206−1	2.662−1	2.222−1
28	41	1.538+0	1.490+0	1.423+0	1.338+0	1.238+0	1.127+0	1.013+0	9.053−1	8.097−1	7.307−1	6.628−1
28	42	1.514+1	1.523+1	1.535+1	1.556+1	1.589+1	1.634+1	1.691+1	1.756+1	1.821+1	1.878+1	1.893+1
28	43	1.541+0	1.493+0	1.420+0	1.322+0	1.200+0	1.062+0	9.224−1	7.947−1	6.880−1	6.040−1	5.343−1
28	44	4.169+0	4.168+0	4.165+0	4.178+0	4.216+0	4.288+0	4.404+0	4.580+0	4.834+0	5.169+0	5.467+0
28	45	1.293+0	1.240+0	1.166+0	1.071+0	9.584−1	8.321−1	7.020−1	5.785−1	4.701−1	3.811−1	3.102−1
28	46	6.300+1	6.527+1	6.890+1	7.420+1	8.094+1	8.898+1	9.860+1	1.105+2	1.255+2	1.437+2	1.607+2
28	47	3.543+0	3.521+0	3.475+0	3.420+0	3.380+0	3.380+0	3.442+0	3.580+0	3.809+0	4.125+0	4.421+0
28	48	7.127−1	6.736−1	6.219−1	5.590−1	4.861−1	4.067−1	3.264−1	2.513−1	1.861−1	1.332−1	9.264−2
28	49	2.561−1	2.471−1	2.330−1	2.137−1	1.897−1	1.620−1	1.326−1	1.041−1	7.842−2	5.695−2	4.005−2
29	30	8.392+1	8.909+1	9.283+1	9.589+1	1.011+2	1.107+2	1.251+2	1.438+2	1.665+2	1.925+2	2.160+2
29	31	8.982+0	8.979+0	8.920+0	8.703+0	8.311+0	7.849+0	7.424+0	7.081+0	6.813+0	6.578+0	6.271+0
29	32	1.360+0	1.010+0	7.422−1	5.434−1	3.989−1	2.967−1	2.261−1	1.781−1	1.450−1	1.210−1	1.013−1
29	33	1.791−1	1.430−1	1.158−1	9.423−2	7.635−2	6.091−2	4.745−2	3.593−2	2.643−2	1.891−2	1.320−2
29	34	8.467−1	6.660−1	5.343−1	4.356−1	3.584−1	2.957−1	2.440−1	2.018−1	1.683−1	1.429−1	1.233−1
29	35	1.127+0	8.785−1	6.975−1	5.616−1	4.548−1	3.671−1	2.935−1	2.325−1	1.835−1	1.455−1	1.166−1
29	36	3.540−1	2.855−1	2.365−1	2.002−1	1.723−1	1.498−1	1.315−1	1.168−1	1.053−1	9.656−2	8.937−2
29	37	3.108−1	2.994−1	2.822−1	2.597−1	2.324−1	2.016−1	1.697−1	1.390−1	1.117−1	8.879−2	7.044−2
29	38	1.297+0	1.253+0	1.186+0	1.101+0	1.003+0	8.959−1	7.876−1	6.862−1	5.978−1	5.241−1	4.596−1
29	39	8.429−1	8.089−1	7.589−1	6.951−1	6.197−1	5.365−1	4.513−1	3.709−1	3.002−1	2.415−1	1.937−1
29	40	7.376−1	7.131−1	6.782−1	6.332−1	5.787−1	5.172−1	4.529−1	3.911−1	3.361−1	2.903−1	2.524−1
29	41	9.119−1	8.768−1	8.280−1	7.656−1	6.908−1	6.071−1	5.208−1	4.392−1	3.676−1	3.088−1	2.608−1
29	42	1.305+0	1.255+0	1.184+0	1.093+0	9.839−1	8.612−1	7.344−1	6.138−1	5.078−1	4.206−1	3.507−1
29	43	2.342+0	2.337+0	2.335+0	2.345+0	2.370+0	2.409+0	2.466+0	2.546+0	2.659+0	2.809+0	2.937+0

Table 5: Effective collision strengths for transitions in C V. ($a{\pm}b \equiv a{\times}10^{\pm b}$).

Transition		Temperature (log T_e, K)										
i	j	4.0	4.2	4.4	4.6	4.8	5.0	5.2	5.4	5.6	5.8	6.0
29	44	3.117+0	3.128+0	3.155+0	3.217+0	3.322+0	3.475+0	3.689+0	3.984+0	4.381+0	4.881+0	5.347+0
29	45	1.176+1	1.182+1	1.192+1	1.209+1	1.235+1	1.272+1	1.318+1	1.370+1	1.423+1	1.468+1	1.480+1
29	46	1.994+0	1.936+0	1.847+0	1.720+0	1.558+0	1.368+0	1.165+0	9.692−1	7.955−1	6.516−1	5.355−1
29	47	4.884+1	5.059+1	5.339+1	5.746+1	6.263+1	6.880+1	7.621+1	8.541+1	9.703+1	1.111+2	1.243+2
29	48	3.466+0	3.338+0	3.167+0	2.967+0	2.744+0	2.507+0	2.268+0	2.045+0	1.849+0	1.680+0	1.519+0
29	49	7.002−1	6.771−1	6.461−1	6.092−1	5.683−1	5.260−1	4.853−1	4.486−1	4.178−1	3.935−1	3.709−1
30	31	1.718+2	1.740+2	1.736+2	1.711+2	1.711+2	1.789+2	1.985+2	2.325+2	2.824+2	3.465+2	4.096+2
30	32	9.304−1	6.823−1	4.959−1	3.610−1	2.641−1	1.933−1	1.407−1	1.012−1	7.160−2	4.981−2	3.409−2
30	33	1.124−1	9.039−2	7.380−2	6.078−2	4.991−2	4.033−2	3.176−2	2.426−2	1.794−2	1.287−2	8.981−3
30	34	4.542−1	3.486−1	2.721−1	2.153−1	1.711−1	1.349−1	1.044−1	7.892−2	5.808−2	4.169−2	2.926−2
30	35	6.705−1	5.235−1	4.156−1	3.339−1	2.686−1	2.138−1	1.665−1	1.263−1	9.302−2	6.664−2	4.655−2
30	36	8.175−1	7.353−1	6.761−1	6.328−1	6.006−1	5.769−1	5.605−1	5.512−1	5.489−1	5.535−1	5.566−1
30	37	1.862−1	1.788−1	1.679−1	1.536−1	1.361−1	1.162−1	9.535−2	7.520−2	5.715−2	4.202−2	3.004−2
30	38	3.110−1	2.988−1	2.806−1	2.566−1	2.273−1	1.941−1	1.593−1	1.257−1	9.555−2	7.032−2	5.032−2
30	39	4.351−1	4.184−1	3.930−1	3.591−1	3.178−1	2.711−1	2.222−1	1.751−1	1.329−1	9.764−2	6.967−2
30	40	4.119−1	3.951−1	3.699−1	3.363−1	2.951−1	2.485−1	2.005−1	1.554−1	1.163−1	8.466−2	6.036−2
30	41	3.973+0	4.034+0	4.129+0	4.292+0	4.543+0	4.908+0	5.428+0	6.153+0	7.132+0	8.361+0	9.555+0
30	42	7.339−1	7.022−1	6.561−1	5.956−1	5.219−1	4.388−1	3.529−1	2.719−1	2.015−1	1.443−1	1.004−1
30	43	6.355−1	6.147−1	5.831−1	5.393−1	4.829−1	4.160−1	3.436−1	2.720−1	2.071−1	1.523−1	1.089−1
30	44	4.863+0	4.947+0	5.068+0	5.252+0	5.523+0	5.902+0	6.393+0	6.984+0	7.646+0	8.337+0	8.867+0
30	45	1.413+1	1.448+1	1.506+1	1.600+1	1.735+1	1.919+1	2.165+1	2.494+1	2.929+1	3.469+1	3.993+1
30	46	1.000+0	9.676−1	9.171−1	8.471−1	7.572−1	6.509−1	5.361−1	4.230−1	3.204−1	2.340−1	1.656−1
30	47	6.505+0	6.632+0	6.817+0	7.095+0	7.503+0	8.066+0	8.790+0	9.653+0	1.061+1	1.161+1	1.238+1
30	48	7.895+0	8.039+0	8.270+0	8.612+0	9.091+0	9.715+0	1.046+1	1.128+1	1.210+1	1.285+1	1.325+1
30	49	2.558+0	2.487+0	2.341+0	2.130+0	1.908+0	1.731+0	1.633+0	1.624+0	1.699+0	1.839+0	1.978+0
31	32	6.197−1	4.457−1	3.193−1	2.298−1	1.665−1	1.209−1	8.750−2	6.267−2	4.425−2	3.074−2	2.100−2
31	33	5.040−2	4.102−2	3.408−2	2.865−2	2.404−2	1.987−2	1.600−2	1.251−2	9.474−3	6.970−3	4.993−3
31	34	2.407−1	1.821−1	1.405−1	1.105−1	8.782−2	6.959−2	5.435−2	4.155−2	3.100−2	2.256−2	1.605−2
31	35	3.261−1	2.539−1	2.020−1	1.635−1	1.332−1	1.076−1	8.523−2	6.583−2	4.946−2	3.618−2	2.582−2
31	36	1.265+0	1.212+0	1.138+0	1.044+0	9.611−1	9.244−1	9.609−1	1.087+0	1.314+0	1.635+0	1.973+0
31	37	9.876−2	9.532−2	9.002−2	8.274−2	7.352−2	6.276−2	5.129−2	4.014−2	3.015−2	2.184−2	1.534−2
31	38	1.682−1	1.623−1	1.534−1	1.415−1	1.265−1	1.090−1	9.064−2	7.297−2	5.740−2	4.459−2	3.439−2
31	39	2.305−1	2.218−1	2.091−1	1.921−1	1.707−1	1.457−1	1.191−1	9.323−2	7.002−2	5.069−2	3.556−2
31	40	1.932−1	1.851−1	1.739−1	1.594−1	1.414−1	1.207−1	9.870−2	7.734−2	5.823−2	4.230−2	2.979−2
31	41	1.364+0	1.370+0	1.388+0	1.426+0	1.493+0	1.596+0	1.737+0	1.914+0	2.118+0	2.341+0	2.526+0
31	42	3.518−1	3.372−1	3.167−1	2.898−1	2.567−1	2.187−1	1.786−1	1.398−1	1.051−1	7.629−2	5.368−2
31	43	3.574−1	3.450−1	3.273−1	3.031−1	2.719−1	2.345−1	1.936−1	1.528−1	1.156−1	8.427−2	5.945−2
31	44	1.938+0	1.957+0	1.984+0	2.023+0	2.073+0	2.132+0	2.194+0	2.252+0	2.303+0	2.346+0	2.352+0
31	45	4.131+0	4.176+0	4.278+0	4.465+0	4.768+0	5.206+0	5.785+0	6.485+0	7.277+0	8.119+0	8.819+0
31	46	5.652−1	5.447−1	5.161−1	4.775−1	4.280−1	3.689−1	3.044−1	2.402−1	1.818−1	1.324−1	9.340−2
31	47	2.346+0	2.375+0	2.416+0	2.473+0	2.547+0	2.634+0	2.727+0	2.815+0	2.892+0	2.958+0	2.974+0
31	48	5.919+0	6.001+0	6.150+0	6.418+0	6.872+0	7.594+0	8.691+0	1.028+1	1.247+1	1.526+1	1.803+1
31	49	3.851+0	4.051+0	4.303+0	4.631+0	5.059+0	5.603+0	6.254+0	6.983+0	7.746+0	8.478+0	8.978+0
32	33	5.195+1	5.786+1	6.429+1	7.213+1	8.164+1	9.300+1	1.065+2	1.222+2	1.393+2	1.553+2	1.647+2
32	34	1.561+2	1.735+2	1.926+2	2.160+2	2.445+2	2.787+2	3.192+2	3.663+2	4.177+2	4.658+2	4.940+2
32	35	2.602+2	2.883+2	3.195+2	3.584+2	4.061+2	4.631+2	5.308+2	6.095+2	6.952+2	7.753+2	8.225+2
32	36	3.079−1	2.641−1	2.287−1	1.979−1	1.697−1	1.430−1	1.182−1	9.631−2	7.808−2	6.365−2	5.219−2
32	37	1.641+1	1.657+1	1.660+1	1.657+1	1.649+1	1.639+1	1.624+1	1.602+1	1.570+1	1.524+1	1.451+1
32	38	2.730+1	2.757+1	2.764+1	2.758+1	2.746+1	2.728+1	2.701+1	2.663+1	2.609+1	2.533+1	2.412+1

Table 5: Effective collision strengths for transitions in C V. ($a{\pm}b \equiv a{\times}10^{\pm b}$).

Transition		Temperature (log T$_e$, K)										
i	j	4.0	4.2	4.4	4.6	4.8	5.0	5.2	5.4	5.6	5.8	6.0
32	39	3.832+1	3.872+1	3.881+1	3.873+1	3.852+1	3.823+1	3.782+1	3.726+1	3.649+1	3.542+1	3.374+1
32	40	4.365+0	4.319+0	4.229+0	4.109+0	3.969+0	3.816+0	3.664+0	3.519+0	3.382+0	3.238+0	3.039+0
32	41	4.887+0	4.824+0	4.711+0	4.563+0	4.393+0	4.212+0	4.032+0	3.865+0	3.716+0	3.577+0	3.400+0
32	42	7.879+0	7.778+0	7.599+0	7.370+0	7.110+0	6.836+0	6.565+0	6.314+0	6.089+0	5.876+0	5.595+0
32	43	1.338+0	1.298+0	1.243+0	1.176+0	1.102+0	1.026+0	9.519−1	8.841−1	8.243−1	7.712−1	7.151−1
32	44	1.252+0	1.204+0	1.139+0	1.061+0	9.746−1	8.851−1	7.986−1	7.204−1	6.531−1	5.961−1	5.421−1
32	45	1.834+0	1.788+0	1.718+0	1.632+0	1.534+0	1.431+0	1.330+0	1.239+0	1.160+0	1.092+0	1.021+0
32	46	2.135+0	2.069+0	1.976+0	1.865+0	1.743+0	1.620+0	1.501+0	1.392+0	1.297+0	1.213+0	1.124+0
32	47	1.112+0	1.071+0	1.012+0	9.389−1	8.568−1	7.707−1	6.871−1	6.116−1	5.471−1	4.932−1	4.439−1
32	48	5.746−1	5.401−1	4.950−1	4.411−1	3.803−1	3.161−1	2.533−1	1.966−1	1.488−1	1.108−1	8.172−2
32	49	2.930−1	2.779−1	2.561−1	2.300−1	2.034−1	1.787−1	1.564−1	1.358−1	1.158−1	9.601−2	7.676−2
33	34	3.143+0	2.991+0	2.748+0	2.442+0	2.101+0	1.749+0	1.408+0	1.101+0	8.385−1	6.242−1	4.547−1
33	35	1.040+1	1.051+1	1.062+1	1.075+1	1.089+1	1.103+1	1.113+1	1.116+1	1.110+1	1.090+1	1.048+1
33	36	6.927−2	5.587−2	4.548−2	3.695−2	2.959−2	2.314−2	1.760−2	1.305−2	9.484−3	6.776−3	4.768−3
33	37	1.207+2	1.251+2	1.300+2	1.365+2	1.449+2	1.554+2	1.687+2	1.854+2	2.062+2	2.299+2	2.497+2
33	38	6.166−1	5.847−1	5.368−1	4.780−1	4.126−1	3.445−1	2.783−1	2.182−1	1.667−1	1.245−1	9.123−2
33	39	2.701+0	2.713+0	2.711+0	2.703+0	2.693+0	2.680+0	2.665+0	2.647+0	2.625+0	2.591+0	2.510+0
33	40	1.231+1	1.237+1	1.234+1	1.224+1	1.211+1	1.196+1	1.178+1	1.155+1	1.127+1	1.089+1	1.031+1
33	41	3.394−1	3.203−1	2.934−1	2.604−1	2.232−1	1.843−1	1.465−1	1.126−1	8.412−2	6.138−2	4.392−2
33	42	1.417+0	1.393+0	1.356+0	1.312+0	1.263+0	1.211+0	1.159+0	1.107+0	1.057+0	1.008+0	9.476−1
33	43	1.903+0	1.816+0	1.679+0	1.510+0	1.343+0	1.215+0	1.141+0	1.122+0	1.146+0	1.191+0	1.214+0
33	44	2.245−1	2.108−1	1.923−1	1.699−1	1.448−1	1.185−1	9.311−2	7.042−2	5.152−2	3.666−2	2.549−2
33	45	2.577−1	2.434−1	2.234−1	1.985−1	1.699−1	1.396−1	1.100−1	8.336−2	6.111−2	4.357−2	3.036−2
33	46	4.381−1	4.225−1	4.023−1	3.789−1	3.536−1	3.277−1	3.025−1	2.794−1	2.590−1	2.410−1	2.226−1
33	47	2.043−1	1.926−1	1.769−1	1.575−1	1.353−1	1.115−1	8.812−2	6.695−2	4.914−2	3.503−2	2.438−2
33	48	1.696−1	1.586−1	1.444−1	1.275−1	1.087−1	8.901−2	7.003−2	5.311−2	3.900−2	2.788−2	1.947−2
33	49	1.274−1	1.230−1	1.159−1	1.059−1	9.358−2	7.964−2	6.537−2	5.212−2	4.079−2	3.171−2	2.464−2
34	35	2.870+1	2.835+1	2.802+1	2.772+1	2.746+1	2.722+1	2.695+1	2.659+1	2.607+1	2.534+1	2.419+1
34	36	3.439−1	2.568−1	1.948−1	1.500−1	1.175−1	9.406−2	7.707−2	6.441−2	5.451−2	4.633−2	3.913−2
34	37	9.174+1	9.502+1	9.864+1	1.034+2	1.095+2	1.172+2	1.270+2	1.394+2	1.549+2	1.726+2	1.874+2
34	38	2.726+2	2.821+2	2.931+2	3.078+2	3.269+2	3.508+2	3.809+2	4.187+2	4.656+2	5.191+2	5.638+2
34	39	6.220+0	6.216+0	6.161+0	6.076+0	5.969+0	5.851+0	5.728+0	5.607+0	5.489+0	5.360+0	5.150+0
34	40	1.288+1	1.289+1	1.280+1	1.265+1	1.247+1	1.226+1	1.202+1	1.174+1	1.141+1	1.099+1	1.039+1
34	41	2.055+1	2.061+1	2.052+1	2.033+1	2.008+1	1.979+1	1.945+1	1.903+1	1.853+1	1.789+1	1.692+1
34	42	3.202+0	3.130+0	3.021+0	2.887+0	2.736+0	2.576+0	2.416+0	2.263+0	2.123+0	1.993+0	1.851+0
34	43	2.479+0	2.364+0	2.185+0	1.961+0	1.740+0	1.563+0	1.451+0	1.403+0	1.406+0	1.433+0	1.438+0
34	44	2.543+0	2.424+0	2.237+0	2.002+0	1.769+0	1.581+0	1.460+0	1.406+0	1.404+0	1.428+0	1.431+0
34	45	6.237+0	6.226+0	6.164+0	6.067+0	5.946+0	5.808+0	5.658+0	5.494+0	5.311+0	5.098+0	4.804+0
34	46	1.174+0	1.119+0	1.049+0	9.672−1	8.788−1	7.882−1	7.010−1	6.219−1	5.539−1	4.968−1	4.449−1
34	47	2.093+0	1.994+0	1.845+0	1.665+0	1.488+0	1.347+0	1.255+0	1.214+0	1.211+0	1.225+0	1.219+0
34	48	6.560−1	6.257−1	5.815−1	5.285−1	4.751−1	4.279−1	3.894−1	3.588−1	3.345−1	3.142−1	2.935−1
34	49	3.824−1	3.694−1	3.482−1	3.186−1	2.817−1	2.400−1	1.973−1	1.576−1	1.236−1	9.644−2	7.519−2
35	36	4.082−1	3.203−1	2.544−1	2.024−1	1.594−1	1.230−1	9.270−2	6.826−2	4.932−2	3.509−2	2.460−2
35	37	1.119+1	1.139+1	1.147+1	1.152+1	1.161+1	1.185+1	1.232+1	1.308+1	1.414+1	1.542+1	1.647+1
35	38	9.705+1	1.003+2	1.038+2	1.082+2	1.141+2	1.215+2	1.311+2	1.434+2	1.589+2	1.768+2	1.917+2
35	39	5.048+2	5.221+2	5.426+2	5.706+2	6.069+2	6.522+2	7.087+2	7.798+2	8.674+2	9.674+2	1.051+3
35	40	5.052+0	4.993+0	4.890+0	4.760+0	4.612+0	4.452+0	4.285+0	4.116+0	3.944+0	3.762+0	3.530+0
35	41	1.235+1	1.231+1	1.218+1	1.199+1	1.175+1	1.147+1	1.117+1	1.084+1	1.048+1	1.005+1	9.470+0
35	42	4.934+1	4.948+1	4.928+1	4.887+1	4.831+1	4.762+1	4.680+1	4.580+1	4.457+1	4.302+1	4.071+1

Table 5: Effective collision strengths for transitions in C V. ($a\pm b \equiv a\times10^{\pm b}$).

Transition		Temperature (log T_e, K)										
i	j	4.0	4.2	4.4	4.6	4.8	5.0	5.2	5.4	5.6	5.8	6.0
35	43	1.615+0	1.556+0	1.478+0	1.386+0	1.286+0	1.183+0	1.083+0	9.917−1	9.110−1	8.389−1	7.647−1
35	44	2.315+0	2.215+0	2.084+0	1.933+0	1.771+0	1.608+0	1.451+0	1.310+0	1.189+0	1.085+0	9.865−1
35	45	4.242+0	4.196+0	4.107+0	3.985+0	3.839+0	3.677+0	3.509+0	3.340+0	3.173+0	3.002+0	2.798+0
35	46	7.845+0	7.481+0	6.912+0	6.206+0	5.511+0	4.962+0	4.627+0	4.506+0	4.553+0	4.681+0	4.730+0
35	47	2.003+0	1.901+0	1.750+0	1.565+0	1.379+0	1.222+0	1.108+0	1.035+0	9.933−1	9.671−1	9.315−1
35	48	9.130−1	8.618−1	7.913−1	7.095−1	6.278−1	5.541−1	4.903−1	4.342−1	3.831−1	3.349−1	2.881−1
35	49	6.337−1	6.125−1	5.774−1	5.283−1	4.670−1	3.977−1	3.267−1	2.608−1	2.044−1	1.593−1	1.240−1
36	37	1.106−1	1.035−1	9.433−2	8.351−2	7.139−2	5.864−2	4.621−2	3.500−2	2.558−2	1.813−2	1.252−2
36	38	2.073−1	1.953−1	1.798−1	1.615−1	1.410−1	1.194−1	9.832−2	7.919−2	6.294−2	4.981−2	3.941−2
36	39	2.618−1	2.443−1	2.222−1	1.963−1	1.675−1	1.375−1	1.082−1	8.192−2	5.986−2	4.241−2	2.928−2
36	40	1.471−1	1.370−1	1.242−1	1.092−1	9.261−2	7.533−2	5.870−2	4.393−2	3.172−2	2.221−2	1.517−2
36	41	1.495+0	1.424+0	1.323+0	1.202+0	1.086+0	1.001+0	9.593−1	9.607−1	9.956−1	1.044+0	1.070+0
36	42	2.733−1	2.540−1	2.297−1	2.012−1	1.699−1	1.378−1	1.071−1	8.004−2	5.771−2	4.037−2	2.755−2
36	43	1.659−1	1.543−1	1.405−1	1.242−1	1.057−1	8.628−2	6.733−2	5.038−2	3.633−2	2.539−2	1.730−2
36	44	7.732−1	7.349−1	6.904−1	6.430−1	5.951−1	5.488−1	5.058−1	4.676−1	4.344−1	4.051−1	3.747−1
36	45	4.686+0	4.476+0	4.181+0	3.832+0	3.510+0	3.293+0	3.221+0	3.296+0	3.485+0	3.719+0	3.861+0
36	46	2.808−1	2.582−1	2.321−1	2.029−1	1.714−1	1.390−1	1.080−1	8.060−2	5.801−2	4.048−2	2.756−2
36	47	9.294−1	8.846−1	8.320−1	7.758−1	7.197−1	6.662−1	6.173−1	5.739−1	5.362−1	5.026−1	4.667−1
36	48	2.872+1	2.870+1	2.854+1	2.829+1	2.798+1	2.758+1	2.710+1	2.650+1	2.575+1	2.482+1	2.348+1
36	49	1.993+2	2.044+2	2.152+2	2.337+2	2.600+2	2.938+2	3.355+2	3.850+2	4.393+2	4.903+2	5.201+2
37	38	1.258+1	1.277+1	1.291+1	1.301+1	1.310+1	1.315+1	1.316+1	1.309+1	1.291+1	1.260+1	1.203+1
37	39	4.742+0	4.763+0	4.755+0	4.723+0	4.664+0	4.580+0	4.470+0	4.341+0	4.194+0	4.025+0	3.793+0
37	40	1.613+2	1.781+2	2.050+2	2.438+2	2.917+2	3.461+2	4.067+2	4.748+2	5.498+2	6.257+2	6.812+2
37	41	2.989+0	2.917+0	2.820+0	2.710+0	2.592+0	2.473+0	2.356+0	2.249+0	2.153+0	2.062+0	1.951+0
37	42	2.067+0	2.017+0	1.946+0	1.862+0	1.769+0	1.673+0	1.581+0	1.497+0	1.424+0	1.359+0	1.282+0
37	43	1.866+1	1.818+1	1.759+1	1.699+1	1.641+1	1.586+1	1.533+1	1.480+1	1.424+1	1.360+1	1.275+1
37	44	1.195+0	1.134+0	1.056+0	9.655−1	8.679−1	7.678−1	6.714−1	5.842−1	5.093−1	4.468−1	3.919−1
37	45	1.438+0	1.375+0	1.295+0	1.202+0	1.101+0	9.979−1	8.995−1	8.115−1	7.370−1	6.750−1	6.165−1
37	46	1.192+0	1.133+0	1.058+0	9.728−1	8.815−1	7.891−1	7.013−1	6.228−1	5.559−1	5.002−1	4.494−1
37	47	1.051+0	9.965−1	9.287−1	8.502−1	7.639−1	6.739−1	5.859−1	5.052−1	4.354−1	3.772−1	3.269−1
37	48	6.728−1	6.362−1	5.895−1	5.327−1	4.666−1	3.940−1	3.209−1	2.534−1	1.958−1	1.497−1	1.140−1
37	49	2.715−1	2.558−1	2.351−1	2.116−1	1.881−1	1.664−1	1.464−1	1.274−1	1.085−1	8.942−2	7.080−2
38	39	1.750+1	1.769+1	1.781+1	1.788+1	1.791+1	1.788+1	1.778+1	1.758+1	1.725+1	1.677+1	1.594+1
38	40	3.415+1	3.708+1	4.178+1	4.860+1	5.709+1	6.685+1	7.785+1	9.032+1	1.042+2	1.182+2	1.285+2
38	41	1.894+2	2.097+2	2.423+2	2.893+2	3.474+2	4.131+2	4.862+2	5.681+2	6.583+2	7.494+2	8.159+2
38	42	5.732+0	5.598+0	5.411+0	5.194+0	4.961+0	4.726+0	4.500+0	4.294+0	4.111+0	3.942+0	3.733+0
38	43	6.855+0	6.645+0	6.388+0	6.116+0	5.843+0	5.575+0	5.314+0	5.059+0	4.808+0	4.547+0	4.229+0
38	44	1.585+1	1.540+1	1.486+1	1.431+1	1.377+1	1.326+1	1.276+1	1.227+1	1.176+1	1.120+1	1.048+1
38	45	4.817+1	5.294+1	6.044+1	7.117+1	8.441+1	9.949+1	1.164+2	1.354+2	1.565+2	1.779+2	1.935+2
38	46	2.684+0	2.552+0	2.388+0	2.204+0	2.008+0	1.810+0	1.621+0	1.449+0	1.300+0	1.172+0	1.054+0
38	47	1.142+1	1.109+1	1.069+1	1.027+1	9.864+0	9.469+0	9.086+0	8.710+0	8.328+0	7.917+0	7.394+0
38	48	1.128+0	1.068+0	9.896−1	8.938−1	7.821−1	6.600−1	5.373−1	4.243−1	3.282−1	2.513−1	1.917−1
38	49	6.860−1	6.584−1	6.216−1	5.803−1	5.414−1	5.106−1	4.900−1	4.794−1	4.770−1	4.795−1	4.765−1
39	40	3.816+0	3.809+0	3.771+0	3.724+0	3.710+0	3.769+0	3.930+0	4.202+0	4.573+0	4.987+0	5.281+0
39	41	2.841+1	3.066+1	3.427+1	3.955+1	4.617+1	5.380+1	6.244+1	7.225+1	8.318+1	9.426+1	1.023+2
39	42	3.419+2	3.786+2	4.371+2	5.211+2	6.247+2	7.420+2	8.726+2	1.019+3	1.180+3	1.343+3	1.462+3
39	43	2.215+0	2.116+0	1.991+0	1.850+0	1.701+0	1.549+0	1.403+0	1.271+0	1.155+0	1.054+0	9.559−1
39	44	5.163+0	4.960+0	4.711+0	4.440+0	4.160+0	3.880+0	3.609+0	3.355+0	3.120+0	2.899+0	2.660+0
39	45	9.219+0	9.769+0	1.063+1	1.188+1	1.346+1	1.532+1	1.748+1	1.998+1	2.279+1	2.566+1	2.774+1

Table 5: Effective collision strengths for transitions in C V. ($a\pm b \equiv a\times10^{\pm b}$).

Transition		Temperature (log T_e, K)										
i	j	4.0	4.2	4.4	4.6	4.8	5.0	5.2	5.4	5.6	5.8	6.0
39	46	3.969+1	3.856+1	3.723+1	3.589+1	3.462+1	3.341+1	3.223+1	3.104+1	2.980+1	2.843+1	2.662+1
39	47	4.415+0	4.236+0	4.013+0	3.766+0	3.506+0	3.244+0	2.991+0	2.756+0	2.543+0	2.347+0	2.142+0
39	48	1.554+0	1.473+0	1.366+0	1.233+0	1.077+0	9.072−1	7.370−1	5.809−1	4.485−1	3.429−1	2.612−1
39	49	6.313−1	5.982−1	5.512−1	4.916−1	4.221−1	3.478−1	2.750−1	2.095−1	1.545−1	1.108−1	7.767−2
40	41	9.605+0	9.589+0	9.525+0	9.430+0	9.309+0	9.159+0	8.974+0	8.749+0	8.483+0	8.158+0	7.689+0
40	42	3.165+0	3.091+0	2.984+0	2.847+0	2.686+0	2.509+0	2.326+0	2.150+0	1.989+0	1.843+0	1.691+0
40	43	1.425+2	1.587+2	1.803+2	2.115+2	2.581+2	3.270+2	4.250+2	5.567+2	7.199+2	8.978+2	1.044+3
40	44	2.887+0	2.776+0	2.623+0	2.437+0	2.228+0	2.009+0	1.795+0	1.601+0	1.433+0	1.292+0	1.162+0
40	45	4.340+0	4.238+0	4.090+0	3.907+0	3.695+0	3.464+0	3.228+0	2.997+0	2.781+0	2.577+0	2.360+0
40	46	2.211+0	2.088+0	1.926+0	1.736+0	1.531+0	1.324+0	1.131+0	9.636−1	8.270−1	7.194−1	6.300−1
40	47	2.608+0	2.481+0	2.320+0	2.135+0	1.935+0	1.730+0	1.531+0	1.351+0	1.196+0	1.066+0	9.498−1
40	48	9.063−1	8.548−1	7.862−1	7.085−1	6.314−1	5.612−1	4.986−1	4.410−1	3.853−1	3.297−1	2.743−1
40	49	3.900−1	3.736−1	3.481−1	3.135−1	2.712−1	2.244−1	1.773−1	1.343−1	9.790−2	6.911−2	4.752−2
41	42	1.235+1	1.218+1	1.194+1	1.165+1	1.131+1	1.094+1	1.054+1	1.011+1	9.667+0	9.193+0	8.593+0
41	43	1.318+1	1.413+1	1.538+1	1.726+1	2.023+1	2.480+1	3.149+1	4.060+1	5.197+1	6.438+1	7.452+1
41	44	1.808+2	2.011+2	2.277+2	2.661+2	3.235+2	4.084+2	5.295+2	6.925+2	8.947+2	1.115+3	1.297+3
41	45	3.535+0	3.382+0	3.199+0	2.990+0	2.760+0	2.518+0	2.277+0	2.052+0	1.852+0	1.678+0	1.511+0
41	46	4.794+0	4.564+0	4.272+0	3.940+0	3.586+0	3.227+0	2.885+0	2.577+0	2.314+0	2.093+0	1.889+0
41	47	1.135+1	1.240+1	1.406+1	1.681+1	2.106+1	2.728+1	3.599+1	4.756+1	6.185+1	7.752+1	9.058+1
41	48	5.442+1	6.033+1	6.921+1	8.157+1	9.669+1	1.139+2	1.332+2	1.551+2	1.790+2	2.029+2	2.196+2
41	49	9.212+0	9.086+0	8.947+0	8.811+0	8.678+0	8.537+0	8.373+0	8.175+0	7.931+0	7.625+0	7.185+0
42	43	2.850+0	2.711+0	2.510+0	2.275+0	2.053+0	1.890+0	1.807+0	1.807+0	1.883+0	2.007+0	2.113+0
42	44	1.122+1	1.173+1	1.235+1	1.327+1	1.479+1	1.725+1	2.097+1	2.617+1	3.283+1	4.037+1	4.686+1
42	45	5.179+0	5.051+0	4.873+0	4.655+0	4.403+0	4.127+0	3.842+0	3.565+0	3.305+0	3.062+0	2.805+0
42	46	2.457+2	2.719+2	3.047+2	3.496+2	4.150+2	5.112+2	6.494+2	8.387+2	1.081+3	1.362+3	1.614+3
42	47	9.449+0	9.856+0	1.040+1	1.129+1	1.281+1	1.526+1	1.893+1	2.400+1	3.036+1	3.734+1	4.304+1
42	48	1.615+0	1.517+0	1.386+0	1.226+0	1.044+0	8.537−1	6.687−1	5.038−1	3.670−1	2.600−1	1.800−1
42	49	7.145−1	6.819−1	6.331−1	5.687−1	4.912−1	4.058−1	3.203−1	2.423−1	1.765−1	1.245−1	8.549−2
43	44	7.661+0	7.522+0	7.315+0	7.047+0	6.720+0	6.344+0	5.943+0	5.542+0	5.159+0	4.793+0	4.399+0
43	45	5.211+0	5.374+0	5.562+0	5.859+0	6.391+0	7.298+0	8.706+0	1.070+1	1.324+1	1.608+1	1.845+1
43	46	4.481+0	4.249+0	3.938+0	3.555+0	3.118+0	2.656+0	2.210+0	1.815+0	1.488+0	1.230+0	1.025+0
43	47	7.617+0	7.378+0	7.057+0	6.670+0	6.225+0	5.737+0	5.237+0	4.756+0	4.314+0	3.916+0	3.526+0
43	48	1.102+0	1.026+0	9.285−1	8.133−1	6.863−1	5.556−1	4.310−1	3.215−1	2.317−1	1.623−1	1.112−1
43	49	3.855−1	3.675−1	3.412−1	3.067−1	2.651−1	2.192−1	1.732−1	1.310−1	9.538−2	6.718−2	4.606−2
44	45	1.559+1	1.690+1	1.876+1	2.165+1	2.604+1	3.252+1	4.167+1	5.394+1	6.917+1	8.594+1	9.993+1
44	46	1.094+1	1.057+1	1.007+1	9.452+0	8.748+0	7.991+0	7.228+0	6.506+0	5.857+0	5.283+0	4.735+0
44	47	4.831+0	4.586+0	4.257+0	3.853+0	3.391+0	2.902+0	2.428+0	2.006+0	1.656+0	1.379+0	1.156+0
44	48	1.643+1	1.592+1	1.530+1	1.466+1	1.401+1	1.336+1	1.272+1	1.207+1	1.142+1	1.075+1	9.957+0
44	49	3.579+0	3.402+0	3.206+0	3.000+0	2.792+0	2.586+0	2.389+0	2.207+0	2.043+0	1.895+0	1.741+0
45	46	3.350+0	3.164+0	2.918+0	2.625+0	2.299+0	1.960+0	1.633+0	1.342+0	1.100+0	9.065−1	7.516−1
45	47	1.854+2	2.057+2	2.312+2	2.661+2	3.172+2	3.926+2	5.007+2	6.476+2	8.329+2	1.041+3	1.220+3
45	48	2.095+2	2.342+2	2.723+2	3.259+2	3.914+2	4.656+2	5.483+2	6.409+2	7.421+2	8.425+2	9.130+2
45	49	3.119+1	3.082+1	3.042+1	3.007+1	2.974+1	2.940+1	2.899+1	2.843+1	2.769+1	2.671+1	2.523+1
46	47	8.836+0	8.587+0	8.234+0	7.783+0	7.246+0	6.648+0	6.035+0	5.450+0	4.923+0	4.456+0	4.005+0
46	48	1.758+0	1.634+0	1.475+0	1.289+0	1.084+0	8.752−1	6.768−1	5.029−1	3.608−1	2.514−1	1.709−1
46	49	6.189−1	5.887−1	5.451−1	4.886−1	4.213−1	3.477−1	2.743−1	2.073−1	1.508−1	1.061−1	7.272−2
47	48	2.219+1	2.154+1	2.075+1	1.992+1	1.909+1	1.826+1	1.743+1	1.659+1	1.573+1	1.484+1	1.376+1
47	49	4.441+0	4.216+0	3.970+0	3.717+0	3.465+0	3.217+0	2.982+0	2.764+0	2.567+0	2.388+0	2.200+0
48	49	3.896+2	3.915+2	4.060+2	4.370+2	4.831+2	5.426+2	6.156+2	7.034+2	8.045+2	9.092+2	9.865+2

Table 6: Comparison of Υ values for transitions of C V. ($a{\pm}b \equiv a{\times}10^{\pm b}$).

T_e (K)		$8.64{\times}10^4$		$1.94{\times}10^5$		$4.32{\times}10^5$		$9.72{\times}10^5$	
i	j	DARC	ZS	DARC	ZS	DARC	ZS	DARC	ZS
1	2	2.84−2	8.48−3	1.99−2	9.46−3	1.41−2	8.91−3	9.94−3	7.23−3
1	3	4.59−3	4.95−3	4.32−3	5.02−3	3.99−3	4.56−3	3.45−3	3.68−3
1	4	1.38−2	1.48−2	1.30−2	1.50−2	1.20−2	1.37−2	1.04−2	1.11−2
1	5	2.30−2	2.47−2	2.16−2	2.51−2	2.00−2	2.27−2	1.73−2	1.84−2
1	6	1.61−2	1.42−2	1.53−2	1.50−2	1.52−2	1.55−2	1.56−2	1.62−2
1	7	2.95−2	4.05−2	3.28−2	4.48−2	3.82−2	5.13−2	4.80−2	6.40−2

DARC: Present calculations from the DARC code

ZS: Calculations of Zhang and Sampson [16]

Table 7: Comparison of Υ values for resonance transitions of C V. ($a{\pm}b \equiv a{\times}10^{\pm b}$).

		DARC			FAC		
T_e (K)		10^4	10^5	10^6	10^4	10^5	10^6
1	2	4.987−2	2.665−2	9.812−3	7.263−3	7.096−3	5.842−3
1	3	5.368−3	4.534−3	3.431−3	4.323−3	4.189−3	3.217−3
1	4	1.625−2	1.361−2	1.029−2	1.294−2	1.254−2	9.632−3
1	5	2.708−2	2.267−2	1.715−2	2.158−2	2.091−2	1.606−2
1	6	1.871−2	1.588−2	1.564−2	1.388−2	1.410−2	1.576−2
1	7	2.674−2	3.000−2	4.836−2	3.737−2	3.941−2	5.721−2
1	8	1.182−2	5.340−3	2.347−3	1.725−3	1.686−3	1.390−3
1	9	1.239−3	1.042−3	8.544−4	1.098−3	1.065−3	8.217−4
1	10	3.800−3	3.129−3	2.562−3	3.275−3	3.176−3	2.452−3
1	11	6.169−3	5.177−3	4.259−3	5.482−3	5.315−3	4.101−3
1	12	5.842−3	3.512−3	3.429−3	2.919−3	2.970−3	3.356−3
1	13	8.990−4	6.556−4	3.540−4	4.225−4	4.065−4	2.935−4
1	14	1.503−3	1.094−3	5.910−4	7.035−4	6.768−4	4.893−4
1	15	2.103−3	1.528−3	8.244−4	9.851−4	9.478−4	6.844−4
1	16	3.493−3	2.143−3	1.342−3	3.607−4	3.844−4	5.897−4
1	17	5.694−3	6.372−3	1.044−2	7.706−3	8.141−3	1.191−2
1	18	2.601−3	1.864−3	1.010−3	6.569−4	6.419−4	5.293−4
1	19	4.795−4	4.159−4	3.509−4	4.278−4	4.149−4	3.208−4
1	20	1.515−3	1.256−3	1.053−3	1.280−3	1.241−3	9.599−4
1	21	2.529−3	2.097−3	1.753−3	2.135−3	2.070−3	1.601−3
1	22	2.238−3	1.567−3	1.491−3	1.138−3	1.158−3	1.316−3
1	23	3.944−4	3.153−4	1.759−4	2.223−4	2.139−4	1.552−4
1	24	6.581−4	5.265−4	2.934−4	3.702−4	3.563−4	2.586−4
1	25	9.187−4	7.367−4	4.099−4	5.182−4	4.988−4	3.618−4
1	26	2.265−4	1.618−4	3.300−5	1.428−5	1.366−5	9.374−6
1	27	4.137−4	2.882−4	6.191−5	1.755−5	1.688−5	1.233−5
1	28	4.074−4	2.924−4	5.959−5	2.569−5	2.457−5	1.686−5
1	29	5.595−4	3.794−4	8.514−5	1.382−5	1.345−5	1.111−5
1	30	2.033−3	1.249−3	7.206−4	1.739−4	1.852−4	2.836−4
1	31	2.206−3	2.695−3	4.397−3	2.936−3	3.105−3	4.569−3
1	32	1.241−3	1.060−3	5.735−4	3.071−4	3.001−4	2.474−4
1	33	2.058−4	2.157−4	1.857−4	2.043−4	1.982−4	1.534−4
1	34	6.395−4	6.491−4	5.568−4	6.122−4	5.937−4	4.596−4
1	35	1.053−3	1.079−3	9.265−4	1.019−3	9.884−4	7.651−4
1	36	9.897−4	9.521−4	9.150−4	5.955−4	6.065−4	6.907−4
1	37	1.737−4	1.616−4	9.827−5	1.225−4	1.179−4	8.571−5
1	38	2.901−4	2.698−4	1.639−4	2.039−4	1.964−4	1.428−4
1	39	4.060−4	3.773−4	2.289−4	2.855−4	2.748−4	1.998−4
1	40	5.883−5	3.597−5	1.239−5	1.126−5	1.077−5	7.416−6
1	41	1.107−4	6.626−5	2.447−5	1.428−5	1.372−5	9.870−6
1	42	1.058−4	6.457−5	2.224−5	2.025−5	1.938−5	1.334−5
1	43	7.456−6	4.356−6	1.133−6	2.609−7	2.484−7	1.629−7
1	44	1.494−5	7.829−6	2.210−6	2.982−7	2.847−7	1.930−7
1	45	1.841−4	1.075−4	4.245−5	1.024−5	9.993−6	8.467−6
1	46	1.169−5	6.808−6	1.774−6	4.098−7	3.901−7	2.558−7
1	47	1.642−5	8.450−6	2.411−6	2.912−7	2.781−7	1.899−7
1	48	9.611−4	7.279−4	4.273−4	9.210−5	9.807−5	1.505−4
1	49	1.256−3	1.649−3	2.573−3	1.492−3	1.579−3	2.332−3

DARC: Present calculations from the DARC code

FAC: Present calculations from the FAC code